



University of HUDDERSFIELD

University of Huddersfield Repository

Elforjani, Badradin A.

THERMAL ENERGY HARVESTING IN WIRELESS SENSOR NODES USED FOR
CONDITION MONITORING

Original Citation

Elforjani, Badradin A. (2018) THERMAL ENERGY HARVESTING IN WIRELESS SENSOR
NODES USED FOR CONDITION MONITORING. Doctoral thesis, University of Huddersfield.

This version is available at <http://eprints.hud.ac.uk/id/eprint/34788/>

The University Repository is a digital collection of the research output of the University, available on Open Access. Copyright and Moral Rights for the items on this site are retained by the individual author and/or other copyright owners. Users may access full items free of charge; copies of full text items generally can be reproduced, displayed or performed and given to third parties in any format or medium for personal research or study, educational or not-for-profit purposes without prior permission or charge, provided:

- The authors, title and full bibliographic details is credited in any copy;
- A hyperlink and/or URL is included for the original metadata page; and
- The content is not changed in any way.

For more information, including our policy and submission procedure, please contact the Repository Team at: E.mailbox@hud.ac.uk.

<http://eprints.hud.ac.uk/>

**THERMAL ENERGY HARVESTING IN WIRELESS SENSOR
NODES USED FOR CONDITION MONITORING**



Badradin Ali Elforjani

Supervised by

Professor Andrew D. Ball and Dr FengshouGu

2017

School of Computing and Engineering
University of Huddersfield

TABLE OF CONTENTS

TABLE OF CONTENTS	2
LIST OF FIGURES	6
LIST OF ABBREVIATIONS	11
ABSTRACT	14
DECLARATION	17
ACKNOWLEDGEMENT.....	18
PUBLICATIONS.....	19
Chapter 1. Research Project Undertaken	20
1.1 Introduction	21
1.2 Maintenance Strategies and Condition Monitoring Techniques	22
1.3 Condition Monitoring Challenges.....	26
1.4 Wireless Condition Monitoring.....	26
1.5 Motivation for Wireless Sensor Network.....	27
1.6 Powering Wireless Sensor Nodes Problems	29
1.7 Energy Harvesting Solution for Wireless Sensor Node.....	30
1.8 Thermoelectric Energy Harvesting	31
1.9 Research Aims and Objectives.....	32
1.10 Research Methodology.....	33
1.11 Research Risk Assessment.....	34
1.12 Thesis outline	35
Chapter 2. Literatures Review: Energy Harvesting Techniques ...	38
2.1 Introduction	39

2.2	Energy Harvesting Technologies.....	39
2.3	Energy Harvesting System.....	42
2.4	Condition Monitoring Techniques.....	43
2.5	Review of the Existing Work on Energy Harvesting System.....	46
2.6	Key Findings.....	59
Chapter 3. Investigation of Wireless Sensor Networks for Condition Monitoring.....		61
3.1	Introduction to Wireless Sensor Networks.....	62
3.2	Architecture of WSNs.....	62
3.3	Wireless Applications for Condition Monitoring.....	63
3.4	Review of WSN for Condition Monitoring.....	67
3.5	Wireless Protocols.....	70
3.6	Key Findings.....	73
Chapter 4. Modelling of Thermoelectric Generator.....		75
4.1	Introduction.....	76
4.2	Background of Model TEG.....	77
4.3	The TEG Module Constructing.....	78
4.4	Basic TEG Equations.....	80
4.5	Development of the Theory.....	82
4.6	Summary.....	86
Chapter 5. Finite Element Analysis of Design of Thermal Module.....		87
5.1	Introduction.....	88
5.2	Bench Mark Simulation.....	88
5.3	Simulation of the Thermal Design.....	88
5.4	Model Geometry.....	89
5.5	Model Boundary Conditions.....	95
5.6	The Mesh Structure of the Thermal Design Model.....	97

5.7	Result and Discussion	97
5.8	Summary.....	100
Chapter 6. Design and Implementation of Thermal Energy Harvesting System		101
6.1	Introduction	102
6.2	Experimental Setup to Evaluate Heat Sinks	102
6.3	System Design and Implementation	103
6.4	Heat source.....	109
6.5	Voltage Booster Design.....	110
6.6	The Buffering Effect of Capacitor.....	112
6.7	Data Acquisition System and Experimental Procedure.....	112
6.8	Results and Discussion	116
6.9	Summary.....	121
Chapter 7. The Optimisation of Thermal Energy System with Temperature Sensor for Monitoring a Gearbox		122
7.1	Introduction	123
7.2	Experimental Setup	123
7.3	Thermal Image	129
7.4	The TEG System Evaluation	131
7.5	Development Features of the TEG Design Test Rig.....	136
7.6	Results and Discussion	140
7.7	Comparison of the Results from Three Different Research Elements	143
7.8	Summary.....	144
Chapter 8. Monitoring of Gearbox Using a Wireless Temperature Node Powered Thermal Energy Harvesting Module		145
8.1	Test Facility and Method	146

8.2	Test Procedure.....	146
8.3	Wireless Measurement.....	147
8.4	Result and Discussion.....	147
8.5	Baseline	148
8.6	Conclusion	153
Chapter 9. Conclusions and Future Work suggestions		155
9.1	Introduction	156
9.2	Conclusions.....	156
9.3	Review of Research Objective and Achievements	158
9.4	Contributions to Knowledge.....	161
9.5	Recommendation for Future Work.....	162
APPENDIX – A.2: Clamp.....		165
APPENDIX – B.1: Clamp support part design - 1.....		166
APPENDIX – B.2: Clamp support part design - 2.....		166
APPENDIX – B.3: Clamp support part design - 3.....		167
APPENDIX – C.1: Clamp support part design - 4		168
APPENDIX – C.2: Clamp support part design - 5		169
APPENDIX – D: Clamp support part design - 6		171
APPENDIX – E: Risk Assessment – University of Huddersfield.....		172
REFERENCE		173

LIST OF FIGURES

Figure 1-1 Thesis structure.....	35
Figure 2-1 Source of energy harvesting source and EH devices (.....	40
Figure 2-2 General block diagram of EH system	42
Figure 2-3 (a) Prometheus sensor node, (b) Everlast prototype sys	48
Figure 2-4 (a) Piezoelectric power RFID shoes with mounted electr....	50
Figure 2-5 Basic configuration for a thermoelectric device.....	53
Figure 2-6 The Seebeck effect	54
Figure 2-7 Thermal to electric conversion with thermoelectric	55
Figure 2-8 Examples of thermal energy harvesting applications[91]	57
Figure 2-9 Design of self-power telemetric wireless sensor node [92] .	58
Figure 2-10 Thermal energy harvesting system.....	59
Figure 3-1 Architecture of Wireless Sensor Node [101]	63
Figure 3-3 Bluetooth history.....	Error! Bookmark not defined.
Figure 4-1 Schematic of Thermoelectric Element{Bottner, 2002 #9}....	79
Figure 4-2 3D Structure of Thermoelectric Generator.....	79
Figure 4-3 Open circuit voltage calculated from Equation (5-13).	86
Figure 5-1 Structure of the thermal design.....	90
Figure 5-2 Structural Dimensions	90
Figure 5-3 Peltier TEG.....	92

Figure 5-4 Aluminium Heat sink (SK 100/100).....	93
Figure 5-5 Thermal insulation material geometry.....	94
Figure 5-6 Insulation material (Bond-Ply)	94
Figure 5-7 Aluminium for cold side	95
Figure 5-8 Aluminium for hot side.....	95
Figure 5-9 Cross Section of thermal design Mesh Structure.....	97
Figure 5-10 Thermal simulation of the temperature distribution fo	98
Figure 5-11 Simulated temperature difference between hot and c.....	99
Figure 5-12 Simulation results of TEG open cuircit voltage of t	100
Figure 6-1 Schematic of experimental setup.....	103
Figure 6-2 Structure of the Thermal EH system.....	105
Figure 6-3 Peltier TEG module from Digi-Key, code number	106
Figure 6-4 Picture of Heat sinks	107
Figure 6-5 Thermal insulation material	108
Figure 6-6 the Hot plate IKA, RCT basic.....	109
Figure 6-7 Schematic diagram of the DC-DC boost converter	111
Figure 6-8 Photo of DC-DC boost converter	111
Figure 6-9 Thermocouple conditioner	114
Figure 6-10 Screenshots measurements made by of DAQ software .	115
Figure 6-11 Experimental step.....	116
Figure 6-12 Heat sink (A)	117

Figure 6-13 Heat sink (B)	118
Figure 6-14 Heat sink (C)	119
Figure 6-15 Measured open circuit voltage.....	120
Figure 6-16 Comparison result of three Heat sinks.....	121
Figure 7-1 Test Rig.....	124
Figure 7-2 Texas Instruments Sensor Tag CC2650K.....	127
Figure 7-3 Texas Instruments CC2540 USB Module	128
Figure 7-4 Thermal CAM S65.....	130
Figure 7-5 The thermal images of the gearbox after (10min)	130
Figure 7-6 The thermal images of the gearbox after (60min)	131
Figure 7-7 Experimental setup for thermal energy harvesting system	132
Figure 7-8 Tooth breakage fault	133
Figure 7-9 TEG module performance for high and low speed gea.....	134
Figure 7-10 Picture of the TEG module held general laboratory	136
Figure 7-11 a) Module with developed clamp, b)illustrated of so	137
Figure 7-12 Photo of TEG module attached to gearbox using besp...	137
Figure 7-13 Results using different clamps.....	138
Figure 7-14 The TEG powered wireless temperature measurement..	139
Figure 7-15 Test system.....	140
Figure 7-16 TEG module performance for high and low speed	141
Figure 7-17 Screen shot of measurement on a mobile phone	142

Figure 7-18 Temperature of gearbox by sensor tag.....	142
Figure 7-19 Comparison of open circuit voltage obtained by expe.....	144
Figure 8-1 Test rig schematic showing sensor placements.....	146
Figure 8-2 Test cycle	147
Figure 8-3 Surface temperature and oil temperature of the gearbo ...	148
Figure 8-4 Results of surface temperature and oil temperature for ...	149
Figure 8-5 Data drive model based on gearbox temperature	150
Figure 8-6 Transmission path of gear mesh temperature	151
Figure 8-7 Results of surface temperature at reduced oil level	152
Figure 8-8 Results of surface temperature at shaft misalignment	153

LIST OF TABLES

Table 1-1 Comparison of maintenance strategies.....	25
Table 2-1 Energy Harvesting opportunities and demonstrated	41
Table 3-1 Maximum data speed for cellular network standards[106] ...	65
Table 4-1 Specification of TE generator	80
Table 4-2 Characteristic TEG parameters	82
Table 4-3 TEG Parameters.....	85
Table 5-1 Specifications of material properties and boundary	89
Table 5-2 Specification of TEG.....	91
Table 6-1 Heat sink specifications	107
Table 6-2 Material properties of insulation materials.....	109
Table 6-3 the hot plate specification	109
Table 7-1 Specifications for the AC motor as provided	125
Table 7-5 Thermal CAM S65 technical Specification	129

LIST OF ABBREVIATIONS

AC	Alternating Current
AE	Acoustic emission
Al ₂ O ₃	Aluminium oxide
ADC	Analogy to Digital Converter
AAKR	Auto-associative Kernel Regression
BLE	Bluetooth low energy
Bi ₂ Te ₃	Bismuth telluride
BM	Breakdown maintenance
BWA	Broadband Wireless Access
CBN	Condition based maintenance
CM	Condition monitoring
DAQ	Data acquisition
DAQS	Data acquisition system
DC	Direct current
EH	Energy harvesting
FEA	Finite element analysis
GAP	Generic Application
GPRS	General Packet Radio Service
G	geometry factor, defined by the ratio of area over length (m)
GSM	Global System for Mobile Communication
I	Electrical current (A)
I _{max}	Input current resulting in greatest ΔT
IOT	Internet of Things
ISM	Industrial scientific and medical
K	Thermal conductivity (W/mK)

K_m	TEG module thermal conductance (W/K)
MEMS	Micro-Electro-Mechanical System
MsM	Magnetostrictive materials
MUC	Microcontroller
N	Number of TEG thermocouples
PFM	Pules Frequency Modulated
PM	Preventative Maintenance
P_{MPPT}	Maximum power point tracking
PVDF	Poor coupling in Piezo thin film
R	Thermal resistance (K/W)
R_m	TEG module electrical resistance (Ohm)
S	Seebeck coefficient
SE	Solar energy
SIG	Special Internet
SHM	Structural Health Monitoring
S_m	TEG module Seebeck coefficient (V/K)
T_a	Ambient temperature (C)
TE	Thermal Energy
TEG	Thermoelectric generator
T_h	Hot side Temperature (C)
T_c	Cold side temperature (C)
TEG	Thermoelectric generator
TinyOS	Tiny Operation System
V	Voltage (V)
VE	Vibration energy
VEH	Vibration energy harvesting
V_{max}	Maximum Voltage
Q_c	Heat load (W)
Q_{max}	Maximum amount of heat
Z	Figure of merit,
WLAN	Wireless local area network

WIMAX	Worldwide interoperability for microwave access
WMAN	Wireless metropolitan area network
WPAN	Wireless personal area network
WSN	Wireless sensor network
WSNs	Wireless sensor networks
WWAN	Wireless wide area network
α	Seebeck coefficient (V/K)
ΔT_{max}	Maximum temperature difference a TEG

ABSTRACT

Presently, wireless sensor networks (WSN) are widely investigated and used in condition monitoring on industrial process monitoring and control, based on their inherent advantages of lower maintenance cost, easy installation and the ability to be installed in places not reached easily. However, current WSN based monitoring system still need dedicated power line or regular charging / replacing the batteries, which not only makes it difficult to deploy it in the fields but also degrades the operational reliability.

This PhD research focuses on an investigation into energy harvesting approaches for powering WSN so as to develop a cost-effective, easy installation and reliable wireless measurement system for monitoring mission critical machinery such as multistage gearbox.

Among various emerging energy harvest approaches such as vibrations, inductions, solar panels, thermal energy harvesting is deemed in this thesis to be the most promising one as almost all machines have frictional losses which manifest in terms of temperature changes and more convenient for integration as the heat sources can be close to wireless nodes. In the meantime, temperature based monitoring is adopted as its changes can be more sensitive to early health conditions of a machine when its tribological behaviour is starting to be degraded. Moreover, it has much less data output and more suitable for WSN application compared the mainstream vibration based monitoring techniques.

Based on these two fundamental hypothesis, the research has been carried out according to two main milestones: the development of a thermoelectric harvesting

(TEH) module and the evaluation of temperature based monitoring performances based on an industrial gearbox system. The first one involves the designing, fabricating and optimising the thermal EH module along with a WSN based temperature node and the second investigates the analysis methods to detect the temperature changes due to various faults associated with tribological mechanisms in the gearbox.

In completing the first milestone, it has successfully developed a TEH module using cost-effective thermoelectric generator (TEG) devices and temperature gradient enhancement modules (heat sinks). Especially, the parameters such as their sizes and integration boundary conditions have been configured optimally by a proposed procedure based on the fine element (FE) analysis and the heat generation characteristics of machines to be monitored.

The developed TEG analytic models and,FE models along with simulation study show that three different specifications of heat sinks with a Peltier TEG module are able to produce power that are consistently about 85% of the experimental values from offline tests, showing the good accuracy in predicting power output based on different applications and thus the reliability of the models proposed. An further investigation shows that a Peltier TEG module based that the thermal energy harvesting system produces is nearly 10 mW electricity from the monitored gearbox. This power is demonstrated sufficient to drive the WSN temperature node fabricated with low power consumption BLE microcontroller CC2650 sensor tags for monitoring continuously the temperature changes of the gearbox.

Moreover, it has developed model based monitoring using multiple temperature measurements. The monitoring system allows two common faults oil shortages and mechanical misalignment to be detected and diagnosed, which demonstrates the

specified performance of the self-power wireless temperature system for the purpose of condition monitoring.

Key words:energy harvesting; wireless sensor networks; condition monitoring; temperature; thermoelectric generator, gearbox monitoring

DECLARATION

This thesis is submitted for the PhD at University of Huddersfield. I state that the work in this thesis was carried out by the author own in accordance with the role of the University of Huddersfield.

The work was undertaken and completed under the guidance of Professor Andrew D. Ball and Dr. Fengshou Gu at the Centre of Efficiency and Performance.

The work was done under the guidance of Professor Andrew Ball and Dr. Fengshou Gu at the Centre of Efficiency and Performance Engineering at University of Huddersfield

ACKNOWLEDGEMENT

First of above, I praise Allah, **the almighty** for giving me the guidance, ability, knowledge, and opportunity to undertake this research study, and blessing me with many great people who have been my greatest support in both my personal and professional. This work was financially funded by Libyan higher education through the Libyan cultural affairs in London. I am very grateful to their support during this project.

I would like to express my sincere gratitude to my supervisor **Professor. Andrew D. Ball**, for the continuous support of my PhD study and research, for his patience, motivation, support, and encouragement.

I am especially grateful to my co-supervisor **Dr. Fengshou Gu**, principal research fellow, for his sincere and warm-hearted support. His abundant experience and great vision in the condition monitoring fields have greatly broadened my mind and provided me with many inspirations.

I have express my very profound gratitude to my parents my dad, **Ali** and my mum, **Fatima**, my wife **Wafa** and my children especially my daughters **Hajer**, **Heba** and **Asma** and my son **Abdaraheem**, and my brothers and sisters, especially my brother **Hossam** for providing me with unflinching support and continuous encouragement throughout my years of study.

Finally, I would like to thank all my relatives back home who supported me throughout my study and many thanks to all my friends back home. My thanks are also to my friends in Huddersfield for their discussions and advice

PUBLICATIONS

- [1] **BadradinElforjani**, Fengshou Gu and Andrew Ball (2016). Thermal Energy Harvesting from Waste Heat of Industrial Machine, Journal of studying Engineering Diagnostics, university of Huddersfield on 16th Dec.2016
- [2] **BadradinElforjani**, Yuandong Xu, Khaldon B, Zhifei Wu, Fengshou Gu and Andrew Ball (2017). Monitoring Gearbox Using a Wireless Temperature Node Powered by Thermal Energy Harvesting, in 23th International Conference on Automation & Computing (ICAC), University of Huddersfield, Huddersfield, UK 7-8 September. 2017
- [3] **BadradinElforjani**, Guojin Feng, Fengshou Gu and Andrew Ball (2017). Thermal Energy Harvesting In Wireless Temperature Sensor Nodes for Condition Monitoring, in 30th International Congress on Condition Monitoring and Diagnostic Engineering Management (COMADEM), University of Central Lancashire, UK on 10th-13th July.2017.

Chapter 1. Research Project Undertaken

With technological developments, industrial machine processes become ever more complex and proper maintenance become ever more important. This project proposes that condition monitoring be conducted by a low power consumption wireless sensor network that will give greater reliability and reduce maintenance and equipment costs.

This chapter starts with a general review of the current situation regarding maintenance management and condition monitoring strategies. Details of condition monitoring techniques are briefly reviewed. Then, the motivation for this research project is presented. Based on these, the aims and objectives of the research are identified. Finally, the outline of thesis contents is given.

1.1 Introduction

Modern industrial machines are becoming increasingly complicated and are often composed of hundreds or even thousands of components. The lifetime of each machinery piece can be limited to the operational speed of machinery is limited to the speed at which it operates, the load to which it is exposed, the components, installation and assembly quality. Unexpected failure of any one of those components may not only incur damage not only to the equipment itself, but can cause major economic loss by the interruption of the operation of the plant. In some major industrial application systems, failures in system can lead to enormous austere consequences that can lead to releases and explosions, etc.[1]. Thus, high attention and effort is being paid to efficient and effective maintenance procedures in recent years.

Machine condition monitoring (CM) is an essential part of condition-based maintenance (CBM), CM provides accurate assessment of machine conditions based on various measurement techniques and comprehensive analysis methods, which is becoming recognized in a wide variety of industries as the most important cornerstone CBM in a wide variety of industries [2].

In the meantime, maintenance costs are soaring with the increasing complexity of machines and safe production. About half of cost of operation on most manufacturing and processing operations due to maintenance [3]. This is ample motivation for any activity that can potentially lower maintenance costs. Machinery CM is considered as one of the effective strategies. Obviously, one important benefit of CM is reducing unplanned interruption of production processes, and others are improved reliability and safety along with, the

reduction of unnecessary maintenance of machines implemented in a time based paradigm[4].

Gearboxes are one of the most significant components in rotating machine. They are used widely in many machines such as helicopter, marine drives, automobiles, trains, wind turbine. Therefore, it is the machine component on that this project will focused on for developing wireless CM techniques.

Numerous different techniques have been developed to monitor and control gearbox health. However, because of the complicity of gearboxes are application environment, especially, ever-reducing cost of production, existing CM techniques are far from industrial requirements. Researchers and manufacturers are continuously trying to discovery maintenance measures to ensure optimal performance, reduce operating costs and extend their working lives while ensuring this does not jeopardise safety [5, 6].

In recent years, wireless sensor node (WSN) technologies have been advanced rapidly. Increasingly, WSN is explored and used for industrial, commercial, and consumer applications including environmental monitoring, temperature monitoring and building health monitoring. WSN has gained worldwide attention because of the great advantage it provides, the ability to monitor and control processes without the complicated wiring required by traditional systems [7, 8].

1.2 Maintenance Strategies and Condition Monitoring Techniques

Increasing profitability of investment in an increasing competitive environment is a difficult challenge facing many companies. One feasible way is to reduce operation costs, effectively reducing per unit cost of production. Maintenance of

plant machinery represents almost half of the production cost [1] so reduction in production costs can be achieved by adopting optimal maintenance strategies[9].

Generally, CM differs from machine to machine in relation to the maintenance objectives. For instance, visual inspection might be appropriate in evaluating the condition of a simple machine, but for processes that are complex, a structured CM system may be required. Selection of CM techniques for CM should always consider both the reason why the monitoring is being carried out and the cost. In last few years, the obvious benefits obtained by the condition monitoring application have led to the growth and expansion of an huge number of new methods. References from [3,10,11]. have discussed machines and CM techniques that are most widely used by researchers

Based on [5,6] maintenance strategies can be classified into three main groups BM, PM, CBM:

1.2.1 Breakdown Maintenance (BM)

Breakdown maintenance (BM); in this method, the machine is simply run until it breaks down after which maintenance take place. The repaired equipment is returned to service within given specifications by replacing or repairing faulty parts and components. Emergency repairs cost three to nine times more than planned repairs, therefore, maintenance plans that rely on reactive maintenance are generally the most expensive. BM is the most expensive maintenance strategy because shutdowns disrupt and stop production runs [12, 13].

One BM advantage is that investment in maintenance is not required as its initial costs are significantly lower. However, drawbacks of BM are evident

because, for instance as the predictability for emergency breakdowns cannot be ascertained, which might lead to other related damages to the plant or can cause lethal accidents, loss in the production and control over maintenance management loss. Thus BM is used where interruption of the production process is not important and maintenance repairs are cheaply and quickly carried out.

1.2.2 Preventative Maintenance (PM)

Preventive maintenance is one of the cornerstones of overall productive maintenance. Also it is called schedule maintenance or time based maintenance that is regularly performed on a piece of equipment to lessen the likelihood of it failing. The maintenance action is carried out at specific time intervals before accident of the fault in the machine and invariably results in maintenance costs, which are less than for breakdown maintenance. In addition the limitation of knowledge of the develop of failure base and lack of scientific methods in fault diagnosis, the determination of the intervals or criteria is usually based on design specifications, previous experience and statistical data. The amount saved depends upon the particular application [14].

PM is widely used and is the first level of maintenance above reactive maintenance. The advantage of this method is that most maintenance can be planned well in advance and that catastrophic failure is largely eliminated. The disadvantages, in addition to the fact that a small number of unforeseen failures can still occur, are that too much maintenance is carried out and an excessive number of replacement components consumed. The main aim of PM is to avoid unexpected catastrophic failures[15, 16].

1.2.3 Condition Based Maintenance (CBM)

Condition based maintenance (CBM) is a maintenance strategy which is undertaken based on the information from monitoring the actual condition of the machinery. It is a maintenance program that recommends maintenance action based on the information collected through CM. CBM is also used in an attempt to avoid unnecessary maintenance, by taken maintenance actions only when there is evidence of abnormal behaviour of the machinery [17, 18]. The main object of CBM is to obtain sufficiently detailed knowledge of the condition of a machine to be able to accurately predict its performance and time to failure, and that can achieved by employing numerous different monitoring techniques.

Table 1-1 shows the comparison amongst the three types of strategies in maintenance. It is seen clearly that the CBM strategy when compared with the others strategies especially can be more effective for maintaining machines that are complicated. Therefore, CBM is commonly used in the industry.

There are various other maintenance strategies such as automatic maintenance, reliability centre maintenance and controlled maintenance. The important objectives of all maintenance work are to maximise design life span, meet safety standards and reduce maintenance costs[19].

Table 1-1 Comparison of maintenance strategies

Strategy	Advantages	Disadvantages
BM	cost is Low	May lead to plant related damage
PM	Reduce the rates of accidents, particularly accidents that can be very catastrophic	<ul style="list-style-type: none"> • Difficulty in determining the intervals for perfect maintenance • High cost of maintenance

CBM	<ul style="list-style-type: none"> • Provides maximum duration of machine operation • Maintenance costs reduced greatly by eliminating unnecessary scheduled 	<ul style="list-style-type: none"> • Extra instrumentation investment • For the analysis on the data, experts is needed
------------	--	---

1.3 Condition Monitoring Challenges

The significant of fault diagnosis and CM have increased with extensive acceptance in both industrial and academic area in last years. Recently, there have been numerous international conference on this research area with several paper publications, studying, several topics in their thousands including techniques for monitoring [5], mechanical modelling and diagnosis of faults [20]. However, such progressive and effective methods are hardly well utilised by industries as most industry would rather make use of traditional techniques that have been developed more than 3 decades ago. Typically, cases for diagnosing fault and CM where using temperature techniques have been well studied for rolling element bearings in academic research areas.

1.4 Wireless Condition Monitoring

Wired online systems for CM have been used successfully for many application in the industry. These wired sensors on the health of the machine provide information with some of these information very reliable that they shut down a machine automatically when an excessive level of vibration is detected. On the other hand, wired online system for CM has been limited mostly to big and critically important industrial machines because their cost are high. With the growing industrial machines being very complex and related cost increase, the

use of wired CM installations have increased with the need for more and upgraded wiring.

Recently, with the development of communication technologies, wireless sensor networks (WSNs) have become increasingly common in CM. There are many benefits of using wireless CM, including lower installation cost, ease of maintenance, reduced connector failure, ease of replacement and upgrading, and improved security. On the other hand, WSNs face many challenges in the industrial environment; these include providing a high enough sampling rate, long-term cost effectiveness and higher security requirement.

1.5 Motivation for Wireless Sensor Network

In recent years WSNs have attracted attention in worldwide because of their potential to facilitate better, the physical environments controlling and monitoring from a remote location[21-23]. WSNs used industry have certain advantages including:

Installation: Recently the price of wiring has risen so that it can be the highest single factor in the cost of a CM project. For example, in dangerous environments where special protected cabling must be used, the cabling can cost around \$2.00 per foot (£4.13 per meter) [24] which makes the wiring many times as expensive as the sensors used.

WSNs can be very economical for hazardous plants areas and where protection applications of high assets are required. Furthermore, they can be ideal areas with access problems for example, mountainous or rural, or across rivers areas [24].

Maintenance: As wire gets old, it can easily cause system failure or crack, and it can take long labour and time to detect the fault and cure it. These cables maintenance is generally much more costlier than the sensors maintaining [23, 25]. Thus, wireless measurement can very effectively reduce such costs because wireless network installation can eliminate the need for very long cables [24].

Security: As is well-known hard wired data communication was, and will continue to be a problem. Industrial wireless networks must be secure to protect the data [26] but more and more secure methods of data transmission are surfacing each year. Bluetooth Low Energy offers various security services for protecting information exchange between two connected devices. However, intrusion prevention and malicious jamming frequencies are basic concerns when applying wireless technology [27].

Mobility and Flexibility: Because WSNs do not require any cables or wiring to the sensors they offer the benefit that the sensors can be easily relocated as and when required. The lack of wiring means plant managers can more easily reconfigure assembly lines to meet changing customer demand. Additionally the lack of wiring means WSNs, without the difficulties in planning a routes of the cable [28].

This thesis is based on two hypothesis. First is the designing and optimisation of extremely efficient the thermal EH module along with a WSN based temperature node by utilizing energy harvesting technologies. Based on the restraints of wireless sensor node, the system should be designed in accordance effective with size and cost, on the principle of energy efficiency.

Second, this research aims also in investigating the analysiing methods to detect the temperature changes due to various faults associated with tribological mechanisms in the gearbox.

1.6 Powering Wireless Sensor Nodes Problems

WSN use has grown with a rapid increase in the number of possible applications, so the problem of powering WSNs has come to the fore: the high power consumption of sensor nodes, for example. In addition, there are limitations placed on the use of sensor nodes because of the high cost of providing cables to supply the sensor node with power. The combined cost of batteries and visits to accessible areas is high, but replacement batteries are not a viable solution for inaccessible areas. Sensor nodes, especially vibration sensors, must be very small, i.e. at most one cubic centimetre, to be suitable. Such extremely small devices are quite limited in the energy quantity, which can be stored in the form of an internal battery, and will be a serious limit on the life of nodes powered by small batteries.

1.6.1 High Power Consumption of Sensor Nodes

Reduce the power consumption of the wireless sensor node is usually critical issue in developing WSN applications. In addition, one main challenge in energy harvesting system that is how to implement power management circuit with a minimum power consumption overhead[29].

Consequently, various researches have been made regarding investigating the power consumption of this type of device and its applications[30].These investigations can help to predict the WSN lifetime, provide recommendations to developers and may optimize the energy consumed by the WSN devices.

Application developers should always adopt best practice in order to reduce the power consumption as much as possible [29, 31].

1.6.2 Energy Source Limitation for Sensor Nodes

In several applications, sensor node lifetime ranges from 2-10 years depending on the detailed application requirements [32]. For example, a sensor node to detect the thickness of the ice on the side of a mountain may have to be in place for years for process of melting to be measureable. Therefore, the lifespan of the sensor nodes must be very lengthy. In that case its energy supply is one of the important considerations that must be addressed.

The limitation in the energy supply and the size of the device generally means limited amount of resources such as memory, CPU performance, and wireless communication bandwidth used for transmission and forwarding range of the data. The necessity in improving another way of powering the actuator nodes and WSNs is of huge importance

1.7 Energy Harvesting Solution for Wireless Sensor Node

To remove the major obstacle of successful deployment of WSNs, the limitation of available energy for the network due to the nodes' high power consumption, and the limited energy capacity and unknown lifetime battery performance, technology for energy harvesting (EH) has become a possible solution to maintain the WSN in operation[33, 34]

Any technique that enabled Energy Harvesting to successfully and reliably maintain the productive life of a WSN would be expected to markedly reduce the cost of maintenance of industrial machinery.

Temperature can be an important parameter in monitoring the condition of many industrial machine components, including gearboxes [35] turbines[36] and bearing [37]. This PhD thesis will focus on temperature monitoring of a gearbox and develop embedded signal processing techniques so that they can become widely applicable.

The work will extend recent theory of thermal energy harvesting to include temperature difference. The computer simulation used when developing the theoretical model has limitations, which has been identified and addressed. The FE models were employed to simulate the maximum temperature difference(temperature difference between hot side and cold side). Furthermore, the computer simulation will be used to help quantify the impact and address the limitations of the theoretical model. A theoretical model will be validated through the experimental work investigation. The Theoretical model produces the quicker results, where the Finite Element model results takes longer with the experimental investigation results taking even longer to produce. A Peltier module CP85438 has been chosen as the TEG module, which was employed to simulate the maximum temperature difference between a hot side and cold side of the module. Additionally, the computer simulation will be used to help quantify and address the limitations of the theoretical model. The theoretical model will be validated by experimental work. The theoretical model produces the quicker results, the Finite Element model results take longer.

1.8 Thermoelectric Energy Harvesting

For energy harvesting system applications in WSN, thermal energy harvesting can be used as power source for many industrial and commercial applications.

Thermoelectric energy harvesting can capture the waste heat as a realistic method to continuously power a WSN.

The thermoelectric generator (TEG) is a device that converts thermal energy (temperature difference) directly into electrical energy, using a phenomenon called the Seebeck effect. It can be used for the direct conversion of heat into electricity from sources such as geothermal energy, solar energy or waste heat. The main advantages are the low maintenance requirement, no moving parts and the potential of utilising heat sources over a wide temperature range. The voltage generated from the temperature difference is determined by the Seebeck effect. Seebeck effect is the basic thermoelectric (TE) operating principle describing the process whereby the two dissimilar materials junctions at different temperatures can generate voltage between them. It will state in chapter 2.

1.9 Research Aims and Objectives

The PhD project aims to develop a wireless temperature node to monitor the health and performance of a working gearbox. The wireless node is powered by thermal energy harvested from the wasted heat generated by the gearbox. Therefore, the wireless monitoring system avoids battery replacement and can thus be maintenance free.

To realise this aim, following five objectives are identified to be the critical milestones to be achieved:

Objective one: Investigate the common CM strategies and techniques, and select one to use to monitor the health of the gearbox. To obtain a detailed

understanding of energy harvesting and thermoelectricity generator design and function.

Objective two: To investigate the WSN network applications to the for condition monitoring fields, including various protocols and challenges. Develop a detailed understanding the Bluetooth Low Energy which will act as the wireless transmission protocol.

Objective three: Provide background information regarding the development of the TEG model. A fundamental theoretical understanding of the generated voltage of the TEG model will be developed. Build and run 3D Finite Element computer model of the thermal design, and validate the model against experimental data.

Objective four: Develop and design a rig suitable to test the TEG and WSN developed. Evaluate the performance of the TEG for THE for three different specification of heat sink, in which an industrial gearbox will be used as both a heat source for the TEG system and the monitored machines for WSN.

Objective five: Evaluate the performance of the TEG for energy harvesting to power the WSN for different test conditions. In addition, investigate the use of a wireless temperature node to monitor and diagnose different faults on a gearbox transmission system under different conditions.

1.10 Research Methodology

The main research involved in the project will complete three different stages:

- The first stage involves the development of the Theoretical model
- The second stage involves the development of FE models
- The last stage involves the Experimental investigation..

- The first stage will develop the theoretical model, defining the maximum of temperature difference through the module parts. This aspect of the Theoretical model's development is linked to the work of name Prijic et, al., (2015).
- The second will develop a full 3D FE model using SolidWorks software. The computer simulation will be used to help quantify the impact of, and address limitations of, the theoretical model. A finite element model will be preferable to an experimental test at this stage as the experimental method will introduce a number of uncontrolled parameters.
- The last stage will provide experimental data to validate the theory model predictions and the simulation results, and will quantify the impact of those parameters which cannot be controlled. The experimental investigation will be carried out on a specially developed test rig, which was designed and built at the University of Huddersfield

1.11 Research Risk Assessment

Experimental work undertaken in this research will be performed in the University of Huddersfield Laboratory. All the laboratory equipment is subjected to the health and safety requirements of the University of Huddersfield's policy (2010 – 2014). The health and safety procedure has been reviewed for the project's experimental work. See appendix (E)

1.12 Thesis outline

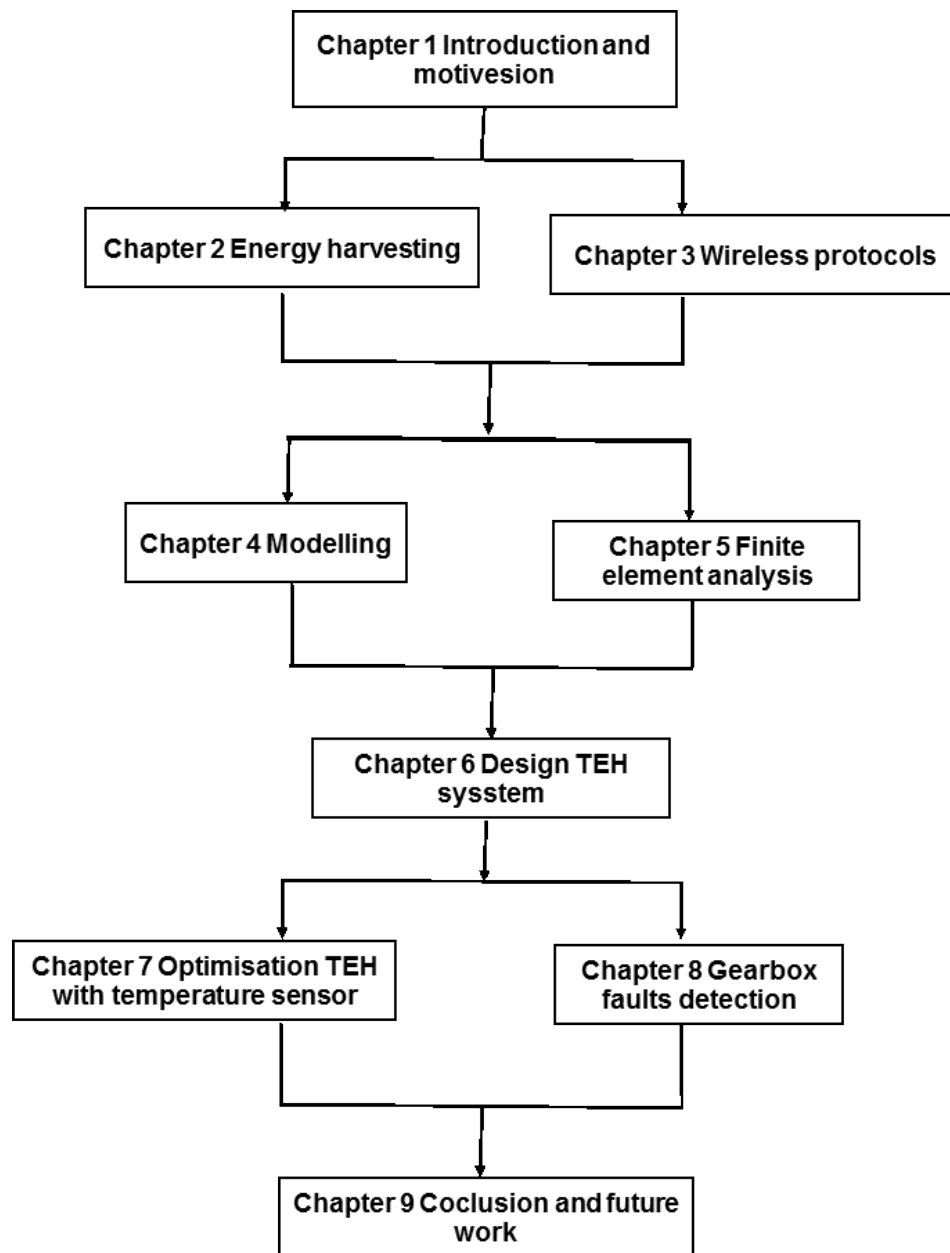


Figure 1-1 Structure of the thesis

The main thesis structure of the thesis is outlined in Figure 1-1. In this section, a brief introduction is given to outline the contents and lay emphasis on of the following chapters:

Chapter One:

This chapter introduced the background to the thesis. It started with a general review of maintenance strategies and the improvement obtainable using WSNs. Common CM techniques were explained. Then, the motivation for the research was presented. Finally, the Aims and Objectives of the research were listed, and an outline of thesis are given.

Chapter Two

Literature survey: this chapter details the literature relating to thermal energy harvesting that is relevant to this PhD thesis. It serves as an introduction to thermal energy harvesting and is intended to provide background information regarding thermoelectric devices and its applications. Then, the physical phenomena of thermoelectricity are explained. Then, thermal and electrical conductivities and energy storage are described. This is followed by thermoelectric generation, its materials and thermometric trade-off. Finally, TE modules are presented.

Chapter Three

The key features for the most common wireless techniques and their applications in CM have been reviewed in this chapter. Then, relative comparisons for the specific purpose for machinery monitoring is made, after which Bluetooth Low Energy and its application are presented. The sensor Tag CC2650STK is presented. Finally, challenges and problems of WSNs and their solutions are discussed.

Chapter Four

Theory analysis – this chapter shows how the theoretical module was developed.

Chapter Five

FE Module - this chapter details how the EF module works.

Chapter Six

This chapter focuses on the experimental investigation of thermal energy harvesting. It describes the thermoelectric generator (TEG) design and how it can be used in evaluating the thermal energy harvesting performance.

Chapter Seven

A thermal system for energy harvesting is designed in powering a wireless sensor node that will monitor the temperature of the gearbox has been presented in this chapter. The system is designed based on the previous chapter. Then, to improve the thermal energy harvesting system efficiency as a new test rig has therefore been developing

Chapter Eight

In this chapter, a wireless temperature node has been applied to detect and diagnose different faults on a gearbox transmission system under different conditions. In which, the wireless temperature node was supplied using a wired power sources without needing for charging problems.

Chapter Nine

Conclusions and achievement overviews for this research concerning the aim and objectives have been presented. The description of the knowledge contribution made in this research, and future work recommendation have also been presented.

Chapter 2. Literatures Review: Energy Harvesting Techniques

Energy harvesting has gained huge advancements in the past few years and a variety of unused ambient energy sources such as solar, thermal, vibration and wind, are converted the harvested energy into electrical energy to recharge the batteries. These kinds of technologies bring great benefits to our routine work and the industrial fields.

Temperature gradients commonly come in numerous household or industrial settings. It is estimated that temperature gradients inherent in the local environment can provide power for sustainable wireless sensor node operation.

This chapter firstly reviews energy harvesting technologies and energy harvesting systems. It also provides a review of existing work in energy harvesting. Finally, thermal energy harvesting is discussed to provide background information regarding thermoelectric devices, thermoelectric materials and a thermoelectric module.

2.1 Introduction

In recent years, there has been a rapid increase in research in the field of energy harvesting (EH). EH is commonly defined as the conversion of ambient energy into electrical energy. It is also called energy scavenging or power harvesting, and is a process by which energy can be obtained from the environment. EH is not new, but a current challenge is how to integrate efficient EH into a modern embedded system such as a WSN, while satisfying the constraints imposed in terms of both the system itself and application environment[38].

2.2 Energy Harvesting Technologies

EH consists of many techniques that capture or harvest a variation of under-used or unused sources of ambient energy such as sunlight, vibration, and radio frequency waves and convert them directly to electrical energy [39]. Energy harvesting provides a very small amount of power and that makes them suitable for powering low energy electronics[40]. Different sources of ambient energy and energy harvesters are illustrated in Figure 2-1. (Wan et al., 2010)

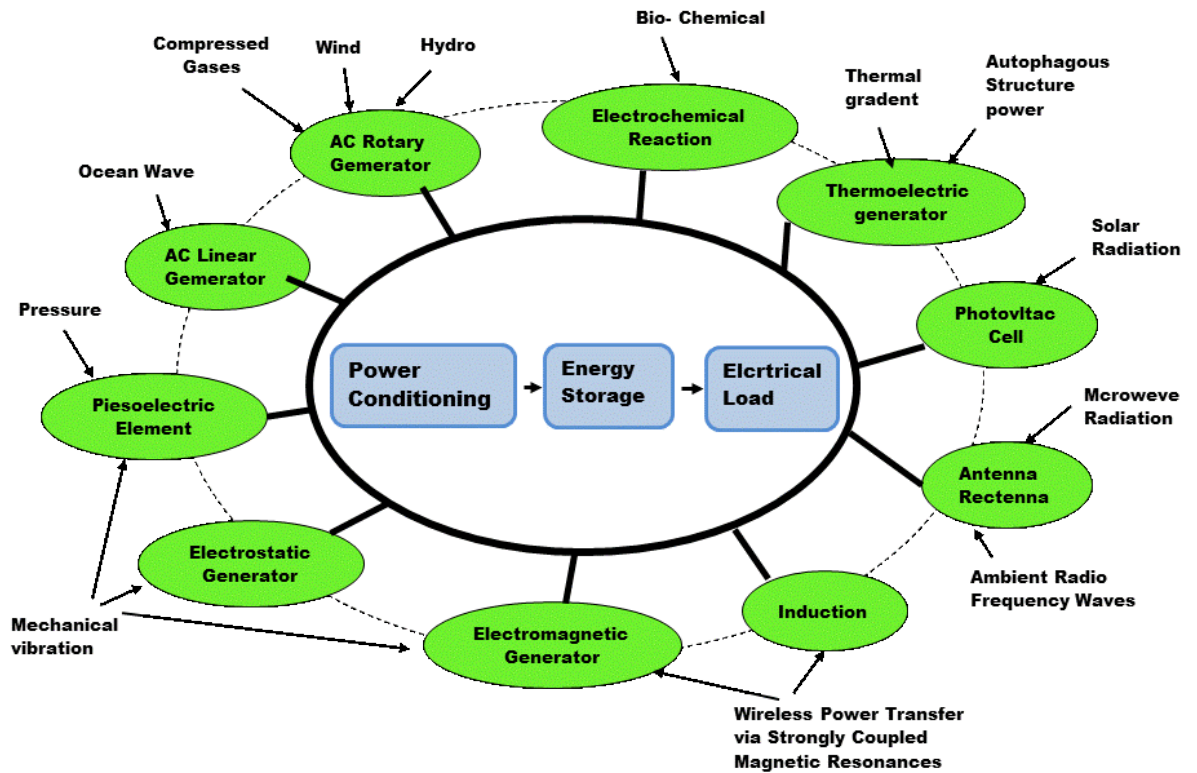


Figure 2-1 Source of energy harvesting source and EH devices [41]

Figure 2-1, shows various sunused and waste ambient energies that can be harvested from the environment. These sources already exist and would be suitable for powering WSNs. Recently, many researchers have investigated the quantity and availability of these energy sources in the environment [41]. Table 2-1 illustrates EH sources performance compilation and their energy density factors[42]. Based on the table, it can be seen that solar power yields the highest energy density in an outdoor environment and, under certain circumstances, can achieve a higher energy density than normal batteries. Solar energy (SE) may be sufficient during the day but it is not available at night. Thus, the energy harvested depends heavily on the specific location and time of day. Obviously, when the solar cells are illuminated using typical indoor light sources the ambient light energy density drops substantially.

Table 2-1 Energy Harvesting opportunities and demonstrated capabilities [42]

Source of energy	Performance	Notes
Ambient light	100 mW/cm ² (direct sunlight) 100μW/cm ² (illuminated office)	Common polycrystalline solar cells are 10%-17% efficient, Standard mono-crystalline cells can reach 20%.
Thermal	a) 60μW/cm ² at 5K gradient b) 135μW/cm ² at 10K gradient	Typical efficiency of thermoelectric generators are ≤ 1% for ΔT < 313K a)
Pressure of Blood	0.93 W at 100 mmHg	When coupled a with piezoelectric generator, the power that can be generated is in the order of μW
Vibration	4μW/ cm ³ (Human, motion-HZ) 800μW/ cm ³ (Machine-kHz)	Predictions for 1cm ³ generators, Highly dependent on excitation (power tends to be proportional to the driving frequency and the input displacement.)
Hand linear generator	2mW/cm ³	Shake-drive flashlight of 3Hz
Push Button	50μJ	Quoted at 3V DC for the MIT Media Lab Device
Heel Strike	118J/cm ³	Per walking step on piezoelectric insole
Ambient wind	1mW/cm ²	Typical average ambient wind speed of 3m/s
Ambient radio frequency	<1uW/cm ²	Unless near a RF transmitter
Wireless energy transfer	< 14mW/cm ²	Separation distance of 2 meters

2.3 Energy Harvesting System

An EH system consists generally of four principal components: mechanism for energy collection and conversion, condition circuit/ electrical power management, device for energy storage and electrical load (e.g. WSN)[43]. Each component can be constructed in numerous ways, according to the needs of the device and the preferences of the designer. Figure 2-2 illustrates an energy harvesting system general block diagram.

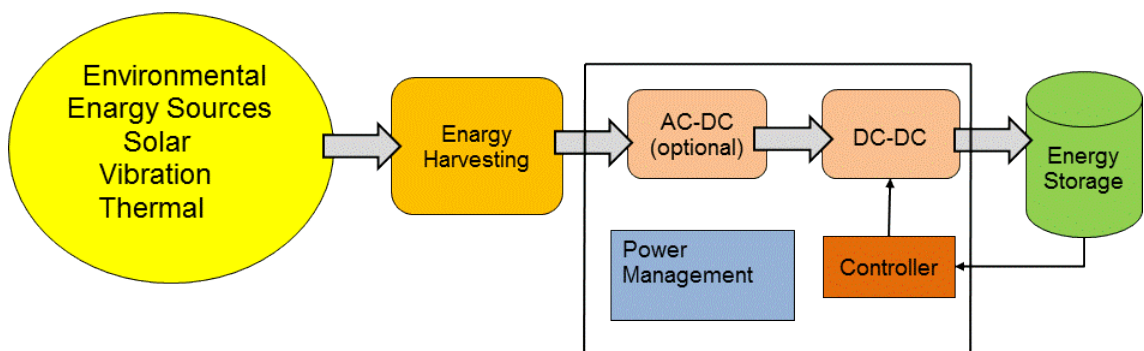


Figure 2-2 General block diagram of EH system

In Figure 2-2, it can be seen that the function of EH is to harvest environmentally available power and convert that into useful electrical energy. Energy harvesters general examples is shown in Figure 2-1 which include solar cells for collecting solar energy, TEG (thermoelectric generator) in harvesting thermal energy, piezoelectric material in converting to electric power from vibration energy, and the antenna arrays in capturing from ambient, radio frequency energy.

The efficiency of the performance is highly significant for a small EH system, and the electric power being generated needs to be appropriately conditioned for the device to be powered, for maximum system efficiency. Power conditioning circuit main objective shown in Figure 2-2 is to process and control the electrical energy flow to the load from the source in a manner that the energy is efficiently used. Another key advantage of power conditioning circuit is to convert and regulate the levels of electrical voltage into suitable levels for the load [44]. In ensuring continuous operation of the load even when the external source of energy is temporarily unavailable or weak, any excess harvested power should be stored either in super-capacitor or in a rechargeable battery as shown in Figure 2-2. The stored energy in the super capacitor is used in charging the battery and to supply power to the sensor nodes. Depending on the local environmental conditions, the power requirements of the load and the specifics of the EH system (i.e. WNS and its control circuitry) will vary, and the design of each individual power harvesting system will be such as to optimise and maintain the operation of WSN.

2.4 Condition Monitoring Techniques

CM techniques will according to the machines or processes being monitored, and the objectives of the maintenance programme. The most commonly used machine and process CM methods are discussion in [3, 7, 45, 46] and are presented in the following a brief summary.

A. Visual Inspection

This technique can sometimes provide a direct indication of machine condition without the need for further analysis. The tools used in visual inspection range from a simple magnifying glass to stroboscopes or low power microscopes.

Visual inspection can be sometimes offer an immediate detection of machine faults without the necessity for additional analysis[47, 48]. It is a very cost-effective method as it costs very little compared with more formal systems based on the use of sensors and monitoring equipment.

Visual inspection is commonly useful in detecting leakage, cracks and corrosion. In addition, it provides a flexible and immediate assessment of machine condition. The problem of different conclusions being drawn by different inspectors for the same machine is because of individual nature of their personal skills and experiences. However, the biggest problem with this technique that the monitoring and information obtained may not be received in sufficient time to take remedial action before a fault develops[48].

This simple technique can be extended to include the use of other human senses such as hearing, touch and smell.

B. Acoustic Emission Monitoring

In recent years, Acoustic Emission (AE) monitoring has been successfully used in many CM applications with industrial machines for detecting leakage, fatigue cracks, damage in ball and roller bearings, etc.

AE describes the elastic, transient waves, within as approximate range of frequency form 100 kHz to 1 MHz that occurs due to changes in the materials microstructure. Sources of AE can occur because of the stress material mechanical deformation, include dislocations creation and movement, crack growth, slip (sliding metals in frictional contact) and mechanical impacts[49, 50].

The AE propagation advantage is that, given a sufficient energy source, external remote material behaviour investigation is possible. This advantage is

quite significant when the interested area is at a location that is inaccessible or an area that prohibits using other monitoring techniques[50].

The mechanisms source that produces AE are largely also responsible for audible air-borne acoustic and vibration waves. All of these can be regarded as CM techniques that are non-intrusive, although it is clear in some regards that AE has advantages over the other two techniques.

C. Temperature Monitoring

Temperature monitoring is extremely well-known and one of the most common monitoring techniques used with industrial machines, both mechanical and electrical machinery. It provides useful monitoring information about the condition of the components in the machines. The most commonly used instruments for temperature measurement of gearbox are thermocouples and resistance thermometers[51]. In addition, this technique has been proved to be exceptionally useful especially where it is difficult to employ conventional surveillance equipment, or in hazardous atmospheres.

D. Performance Monitoring

A machine or process is designed to perform certain functions. With the performance monitoring technique, the main aim is to confirm that it performs its required function (whether converting energy from one form to another or producing quality products) at the required rate with the necessary efficiency. The condition of a machine or a component can be indicated by data or information obtained from performance monitoring [52]. E.g., tool wear may result in product dimension increase and by checking the quality of the product quality, the extent at which the tool has worn out can be assessed. It is a steady state monitoring technique and its problem is that its feedback information may

not be provided on time or well enough in advance of a fault occurring. It can also require highly accurate transducers in order to determine useful outputs[3].

E. Vibration Monitoring

All rotating and reciprocating components such as electric motors produce a wide range of vibration frequencies. Even two outwardly identical machines will have different signatures due to small dimensional and assembly differences. With vibration monitoring a sensor picks up the vibration signals generated by a machine, and these are analysed to determine the condition of the machine [51]. There are many reasons for the wide use of vibration monitoring, possibly the most important is that almost every machine or process will produce vibration in one form or another while in operation. Another reason is the vibration mechanisms of most machinery and structures are theoretically understood, making it possible to predict the characteristics of vibration responses due to specific faults. This is due to its established ability in detecting the existence of early faults [48,53].

However, vibration monitoring is not appropriate for all CM purposes as it provides vibration related information and certain types of faults, such as wear, may not produce significant change in vibration levels. Nevertheless, vibration CM is the predominantly used and most cost-effective technique [18].

2.5 Review of the Existing Work on Energy Harvesting System

There are numerous research works and experimental investigation recorded in the literature on harvesting environmental energy source for powering WSNs.

2.5.1 Solar Energy (SE)

Solar energy is one of the most common source of energy harvested from the environment. Solar cells which is an energy harvester, where the photovoltaic effect is used in converting directly to electric power from solar radiation [55]. Normally, the voltage being generated for a solar cell depends on the material of the cell and the level of the input solar radiation [56]. However, the current being generated for a solar cell is proportional roughly to the solar cell area. From a single solar cell, the current and voltage is not big enough in meeting the sensors nodes energy requirement, so several solar cells in parallel or series are combined in a solar panel of array in providing a suitable current and voltage [57].

According to some researchers the solar energy density outdoors at midday is about 100 mW/cm^2 , per centimetre square indicating that in a 1 cm^2 , electrical power of 100 mW from the sun can be harvested by the use of the solar panel. Conversely, based on (Randall) the light energy density in indoor environments is almost $100 \mu\text{W/cm}^2$ [58]. Amorphous silicon solar cells and thin film polycrystalline are normally used commercially due to their relatively low cost and also low efficiency of between 10 to 13% [58].

Recently, various applications of solar EH have claimed a better performance and greater energy conversion. Permethus [59], Helimote [59], Everlast [60], and Ambimax [61] are different prototypes of solar harvesting sensor nodes, see Figure 2-3.

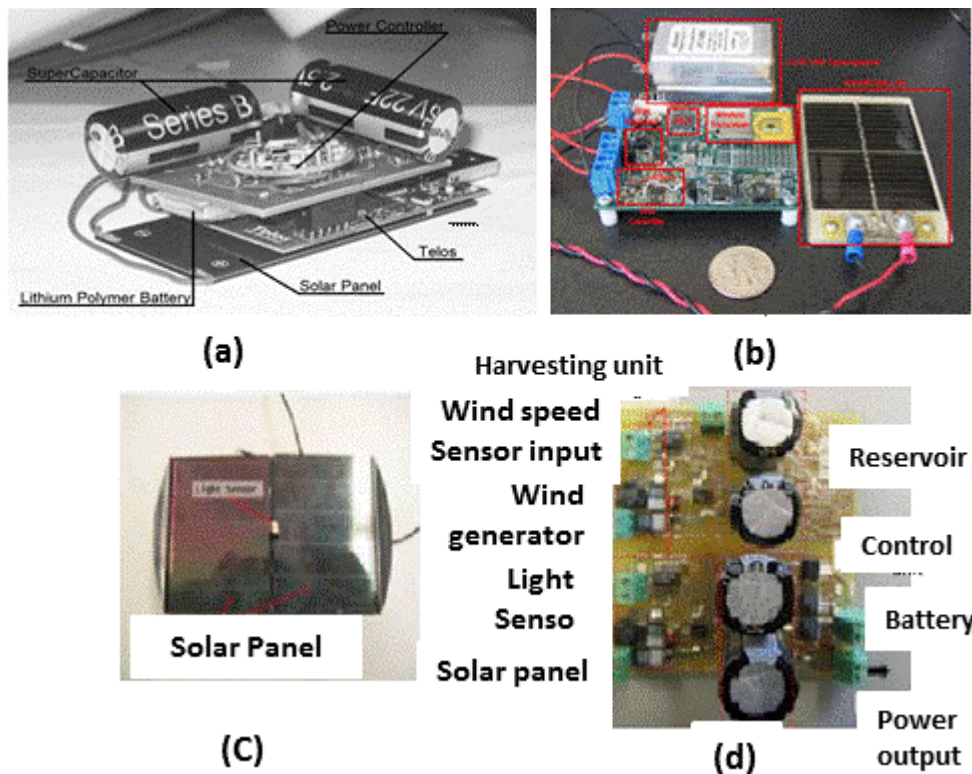


Figure 2-3 (a) Prometheus sensor node, (b) Everlast prototype system, (c) Ambimax solar panel with light sensor, (d) AmbiMax board with super-capacitor [59, 61]

Prometheus and Heliomote are prototypes EH systems where connection between the storage device and solar panels takes place. A Prometheus photo is shown in Figure 2-3(a). In this design, there is direct connection between the solar panel and a super-capacitor. This means that this prototype has been specially designed for super-capacitor with low voltage as much less power is generated by the solar panel than P_{MPP} (maximum power).

Everlast is another prototype of solar panels, which is a super-capacitor operating platform for energy harvesting (see Figure 2-3(b)). That is, it is a combined system with sensors, radio, energy harvesting subsystem and low power MCU. This type of technique is simple, easy to design and cheap to

construct. The addition, the components of EH systems are: solar cells, a 100F super-capacitor, PFM regular and Pules Frequency Modulated (PFM) controller.

There is another an autonomous energy harvesting called Ambimax, which is for multi-supply wireless sensor nodes. The Ambimax not only convert solar energy but also can be harvested even wind energy (see Figure 2-3 (d)). Each source of power has its individual harvesting system charging a super-capacitor. The super-capacitor energy stored is used in charging the battery and supplying power to the sensor node.

2.5.2 Vibration Energy (VE)

Vibration energy is another example of general source of energy that, from the environment, can be harvested. Indeed, EH of mechanical vibration is considered to a very effective way of converting environment energy directly into electricity [62]. As an environmental energy source vibratory motion is generally available and easily accessible, and regularly used to power portable or wireless devices. Examples of vibrations that can be used are those occurring in buildings, transport, human activities and industry. Numerous research studies on EH of vibration energy have been carried out which show that the density of power from vibration that can be harvested is almost $300 \mu\text{W}/\text{cm}^3$ [63]. Any device that can harvest into electricity, mechanical motion can be categorized as piezoelectric, electromagnetic and electrostatic [64, 65]. A coil oscillates, in electromagnetic transformers, in a magnetic field that is static and induces across the coil a voltage. Piezoelectric transformers exploit the characteristic of certain materials such as ceramics or crystals in generating an electric voltage due to an applied mechanical force [66]. In the case of

electrostatic transformers, electric charge on changing capacitor plates generates a voltage.

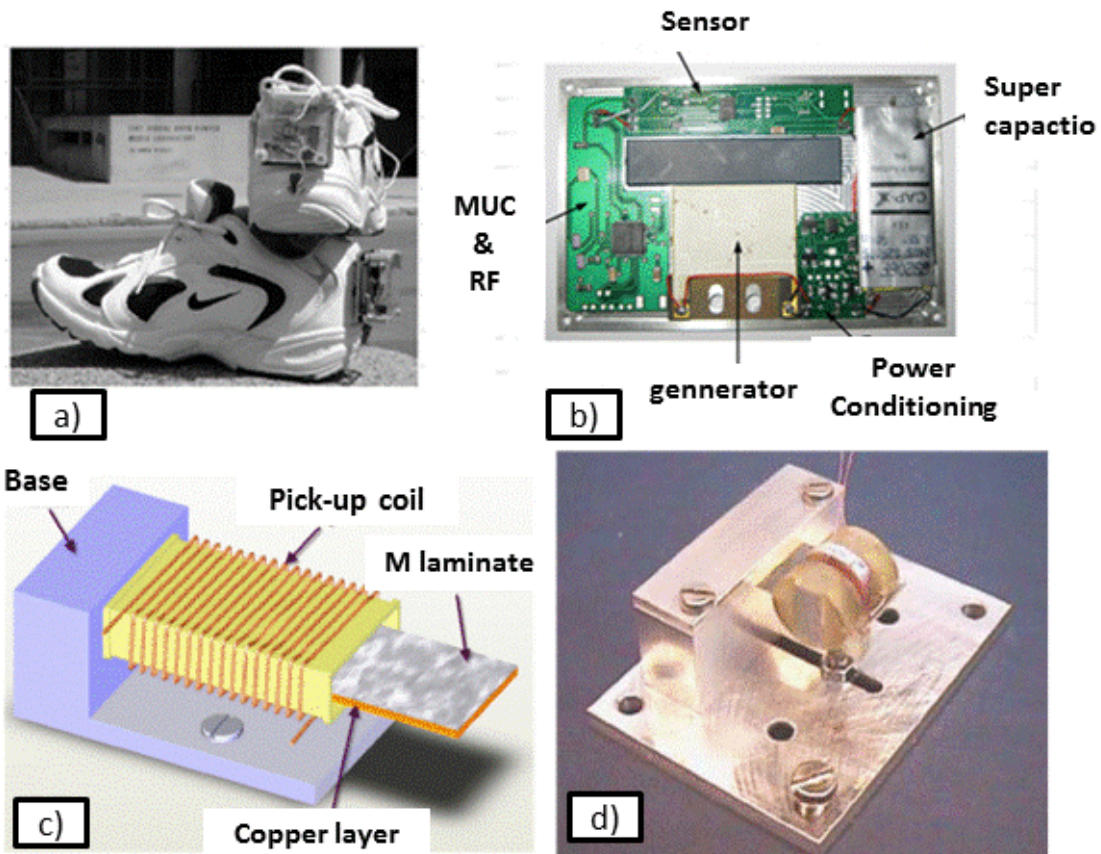


Figure 2-4 (a) Piezoelectric power RFID shoes with mounted electronics, (b) Vibration power wireless sensor node, (c) electromagnetic vibration-based micro-generator device, (d) Electrostatic transformer [66, 67]

Shenck et al., [66] presented a piezoelectric powered RFID (Radio Frequency Identification) system as shown in Figure 2-4(a). This used a specially designed shoe to convert energy from human movement under normal working conditions, to generate about 10 mW of power. From human activities, the mechanical energy is a promising source of renewable energy.

Roundy and Wright have made a similar proposed using piezoelectric generators as shown Figure 2-4(b) as a smart way in powering wireless sensors [68]. Other EH researcher that are vibration-based has included electronic

textiles that are wearable [69], and electromagnetic micro-generator devices that are also vibration based to power sensor systems that are intelligent [70].

Meninger et al., developed an electromagnetic converter from vibration to electricity that produces electrical power of $2.5 \mu\text{W}$ per cm^3 [71]. Similar research by Mitcheson, et al., has indicated that up to $4 \mu\text{W}/\text{cm}^3$ can be achieved from vibration microgenerators (of order 1 cm^3 in volume) with typical human motion (5 mm motion at 1 Hz), and up to $800 \mu\text{W}/\text{cm}^3$ from machine induced stimuli (2 nm motion at 2.5 kHz) [72]. However, at present, there is inadequate management circuits with ultra-low power in conditioning this generation of micro-power.

Magnetostrictive materials (MsM) are a class of compounds that change their shape or dimension when they are subjected to a magnetic field. The mechanism of magnetostriction can be seen Figure 2-4(c). The principle of vibration EH is mainly based on the Villari effect[67]. Wang and Yuan [73] were amongst the first to propose the feasibility of using amorphous metallic (Metaglas 2605SC) glass as a MsM suitable for harvesting power from mechanical vibration.

2.5.3 Thermal Energy (TE)

Thermal EH is the process of converting thermal energy to electrical energy by using a TEG, such as a thermocouple. There are various well-known methods for converting thermal energy directly into electrical power such as the Seebeck and the piezo-thermal effects, and others are currently under investigation [74]. Basically, electric current is generated by heat flow through a thermoelectric (TE) material[76]. The output power of a TEG depends on its area and the

temperature difference from one side of the element to the other. However, TEGs can be used for powering CM WSNs in domestic and industrial environments, and many papers have been presented on the TEG in the past decade[75-77].

Previous research studies for thermal energy harvesting have demonstrated that TEGs that Seebeck effect based are popular devices for converting thermal energy to electrical power [78]. The electrical power produced is proportional to the temperature difference between the hot and cold side junctions. Hudek and Amatucci have presented a summary of the performance of TE modules performance summary, capable of generating from between 1-60 $\mu\text{W}/\text{cm}^2$ for temperature difference at 5K or less [74]. Watkins, et al., achieved the highest power density with a module that can produce 6.1mW/ cm^2 at 2.7K temperature difference, but 0.25 V/ cm^2 of open circuit voltage [79].

2.5.3.1 Thermoelectric Generator

Thermoelectric generators (TEGs) are solid state devices which means that they have no moving parts, produce no noise and involve no harmful agents. TEGs are the most widely adopted devices for waste heat recovery. The ability to generate electrical power from a temperature difference across a material is due to the Seebeck effect [80]. The Seebeck effect was first discovered by Johann Seebeck in 1821, who found that when the two junctions are at different temperatures, a low voltage is generated. The Seebeck's effect can be observed in a thermocouple made of two dissimilar conductors. Figure 2-5 shows a schematic for a thermoelectric. In addition, Seebeck effect based TEG (Thermoelectric generator) is one device that is quite popular being used in harvesting thermal gradient energy.

In 2000, Simon [81] reviewed the devices have long been used in cooling application for electronic devices, and in 2005, Luo[82] illustrated that the prototype thermoelectric can save more than 38% of the power consumption compared with that of conventional electric water heaters. It is of great practical interest in building energy saving, supplying hot water for carriages, ships and other analogous movable spaces. In 2013, Siviter et al [83] suggested the large-scale application of thermoelectric heat pumps to improve the efficiency of power plants based on the Rankine cycle. When used in electrical power generating mode, TE devices are usually referred to as TEGs. Rowe [84] provides an overview of earlier applications and assesses the potential of TE power generation as an alternative source of electrical power.

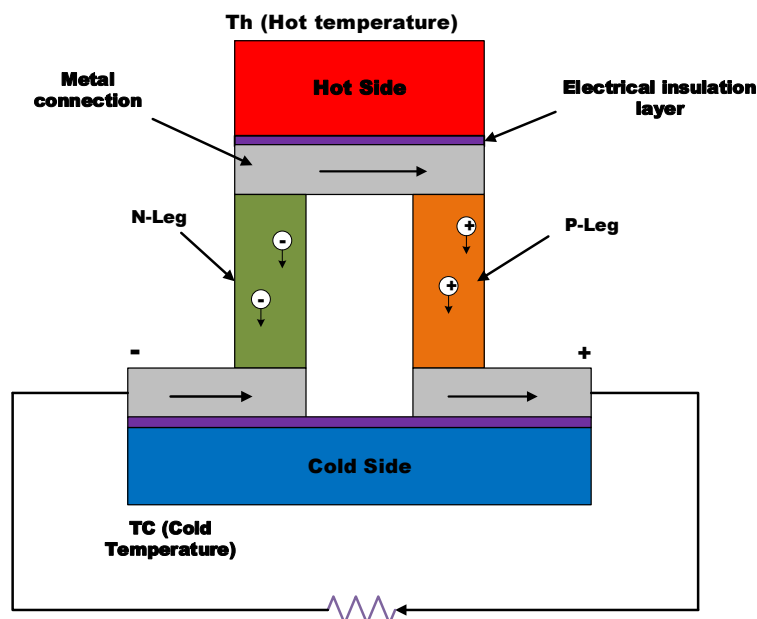


Figure 2-5 Basic configuration for a thermoelectric device

2.5.3.2 Seebeck Effect

In general, when two dissimilar conductors, A and B constitute a circuit, a current will flow as long as the junctions of the two conductors are at different

temperature. Conductors A is defined as being positive with respect to conductor B if the electrons from A to B at the colder junction as shown in Figure 2-6.

The TEG module V_G (open circuit voltage) can be calculated from the temperature difference ΔT between hot side (T_h) and cold side (T_c):

$$V_G = N\alpha_{ab}\beta\Delta T \quad (2-1)$$

Where N denotes the number of thermocouples used, α_{ab} is the thermocouple materials seebeck coefficient and β thermal coefficient, and α_{ab} is the Seebeck coefficient of thermocouple materials. It can be seen that with the increase of the number of thermocouple in the TEG module, the open circuit voltage will be larger.

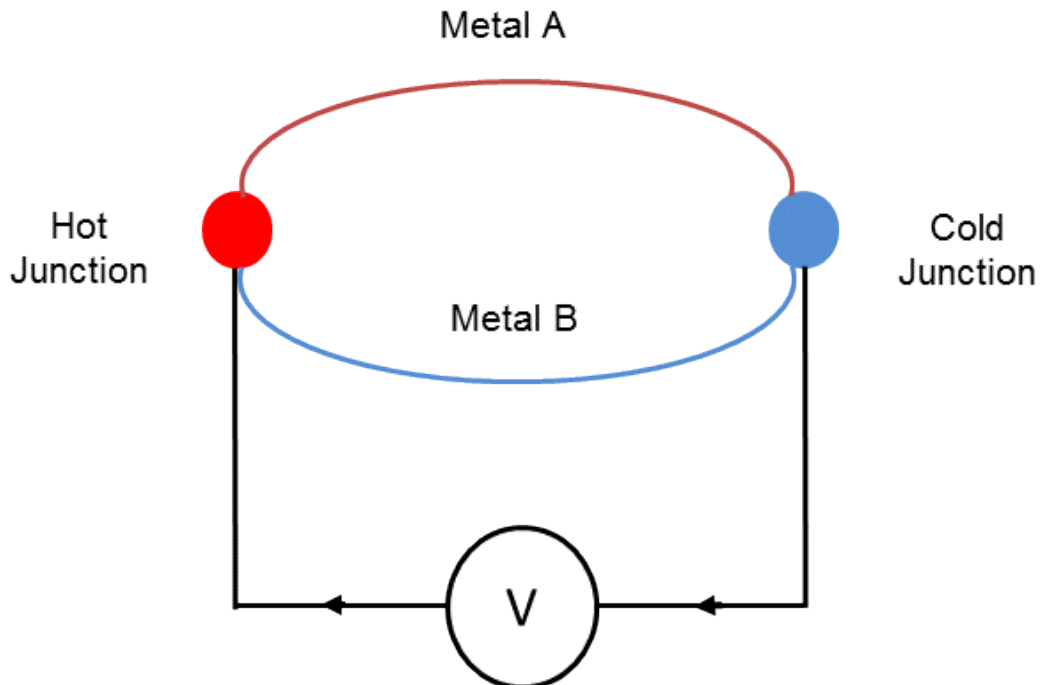


Figure 2-6 The Seebeck effect

TE devices are often comprised of a number of semiconductor elements of both N-type and P-type which are connected electrically in series and thermally in parallel as shown in Figure 2-7. When heat flows through the cell the N-type components are loaded negatively (excess of electrons) and P-type components are loaded positively (deficit electron). If the thermal gradient is such that the heat is flowing from the “top” to the “bottom” of the TE device (see Figure 2-7), a voltage will be produced and an electric current will flow. The voltage from each element is added such that a device comprising many such elements produces a usable voltage. Each p- and n- pair is referred to as a thermocouple.

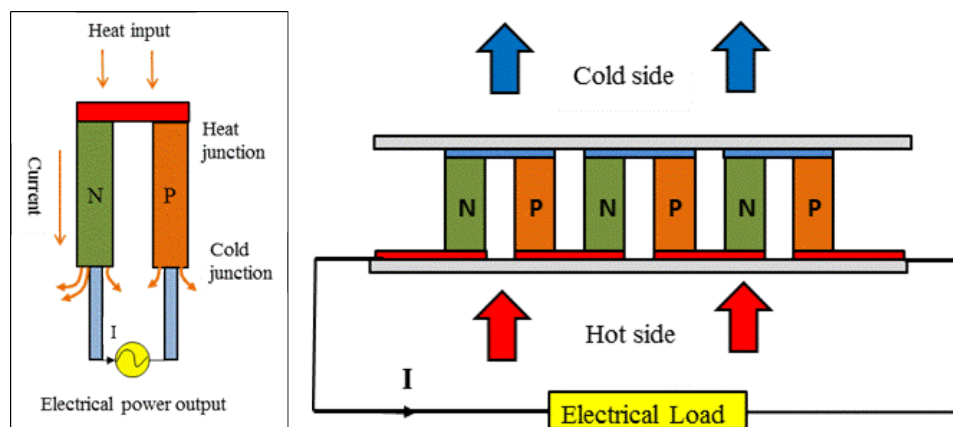


Figure 2-7 Thermal to electric conversion with thermoelectric

2.5.3.3 Thermoelectric Materials

High coefficient of Seebeck, high electric conductivity and low thermal conductivity are characteristics of a good TE material. When a TE material are used for designing, there is usually a trade-off regarding keeping the thermal conductivity low and the electric conductivity high [85]. This is because the transportation of both the heat and electric current is the responsibility of the electrons. Lattice vibrations, called phonons, can also transport heat and the

reduction of this contribution to the conductivity of heat when new materials are being developed is of significant importance.

Materials such as glass, due to the way their material lattice is being organized, have a low thermal conductivity [86]. Though glass does not allow electrons to flow, it makes them poor TE material. Crystalline materials are good TE materials as they scatter their phonons without the disruption of their electrical conductivity. Crystalline semiconductors are known today as the best TE materials, as more researchers and scientists are working hard to develop and improve their properties as seen in [87-89] for example.

The most commonly TE material used is the Bismuth telluride (Bi_2Te_3) which was first suggested in 1945 as a TE material [90]. Its properties depends strongly on the crystal size, carrier concentration and crystal orientation. Hence, making the properties of the material different for Bi_2Te_3 that is supplied by various manufacturers [73].

2.5.3.4 Thermoelectric Module

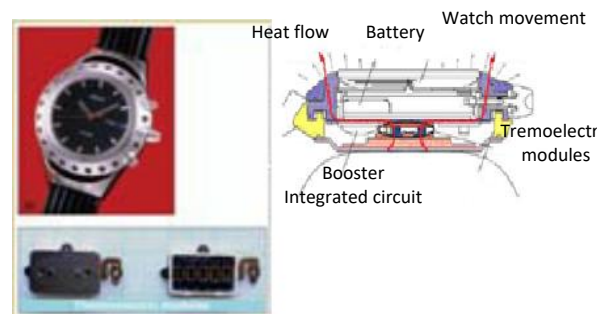
The TE pellets in a TE module are connected electrically in series with a small metal plate. Such connectors are typically made from aluminium or copper for good thermal and electric conductance [91]. The connectors are mounted on a ceramic material sheet on the cold side which is both a good electric insulator and thermal conductor. Aluminium oxide (Al_2O_3) is a common material used as they are cheap, retains the right thermal conductor and are stiff. On the cold side, the thermoelectric pellets are mounted on the metal connectors, and then connected together on the hot side using additional metal connectors. The entire package is then covered using another ceramic material layer.

2.5.3.5 Typical Thermal Energy Harvesting Systems

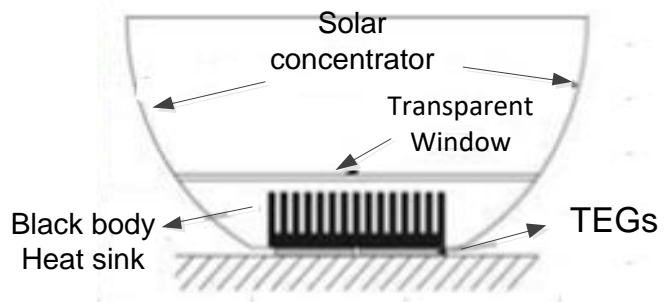
In the literature, several thermal EH applications have been proposed. One example of thermal EH is the Seiko Thermic watch, as illustrated in Figure 8-2Figure 2-8(a). A TEG is used in harvesting heat from the body and converting it into electrical energy in order to drive the watch. The thermal EH system consists of a series TE module, DC-DC voltage booster and a lithium-ion battery. A difference in temperature of about 1Kelvin, between the room temperature environment and the wrist, can be converted to $22 \mu\text{W}$ [74].



(b)



(a)



(c)

Figure 2-8 Examples of thermal energy harvesting applications[92]

Leonov et al., have been considered similarly work, which they designed the thermal energy harvesting system using TE power generator to convert body heat into electrical power, see in Figure 2-8(b)[92]. The voltage output of the TEG module is usually very small hence, a DC-DC booster is usually added in boosting the voltage being harvested and then store the power into a

rechargeable signal of 1.2V NiMH battery. The average rate at which power was harvested by the thermal EH system during the day was almost $250\mu\text{W}$ corresponding to about $20\mu\text{W}/\text{cm}^2$ with 10 kelvin temperature difference, which in an improvement from the solar in indoor case.

In another thermal EH system, Sodana et al, presented thermal EH system with solar with a solar generator placed in a greenhouse as shown in Figure 8-2(c). The solar thermal EH system used a TE module between the ground and the heat sink. The converted power was used in recharging a 300mA NIMH battery. At ΔT estimation of 25K, the energy being harvested was able to recharge in 3.3mins, an 80 mAh battery. The authors have explained that TE generator can be used as photovoltaic devices alternative though there are some discussions on how the solar thermal EH power of the management element are designed

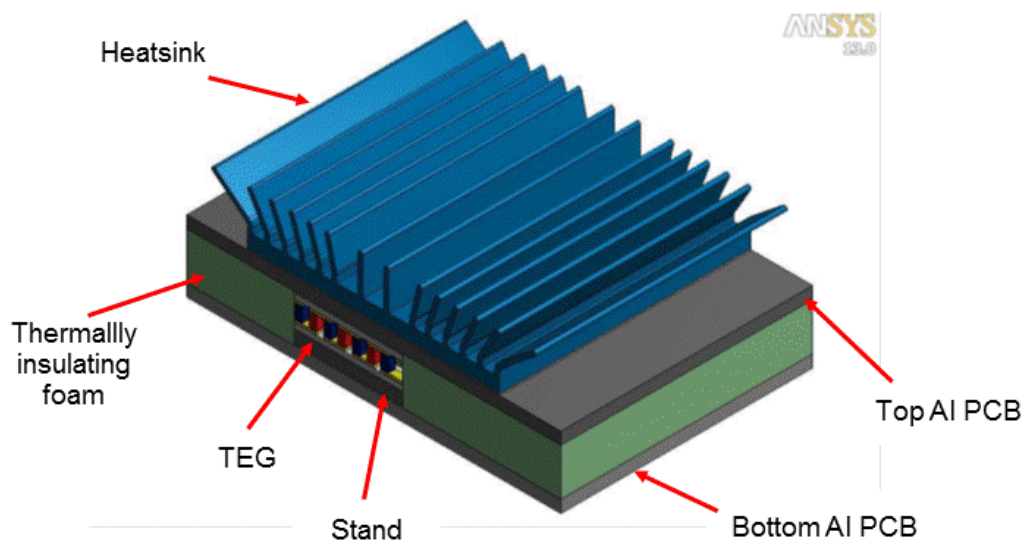


Figure 2-9 Design of self-power telemetric wireless sensor node[93]

In another thermal energy harvesting research, Aneta et al.,[93] developed an energy harvesting system to power WSN, as Figure 2-9 depicts a prototype. A TEG module is used in converting energy between the ambient and a hot chuck

with computer controlled temperature as the source of heat, from temperature difference. The harvested energy is used to charge super-capacitor which is used there is no harvested energy or the harvested energy is not adequate for continuous node operation.

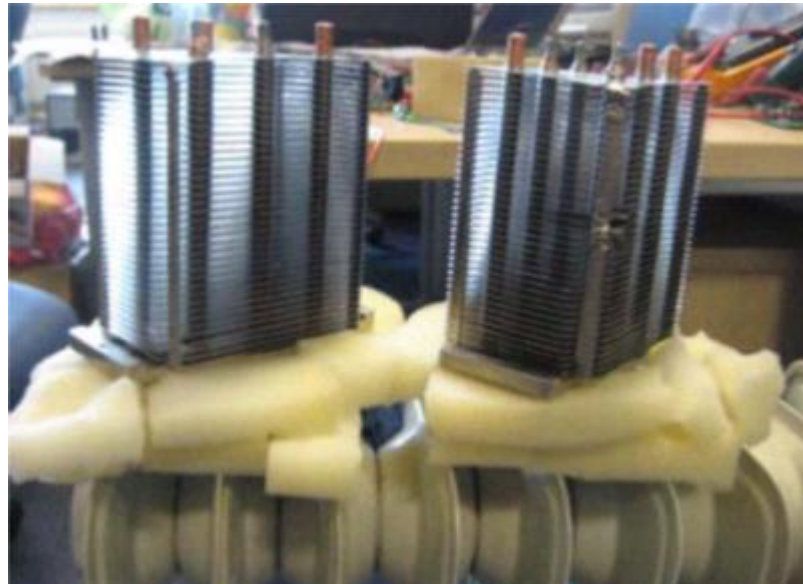


Figure 2-10 Thermal energy harvesting system[94]

Similar work has been done by Xin Lu and Shuang Hua [94]. They designed a thermal energy harvesting system as shown in Figure 2-10, that can harvest heat energy between radiator as heat source and ambient, from a temperature gradient and converting it to electrical energy in powering the ZigBee electronics. The results from the experiment shows that a maximum power of 150mW by the prototype can be harvested, and when the voltage being harvesting is as low as 0.45V, the system can operate normally continuously.

2.6 Key Findings

It is clear that EH technology can enhanced for the performance of a WSN. There are numerous different designs of EH systems using much the

same components (e.g. battery and/or WSN) because each type of energy source will require its own EH system and the systems tend to be very specific to the energy being harvested. Researchers haven't point out that their system structure of their system was most efficient. As each platform is typically designed for a particular sensor node and focused only in harvesting one power source type, cannot expand easily, the systems in harvesting another form of energy and use it for other forms of applications. Similarly, even when the energy source is defined and the EH device selected there will be a range of possible designs depending upon the electronic and/or mechanical components chosen. In addition, there is no clear procedure for EH design that have been introduced to guide the researcher in the literature, a new system for energy harvesting. The researcher follows a procedure of trial and error in improving a new system of energy harvesting, with this procedure being considered as inefficient. Therefore, if there a procedure for a simple and efficient design that can be followed, the design progress for harvesting energy can be simplified and the time for improvement can be shortened.

There are two concerns are noted when energy is converted from ambient heat flow, especially for small scale of thermal EH systems. The first one is that the ambient temperature difference small value produces a very low voltage output that can recharge a battery or to power a device or that can even power a boost harvester. Therefore, finding a means in increasing the temperature difference or at least, maintain a large thermal EH designs temperature difference is very significant. Hence, consideration should be given to increase the heat transfer in thermal EH systems. Secondly, the fluctuation of the ambient temperature

may produce fluctuations of the output of voltage of the TEG. Thus, a boost converter and a heat sink are both components that are vital in the thermal EH.

The essential target in this research thesis is designing and implementing a self-sustaining and self-powering micro-system for energy harvesting in order to power sensor node that are wireless.

Chapter 3. Investigation of Wireless Sensor Networks for Condition Monitoring

In the last few years, Wireless Sensor Networks have seen numerous improvements, with new wireless protocols, such as Bluetooth Low Energy, Wi-Fi, and ZigBee developed for different types of applications. These techniques can be of significant benefit both to our daily personal lives and to commerce and industry.

This chapter reviews the main features of the most popular wireless transmission techniques and typical applications in the condition monitoring. Then, they are compared the specific purpose for machine condition monitoring. In addition, a review of wireless sensor networks used for condition monitoring is presented. Finally, challenges and problems for employing wireless techniques for condition monitoring are discussed.

3.1 Introduction to Wireless Sensor Networks

The use of WSNs is a field of growing interest and has developed substantially in recent years. The WSN typically consists of a number of individual sensor nodes that are able to collect information by measuring locally varying parameters such as temperature, vibration, humidity, sound level, etc. Such uses of WSNs include numerous applications in fields such as Structural Health Monitoring [95-97], environmental monitoring, military applications, industrial condition monitoring, control applications, and .medical diagnostics[98].It has also played an important role in the emerging Internet of Things (IOT)[100].The IOT also is the inter-connection of physical devices, such as industrial machines, using embedded sensors and their associated electronics, software and a connecting network such that the sensors collect and exchange data providing information on and, even, control of a machine or process[101].

3.2 Architecture of WSNs

The WSNs are a major development of wired sensor networks where hard-wire communication cables are no longer required and have much lower installation and maintenance costs. The architecture of the WSN will usually include consideration of the types and positions of the sensor nodes, sink node, public

communication network (internet connection), the task manager and end user [102].

Today there are many small, smart and inexpensive sensor nodes available, designed to collect data and track information useful to the end user[103]. These sensors nodes can communicate with each other wirelessly to cooperate and configure a network, collect data from the local environment and disseminate it. Figure 3-1 shows the architecture of WSN that included the sensor nodes and the transfer of data by nodes close to each other via wireless connection to a sink node. The sink node serves as a gateway and has greater processing ability, it communicates with the task manager node. The connection between the sink and task manager nodes is by public network, internet or satellite.

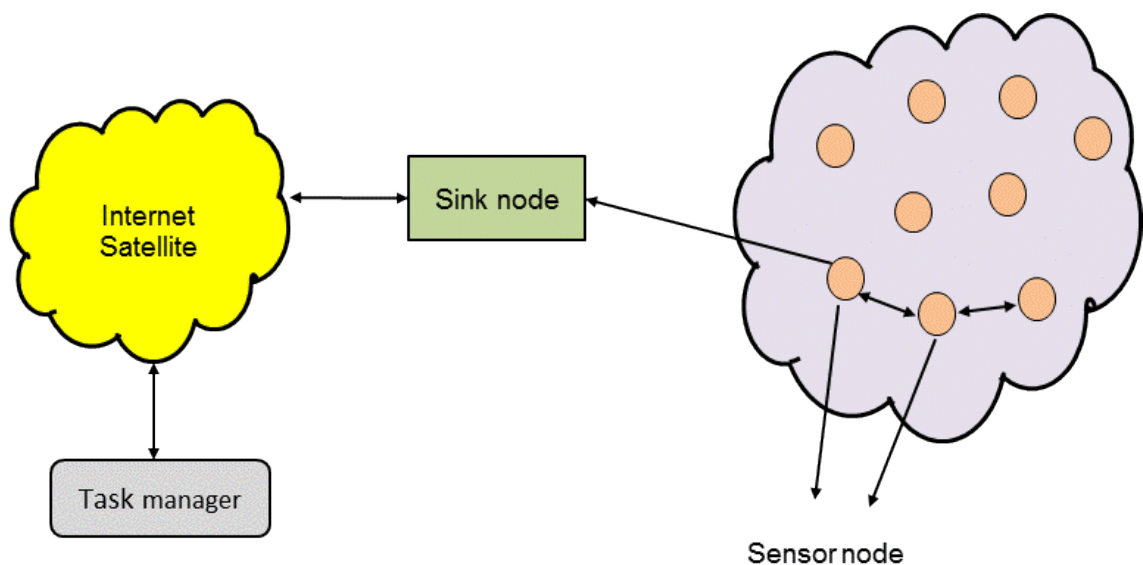


Figure 3-1 Architecture of Wireless Sensor Node[102]

3.3 Wireless Applications for Condition Monitoring

In the past few years, Wireless sensor technologies have made massive progress and many wireless protocols have been developed for numerous

specific applications; these include Bluetooth, Wi-Fi, ZigBee, mobile communication, RFID, etc. Condition based maintenance is one area which has benefits greatly from these developments.

Wireless network techniques will vary according to their application, including signal range, and are usually classified into four groups [104]: wireless personal area network (WPAN), wireless local area network (WLAN), four different categories [104]: They are WLAN (wireless local area network), WPAN (wireless personal area network), WWAN (wireless wide area network) and WMAN (wireless metropolitan area network). In general, cost and the power consumption increases with signal range and bandwidth.

3.3.1 Wireless Personal Area Networks

Wireless personal area networks are generally described as short range and low of power, and is suitable for monitoring industrial machinery within a factory. The advantage of this type of network is the possibility of ad-hoc mode connections. They have been widely and successfully applied, mainly because of such features on low rate, low cost, limited power, and short distance transmission [105].

The most common protocols for wireless personal area networks are IEEE 802 (e.g. Bluetooth), IEEE 802.15.3 and IEEE 802.15.4. In addition, there are also some commonly used short range and low power protocols such as RFID, NFC, IRDA, which are not relevant to the IEEE.

3.3.2 Wireless Wide Area Network

The popular and extremely well-used cellular network is a type of the WWAN. In the last decade, WWAN has developed enormously and gained success in its

applications in the form of trade products. It also provides for users the possibility to create wireless connections over a wide geographic zone with either private or remote public networks. Table 3-1 shows the maximum data speed for several presently available cellular networks [106].

The packet data communications is General Packet Radio Service (GPRS) built on top of the Global System for Mobile Communication (GSM) technology to offer a maximum upload of 40 kbps. Theoretical evaluation of GSM has demonstrated that the maximum possible download could be as high as 384 kbps [107].

Table 3-1 Maximum data speed for cellular network standards [106]

Protocols	Standard	Download	Upload
2.5G	GPRS	114 kbps	20 kbps
2.75G	EDGE	384 kbps	60 kbps
3G	UMTS	384 kbps	64 kbps
	W-CDMA	2 Mbps	153 kbps
	HSPA 3.6	3.6 Mbps	348 kbps
	HSPA 7.2	7.2 Mbps	2 Mbps
Pre-4G	HSPA 14	14 Mbps	5.7 Mbps
	HSPA+	56 Mbps	22 Mbps
	WiMAX	75 Mbps	30 Mbps
4G	WiMAX 2	1 Gbps	500 Mbps

	LTE advanced	1 Gbps	500 Mbps
--	--------------	--------	----------

3.3.3 Wireless Metropolitan Area Network

Recent improvements to wireless metropolitan area networks (WMANs) have provided data rates of hundreds of Mbps over a wide range. WMAN is also the official trademark of the IEEE 802.16 working group on Broadband Wireless Access Standards. The Worldwide Interoperability for Microwave Access (WiMAX) forum promotes conformity of communication using IEEE 802.16 as its base. The purpose of WiMAX is to ensure broadband internet connectivity of WLANs and LANs. The WiMAX technology is often called the technology for the Last Mile Access. The maximum theoretical data transmission rates for WiMAX are 75 Mbps with this number decreasing with increase in distance from the base station [108].

3.3.4 Wireless Local Area Network

Wireless Local Area Network (WLAN) is a wireless network that links one computer to other computers or devices using wireless. IEEE 802.11 is a set of general specification for WLAN, the most popular of which is Wi-Fi[109]. Most modern WLANs are based on these general specifications, and the term Wi-Fi used in general English is a synonym for WLAN. Wi-Fi products which comply with Wi-Fi Alliance interoperability certification testing might use the Wi-Fi CERTIFIED trademark[110]. The transmission speed of WLAN has improved from 11 Mbps to 300 Mbps. Thus, Wi-Fi is fast enough to carry adequate data at a rate suitable for modern CM systems, which is a significant advantage. But its high cost and high power consumption has limited its use in CM. Nevertheless,

Wi-Fi generally is suitable for continuous CM measurement where a suitable power supply is available.

3.4 Review of WSN for Condition Monitoring

Attracted by the potential benefits and opportunities of WSN, many research works have been carried out for condition monitoring purposes and some industrial products have become available on the market. This section reviews work in the condition monitoring area.

3.4.1 Review of research`s works

Peng Guo and Nan Bai[113] used temperature trend analysis to monitor a gearbox`s operating conditions. The Auto-associative Kernel Regression (AAKR) method is used to model the normal behaviour of gearbox temperature and give temperature estimates. The method has the benefit of being computationally remarkably simple and should thus have immediate appeal to wind industry practitioners.

When the gearbox has an incipient failure, the temperature residual between the AAKR model estimate and real measurement will become significant. With moving window residual statistics, these incipient failures can be detected in a timely way. With suitable choice of the parameters available to the user (window size, vector parameter selection, thresholds etc.), the method should show useful for wind turbine condition monitoring more widely.

Xin Xue in 2007, proposed[114] a CM system for induction motors which used WSN for vibration level and temperature measurements. The sensor nodes were from Crossbow Inc., that hosted an Atmel 128LCPU running the Tiny Operation System (TinyOS). The WSNs were placed on the stator and rotor

with the data is being transmitted to a base station that is located 300cm away. The base station is connected to a server computer through a serial port cable. A laptop can be used as a server computer as well. All the data collected is saved in the data base and the signals can be processed by using various signal processing techniques. The results obtained showed that data from wired sensors were more reliable more than data from wireless sensors. The presence of the magnetic field of the induction motor caused losses in the data transmitted by wireless communication between the sensor nodes and the base station. However, this work demonstrated that it was possible to collect data from sensors located in positions wired sensors could not reach. Note that the temperature sensor had a sampling rate set at 10 Hz whereas the acceleration sensor was set at 100 Hz.

In 2013, Amir Shahidi, et al.[115] proposed a single, novel, sensor capable of simultaneously measuring the temperature and vibration signature of a bearing case using inductive coupling.

These researchers measured the bearing temperature in the range from 20 °C to 90 °C for a Timken MMC9112K Deep Groove Ball Bearing at rotational speeds from 1280 rpm to 3250 rpm. The results showed that the single sensor was capable of remotely measuring both temperature and vibration of a bearing case using inductive coupling. The temperature sensor was able to measure the temperature of the bearing up to a maximum of 90 °C for different speeds. The sensor was shown to be able to detect such vibration frequencies as ball spin, and cage and outer race fault frequencies with high accuracy.

In 2012, Gupta et al[116], used a RF temperature sensor for CM of mechanical face seals. The system was validated using a HFSS-ADS EM circuit co-

simulation model. The results showed an excellent match between simulation and the measured values of the resonant frequencies at room temperature. In addition, the measurement trend followed an energy equation with respect to temperature from 25-80°C with temperature uncertainty of less $\pm 5\%$.

In 2013, G. Feng et al [117]. Investigated commonly used wireless protocols and their applications to CM. It was confirmed that IEEE802.15.4 is most suitable for establishing wireless CM systems because of its low power consumption, low cost and its capability of setting up large-scale network. In addition, the result showed that the amount of data communication the wireless network can be reduced by 95% and it supports the performance to monitor the simulated bearing faults.

In 2014, Ricardo et al., [118] they compared different thermal insulating materials that can be used to avoid exceeding the maximum operational condition in wireless temperature measurement system, called "eBiscuit" that due to its size, format and location in the metal rack conveyor belt in the oven, is able to measure the temperature a real biscuit experience while baking. Data acquired by the "eBiscuit" is transmitted using ZigBee technology to a base station where information is stored and processed. The experimental results with real tunnel ovens confirm its good performance, which allows detecting production anomalies early on.

In 2013, Di Peng and Shengpeng Wan [119] proposed a design of remote wireless temperature monitoring systems, places multiple nodes in different areas. Based on ZigBee technology, a remote wireless networking temperature monitoring of a lot of equipment scattered in different locations of factories and companies. The system uses infrared temperature sensor TS118-3 assembly

temperature information. Each node collected measured the temperature of the object information. Then it transfer data to the coordinator node via wireless multi-hop routing. The receiving node uploads the data to a computer by RS232.PC software displays real-time temperature information.

Dasheng Lee [120] developed a wireless and powerless sensor node integrated with a MEMS accelerometer, a signal processor, a communication module, and a magnetic self-powered generator for application of an easily mounted network sensor for monitoring motors.By using induction power that is generated by the motor's shaft rotation, the sensor node is self-sustaining; therefore, no power line is required.The test results show that, the novel sensing node developed in this study can effectively enhance the reliability of the motor monitoring system and it is expected to be a valuable technology, which will be available to the plant for implementation in a reliable motor management program.

3.5 Wireless Protocols

Because of the different applications and area requirements protocols for wireless communication in the WSN have been developed and used which include Bluetooth, Wi-Fi, 6LoWPAN and ZigBee. Protocols have also been developed for special requirements in industries such as ISA100.11a and WirelessHART.

3.5.1 Wi-Fi

Wi-Fi is by definition a technology for wireless local area networks (WLANs) which describes network components based on the IEEE 802.11 Sanders adopted by the Wi-Fi Alliance[108]. Wi-Fi also is a wireless network technology that allows computers and other devices to communicate using a wireless

signal connecting computers together and usually has a restricted signal range; indoor range is approximately 40 meters.

2.4/5 GHz is the frequency band in which Wi-Fi operates. This frequency band is one of the ISM (industrial scientific and medical) frequency bands that is license-free, meaning that additional traffic fees is not incurred. For data transmission to occur, the theoretical data speed rate ranges from various Mbps in IEEE802.11b to around 600 Mbps in IEEE 802.11n. It should be noted that this data rate can be significantly affected by the number of users that coexists on the network and the strength of the signal. An additional, an advantage of Wi-Fi is fast data transmission speed and its use has been explored for remote monitoring systems[121]. However, there is an important issue; long latency and the consumption of power mean that the Wi-Fi is not a good applicant for WSN applications that are battery powered. Moreover, because of wide commercial availability of Wi-Fi, one significant concern is its security during industrial applications.

Recently, Wi-Fi Halow, which is a new Wi-Fi solution for low power, has been introduced based on the IEEE802.11ah specification by the Wi-Fi Alliance in satisfying the necessary requirements for applications in IOT [121].

3.5.2 Bluetooth Low Energy

Bluetooth Low Energy (BLE), is a wireless personal area network technology designed and market by the Bluetooth Special Interest Group (SIG) aimed in novel applications in the security, healthcare, fitness and industrial area [122]. The Bluetooth Special Interest Group (SIG) introduced the Bluetooth Low Energy BLE to attract application developers of emerging IOT. BLE was first

specified in Bluetooth 4.0 [123] and further enhanced in Bluetooth 4.1 [124] and 4.2 [125].

designed at novel applications in the healthcare, security, fitness and industry area

Nevertheless, for Bluetooth to be suitable for many of IOT applications, it must decrease the power consumption [126], so that it can be employed in battery – power devices for a longer period. In fact, as mentioned above, IOT devices have to be connected, but power consumption is usually a real concern. The consumption of power for BLE is lower when compared to Wi-Fi, making it very suitable for wireless applications that are battery powered [127]. In addition, in contrast with the previous Bluetooth, BLE has been designed as a low power solution for control and monitoring applications [128]. BLE also is technology-addressing device with an ultralow power and very low capacity battery. It also allows for a maximum data rate over a 50m distance of up to Mbps in the frequency band of 2.4 GHz. The advent of BLE has occurred while other low-power wireless solution such as ZigBee, 6LoWPAN and Z-Wave have been steadily gaining momentum in application areas that require multi-networking [129], [130].

BLE is application that requires the periodic or episodic small amounts of data transmission. The maximum consumption of power is around 15 mA with an average power consumption only at about 1 μ A. This can be achieved by making the time of transmission only a few ms (mili-second) [131]

3.5.3 ZigBee

ZigBee is a standard protocol for high level, low power devices targeted at building and home automation, industrial control and monitoring, embedded sensing and energy automation system based on IEEE 802.15.4. Zigbee is less expensive and simpler than other presently available WPANs such as Bluetooth or Wi-Fi. The main features of ZigBee are low data rate, network flexibility, very low power consumption and support for various different topologies, which make it suitable for WSNs[132]. However, it is claimed that ZigBee cannot meet, for some industrial applications, all their requirements, e.g., it cannot be used to serve within a specified time cycle, a high number of nodes[133].

3.5.4 6LoWPAN

6LoWPAN is a simple low cost communication network that allows wireless connectivity in applications with limited power. From industrial point of view, the 6LoWPAN benefits are their ability to directly communicate with other IP devices through an IP network (e.g., Ethernet, Internet) or locally. In addition, it can utilise existing system security and architecture, establish application level data models, management tools for service network etc. [134, 135].

3.6 Key Findings

This chapter reports on the several of wireless protocols found that meet the requirements of different CM applications. It has also been reported that each of the technology has both disadvantages and advantages as all the technology can be used for asset Management applications, as no single technology will meet, at this time, all requirements. In particular, the power consumption for

wireless protocols is successfully and rapidly developing with the emerging IOT.

Protocols such as ZigBee, BLE and Wi-Fi increasingly provide good commercial support and are available at cost effective price. All can be utilised for CM where cost is a concern, as strict data reliability is not required.

Chapter 4. Modelling of Thermoelectric Generator

The purpose of this chapter is to provide background information regarding the theory development of the TE module. A fundamental theory understanding of a thermoelectric generator (TEG) will then be developed.

This analysis is based on previous work by Prijic et al., (2015) on voltage generation in a TEG module. In addition, this chapter presents the results of an investigation of the TE generator parameters.

4.1 Introduction

A thermoelectric generator (TEG) is a solid-state device with no moving parts based on a Peltier module capable of converting heat energy directly into electrical energy. Increasingly, the TEG is being used, especially in the electronics industry, to solve problems such as reducing energy costs and to resolve environmental issues [138]. In Chapter 2 is mentioned, the power derived from the device is highly dependent on the siting of the device, the TEG design and the local environment [139]. Generally, the local conditions can be identified using appropriate environmental sensors, or from previous environmental surveys, and the details and parameters of the TEG can be found on the manufacturer's own datasheets.

Modelling EH mathematically is a way considered to be efficient in analysing and characterise the power output of the energy generation of the EH device [140]. Mathematical modelling together with computer simulation can be used to effectively enhance the understanding, and evaluation of the performance, of a TEG. The various parameters and physical properties that affect the performance of the TEG also have to be evaluated to predict its likely best performance. This optimisation of operating parameters can be achieved using hand calculations [93]. In addition, if the TEG contains a huge amount of thermocouples, a low cross-sectional area value for each element and low internal thermal conductance value will be needed in maintaining the temperature difference, ΔT , between the hot and cold junctions, and achieve a higher open circuit voltage V_G across the junctions.

4.2 Background of Model TEG

As stated in Chapter 2, the development of new thermoelectric TE materials has led more and more researchers to focus their attention on the design of TEGs to harvest the thermal energy available from temperature gradients in local environments[141]. Thermoelectric modules are specialized so that every manufacturer offers a family of such modules suitable for each kind of application.

Each manufacturer tests and calibrates their TEGs, and provides performance curves and limit values [142]: ΔT_{\max} , I_{\max} , V_{\max} and Q_{\max} , are respectively the maximum temperature difference that can be sustained between the cold and hot ceramic plates, I_{\max} is the current at the input produced at ΔT_{\max} across the TEG module, V_{\max} is the DC voltage produced at ΔT_{\max} , Q_{\max} , is the maximum amount of heat dissipated at the cold side. Note that Q_{\max} , is not that maximum possible amount of heat that can be handled by the TEG, rather the heat flow corresponding to the current I_{\max} .

To obtain the highest performance from the TEG it is necessary to optimize the operating parameters. This is done using simple calculations, then simulating the overall cooling system using commercially available CFD software. To do this, it is important to know the basic physical properties for the TEG material. However, most manufacturers do not provide this information in their datasheet and thermal designers often find it difficult to obtain the relevant physical properties [108, 121].

Therefore, the fundamental physical properties α , ρ and K of the TEG materials are often calculated using the information (ΔT_{\max} , I_{\max} , V_{\max} and Q_{\max}) available in the datasheets.

4.3 The TEG Module Constructing

To develop a TEG module, the TEG structure must be known. Figure 4-1 shows structure of a TEG module used to harvest the thermal energy flow due to a temperature difference directly to electrical power. Generally, the TEG module is built with several pairs of N-type and P-type semiconductor legs, connected in series and joined by metal interconnects (generally Cu). These legs are soldered in parallel, sandwiched between ceramic plates, see Figure 4-2. The flow of thermal energy will be conducted to the module hot side from the heat source, through the module and will be dissipated from the cold side into the ambient air.

The many thermocouple “legs” that form the core of the TEG module can be modelled as a single P-N type semiconductor couple, see Figure 4-2, whose size is that of a single couple multiplied by the number of couples (N) within the module. By analysing each parameter design function, the TEG system model is then divided into heat exchanger and a TEG part.

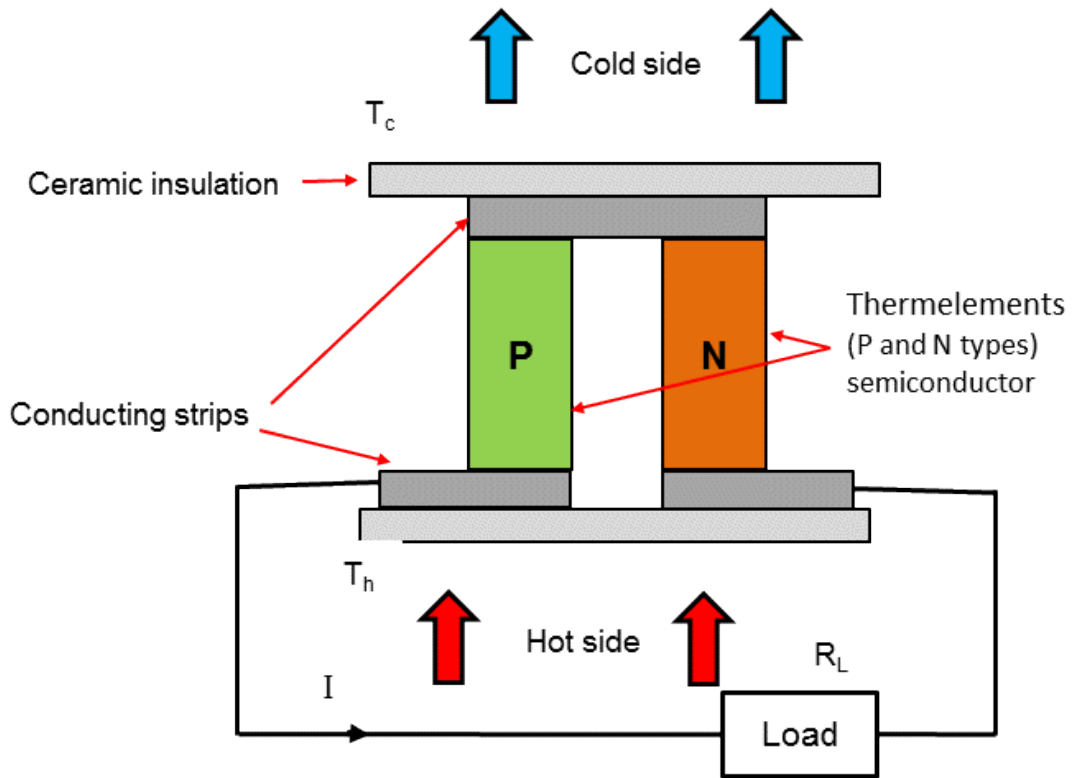


Figure 4-1 Schematic of Thermoelectric Element[143]

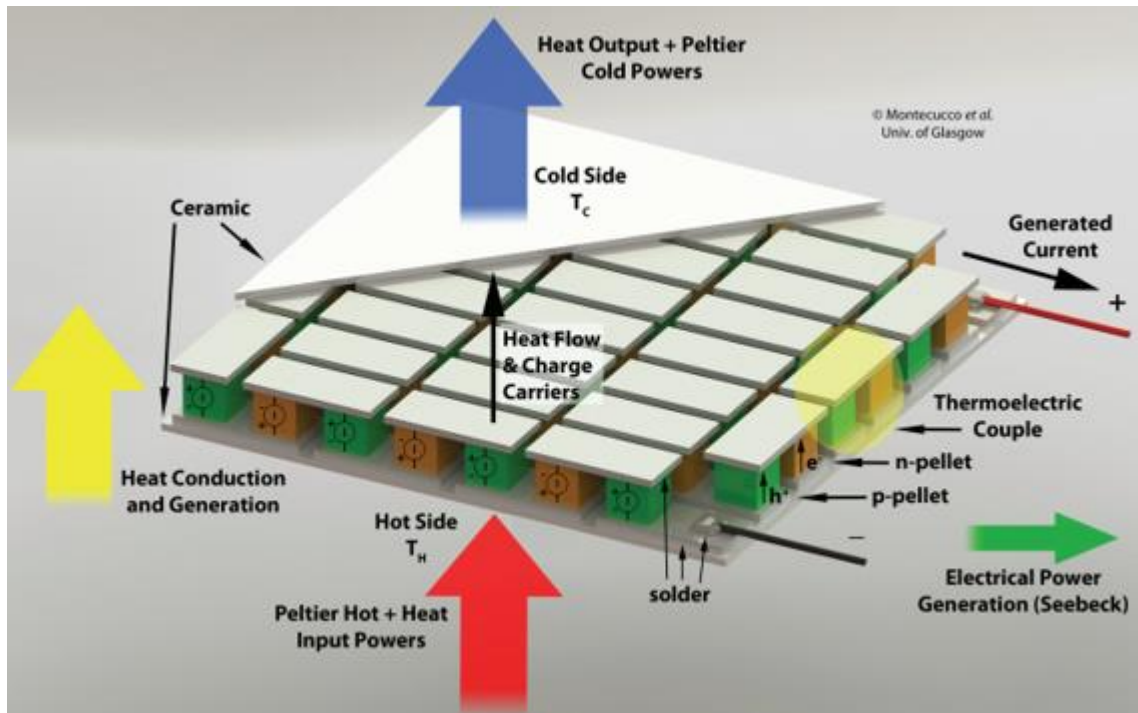


Figure 4-2 3D Structure of Thermoelectric Generator[144]

4.4 Basic TEG Equations

The analysis starts with one-dimensional thermal equations of the TEG which are available in the literature see[78, 108, 121, 142, 145]. It is noted that the temperature will affect the thermoelectric properties of the TEG.

The following equations (4-1/2/3) for TEG are available in the literature[146]:

$$Q_c = 2N \left[\alpha I T_c - \frac{1}{2} I^2 \frac{\rho}{G} - KG \Delta T \right] \quad (4-1)$$

$$V = 2N \left[I \frac{\rho}{G} + \alpha \Delta T \right] \quad (4-2)$$

$$Z = \frac{\alpha^2}{\rho k} \quad (4-3)$$

Where, N is number of couples in the TEG, α is the Seebeck coefficient [V/K], I the electrical current generated [A], T_c is the temperature at the cold side [K], ρ [Ωm] is the electrical resistivity of the TEG, G [m] a geometrical factor, the ratio of the cross-sectional area/length of each thermoelectric element, and K [$W m^{-1} K^{-1}$] is the thermal conductivity of the TEG, and ΔT is the temperature different $\Delta T = (T_h - T_c)$ as seen in table 4-1. And Z is the figure of merit[121]:

Table 4-1 Specification of TE generator

Parameter [CP85438-12708]	Value	Unit
Max. temperature difference ΔT_m (hot-to-cold side)	68	K
Max. Current	8.4	A
Max. Voltage	15.4	V
Dimensions	40x40x3.8	Mm
Resistance R_{TEG}	1.5	Ω
Max. operation temperature	138	$^{\circ}C$
Ceramic (alumina) plate thickness h_{CER}	2x0.8	mm
Thermocouple leg dimension(1xwxh)	1x0.7x2.2	mm
Number of Thermocouple	127	

The thermal balance equations for the TEG can be transformed in terms of the module parameters S_M , R_M and K_M given by [78]:

$$R_M = \frac{2N\rho}{G} \quad (4-4)$$

$$K_M = 2NkG \quad (4-5)$$

$$S_M = 2Ns \quad (4-6)$$

Where, R_M , K_M and S_M are devices electric resistance, devices thermal conductance and device Seebeck Voltage respectively. Using Eqs (4-4) - (4-6), we can rewrite Eqs (4-1) – (4-3) as follows:

$$Q_c = S_M T_C I - \frac{1}{2} I^2 R_M - K_M \Delta T \quad (4-7)$$

$$V = S_M \Delta T + IR_M \quad (4-8)$$

$$Z = \frac{S^2 M}{R_M K_M} \quad (4-9)$$

Using the relations (4-7), (4-8) and (4-9) the characteristic parameters of the TEG can be derived as follows:

$$\Delta T = \frac{1}{K_M} (S_M T_C I - \frac{1}{2} I^2 R_M) \quad (4-10)$$

$$\frac{d\Delta T}{dI} = \frac{1}{K_M} (S_M T_C - IR_M) \quad (4-11)$$

$$I = \frac{S_M}{R_M} T_C \quad (4-12)$$

$$\Delta T_{\max} = \frac{1}{2} Z T_C^2 \quad (4-13)$$

$$V_{\max} = S_M \Delta T_{\max} + I_{\max} R_M \quad (4-14)$$

$$I_{\max} = \frac{S_M}{R_M} (T_h - \Delta T_{\max}) \quad (4-15)$$

$$\Delta T_{\max} = \frac{1}{2} Z (T_h - \Delta T_{\max})^2 \quad (4-16)$$

The module parameters S_M , R_M and K_M are obtainable from TEG specification parameters such as I_{\max} , ΔT_{\max} , Q_{\max} , T_h and V_{\max} which are given on manufacturer's datasheets, and can now be used to calculate the parameters of the proposed model in table 4-2 [121, 147]:

$$R_M = \frac{(T_h - \Delta T_{\max}) V_{\max}}{T_h I_{\max}} \quad (4-17)$$

$$K_M = \frac{(T_h - \Delta T_{\max}) V_{\max} I_{\max}}{2 T_h \Delta T_{\max}} \quad (4-18)$$

$$S_M = \frac{V_{\max}}{T_h} \quad (4-19)$$

Table 4-2 Characteristic TEG parameters

Parameter	Value	Units
Z	0.002526	1/K
S_M	0.05133	V/K
K_M	0.7355	W/K
R_M	1.4177	Ω

4.5 Development of the Theory

The TEG is made of two different semi-conductors materials, sandwiched in-between ceramic plates. They are the cold and hot sides of the generator which the outer faces of ceramic plates. Certain phenomena which occur in TEG modules, should be determined before constructing the module. One essential characteristic underpinning the TEG module is the Seebeck effect, which occurs

when two dissimilar junctions materials are, at different temperatures, held together, with voltage being generated between both junctions, see Figure 4-1.

Because of the temperature difference ΔT across the TEG between the cold side T_c and the hot side T_h , a voltage is generated, the open circuit voltage V_G is given by [148]:

$$V_G = N\alpha_{ab}\beta\Delta T \quad (4-20)$$

Where the number of thermocouples is denoted by N and α_{ab} is the thermocouple materials coefficient of Seebeck. The coefficient β is determined by the TEG thermal conductance, and is controlled largely by the thermal conductivity of the ceramic plates K_{CER} .

The coefficient β has been calculated as [149]:

$$\beta = \frac{K_a}{K_a + 2K_{TEG}} \quad (4-21)$$

Where

$$K_a = \lambda_a \frac{A_{TEG}}{h_a} \quad (4-22)$$

Where, A_{TEG} is the TEG area, and λ_{CER} is the ceramic plates thermal conductivity, and h_{CER} is the thickness of the ceramic plates.

$\Delta T_{TEG} = T_{hj} - T_{cj}$, i.e., the effective difference in temperature across the TEG junctions. The cold junction T_{hj} , is given by [149]:

$$\Delta T_{TEG} = \frac{K}{K + 2K_{TEG} + \frac{2\alpha_{ab}^2 Tm}{R_{TEG} + R_L}} \Delta T \cong \frac{K}{K + 2K_{TEG}} \Delta T = \beta\Delta T \quad (4-23)$$

The TEG internal thermal conductance K_{TEG} has been given in[93]:

$$K_{TEG} = 2N\lambda \frac{A}{h} = 2N\lambda G \quad (4-24)$$

Where, λ_{COP} is the thermocouple material thermal conductivity, A and h are the cross-sectional area and height of a single thermocouple (equal to the thickness of the TEG) respectively. A geometric factor, G is defined as $G = \frac{A}{h}$, and the TEGs internal electric resistance, R_{TEG} , is given by:

$$R_{TEG} = \frac{2N\rho h}{A} = \frac{2N\rho}{G} \quad (4-25)$$

Where, ρ is the thermocouple material electrical resistivity.

If a resistive load R_L is connected to the terminals of the TEG to enable the flow of current I_L , the voltage across it is[93]:

$$V_L = \frac{R_L}{R_L + R_{TEG}} V_G \quad (4-26)$$

The output power, P_L delivered by a signal from the thermocouple to the load, R_L by the TEG is:

$$P_L = \frac{V_L^2}{R_L} \left(\frac{R_L}{R_L + R_{TEG}} V_G \right)^2 \cdot \frac{1}{R_C} = \frac{R_L}{(R_L + R_{TEG})} N^2 \alpha_{ab}^2 \beta^2 \Delta T^2 \quad (4-27)$$

Maximum power is delivery by the TEG under the condition of impedance matching, for a DC voltage this occurs when the external resistance is equal to load resistance. That is, $R_L = R_{IN}$:

$$P_{L\max} = \frac{N^2 \alpha_{ab}^2 \beta^2 \Delta T^2}{4R_{TEG}} = \frac{N \alpha_{ab}^2 \beta^2 \Delta T^2 G}{8\rho} \quad (4-28)$$

Table 4-3 TEG Parameters

Parameter	Value	Units
Z	2.52×10^{-3}	1/K
S_{TEG}	0.05133	V/K
K_{TEG}	6.325×10^{-1}	W/K
R_{TEG}	1.5	Ω
α_{ab}	200×10^{-6}	V/K
ρ	5.6×10^{-3}	$\Omega \cdot m$
K_{CER}	20	W/ (m. K)
λ_{COP}	1.5	W/K. m
G	1.685	mm
A_{TEG}	278	mm ²
PF	2.2	

The power factor seen in table 4-3, i.e. the maximum output power value for $\Delta T = 2.2$, (difference in unit temperature), and $A_{TEG} = 1$ (unit face TEG area), is given by:

$$PF = \frac{P_{Lmax}}{\Delta T^2 A_{TEG}} = \frac{N^2 \alpha_{ab}^2 \beta^2}{4 R_{TEG} A_{TEG}} = \frac{\alpha_{ab}^2 \beta^2}{8 \rho} \cdot \frac{NG}{A_{TEG}} \quad (4-29)$$

The internal thermal conductance and power factor are significant in evaluating the performance of TEG for EH implementation. The higher the power factor value, the better power-generated transfer. A lower internal thermal conductance value is important to maintain the difference in temperature ΔT and achieve high values of output voltage.

Figure 4-2, shows represents open circuit voltage for the TEG calculated from Equation (4-13). According to the figure, the voltage V_G obtained from a temperature difference 6.8 C° is 170 mV.

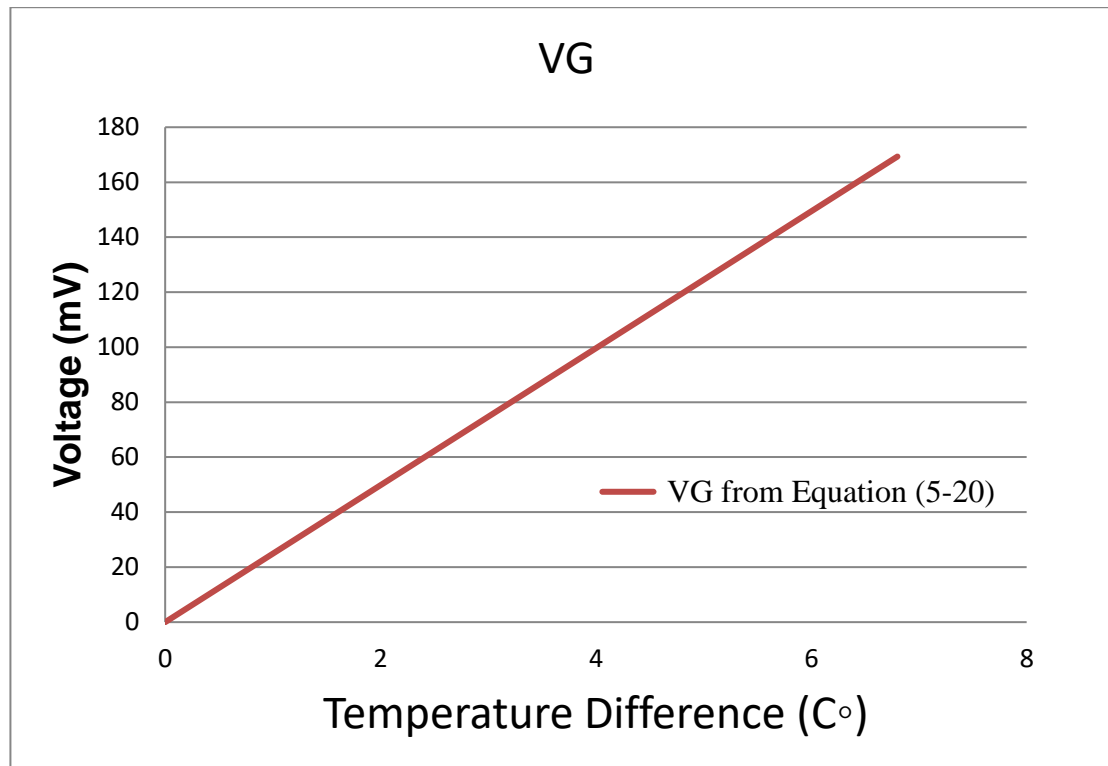


Figure 4-3 Open circuit voltage calculated from Equation (4-13).

4.6 Summary

In this chapter, a computational design of a TEG module has been developed. Starting, from values of internal parameters of a commercial thermoelectric module given on the manufactures' datasheet, initial estimates of relevant values of the elements of a thermal module were made.

After these parameters were obtained, the thermoelectric of the TEG was evaluated as power generator. The model developed has been shown to have a predictive value: the open circuit voltage has been calculated for the module at a given temperature difference, 6.8 °C as the result confirmed that using such thermoelectric devices can be a possible tool for power generation in supplying circuits with low power.

Chapter 5. Finite Element Analysis of Design of Thermal Module

In this chapter, SolidWorks Premium, a commercially available software package was used to design a Peltier thermoelectric generator module.

SolidWorks Premium has the capability of carrying out a Finite Element Analysis and Simulation and this was used to predict product performance.

The model, heat source, boundary conditions are introduced and described, as is the mesh structure used in the Finite Element Analysis. The chapter concludes with a presentation of results obtained of model predictions.

5.1 Introduction

This chapter will describe the creation of a model of a TEG in sufficient detail, including all its essential structural elements to perform a detailed Finite Element (FE) simulation. The simulation of transient thermal behaviour was undertaken using SolidWorks software, selected due its ability to execute the most commonly needed FE analyses and construct complex geometrical shapes. The simulation results are described in this chapter.

5.2 Bench Mark Simulation

A benchmark simulation was completed to validate the reliable application of the thermal parameters as described in Section (4.5), and confirm the accuracy of the thermal software simulation compared to calculation compared to the hand calculations carried out in Chapter 4.

5.3 Simulation of the Thermal Design

The SolidWorks software provides both the capacity to construct a 3-D model, with the necessary thermal features, and simulate the likely thermal behaviour. To determine the optimum thermal parameters and simulation methodology it is necessary to have accurate thermal characteristic for the TEG module.

The software requires the temperature of an object for two sets of calculations: First is the surface heat flow which is the heat input to the surface of the object. Second is the thermal energy flow through the TEG. This will determine the temperature distribution across the module; generate electrical energy, depending on boundary conditions.

A thermal model of dimensions (131 mm * 63 mm * 50mm) about size (see Chapter 6) was generated and assembled in the SolidWorks software and a thermal transient simulated, based on a given temperature difference and the material properties of the structure, as given in Table 5-1[150]. The initial design temperature for the system was set to 25°C, setting also the transient analysis duration to one hour, matching the experimental time as will be seen in Chapter 7.

Table 5-1 Specifications of material properties and boundary conditions as provided by manufacture[150]

Property	TEG (Peltier)	Heat sink	Aluminium	Thermal insulation
Density (Kg/m ³)	7530	2700	2700	1880
Specific heat (J/Kg.°C)	544	900	960	700
Thermal conductivity (W/m.K)	20	30	120	2.5
Mass (g)	21	364	49	8

5.4 Model Geometry

Figure 5-1 shows a 3D geometrical diagram of the TEG. All dimensions are in millimetres and the material type is solid deformable as shown in Figure 5-2. In this research a simple low-cost design will be shown to produce, in a convenient way, a small voltage from the heat energy dissipated by a gearbox.

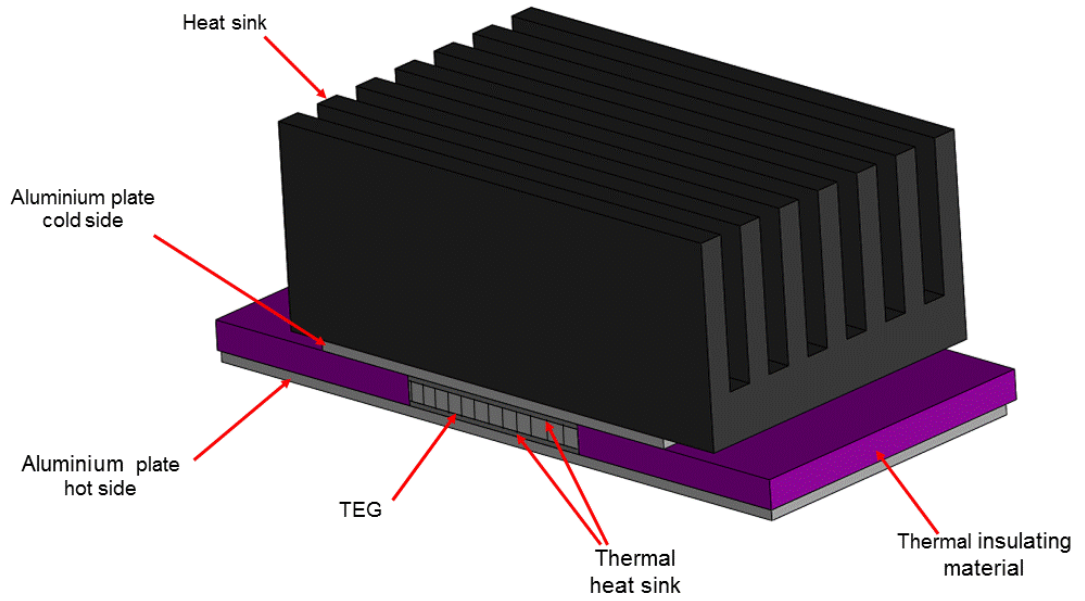


Figure 5-1 Structure of the thermal design

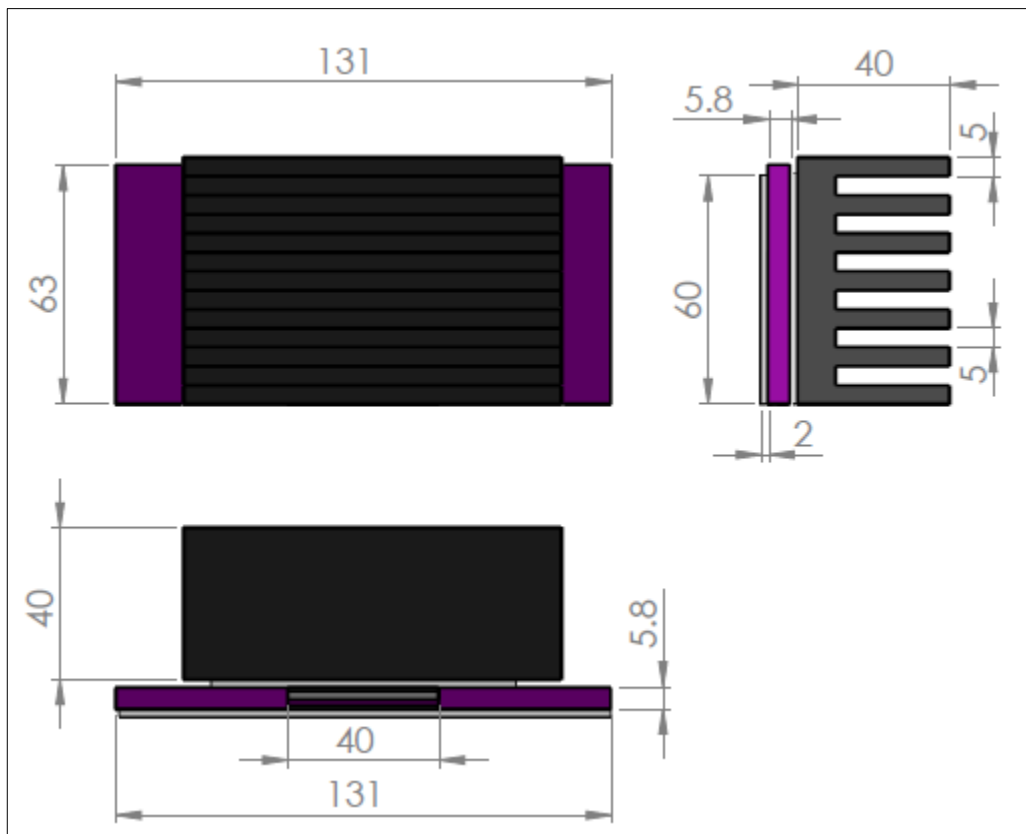


Figure 5-2 Structural Dimensions

In the following sections each element in the structure, as shown in Figure 5-1, is described and its function explained.

5.4.1 Peliter

The choice of the thermoelectric generating mechanism in the successful design of a TE generator is of utmost importance. Here a Peltier TEG was chosen. See Chapter 2, the Peltier effect and Seebeck effect, and how they are used in TE generators. A commercially available Peltier TEG module from Digi-Key, code number CP85438[150]., specifications in Table 5-2[49], was chosen as the TE module due to its low cost, small size and acceptable power factors and thermal conductance values.

A TE module, shown in Figure 5-3, is comprises generally of TE elements in their hundreds, formed by electrically connecting in series, N-type and P-type semiconductors and thermally sandwiched parallel between ceramic plates, having role of the cold and hot sides of generator. The most common thermoelectric material, from which the thermoelectric couples are, is made of from Bismuth Telluride ($B_{i2}T_{e3}$). Bismuth Telluride ($B_{i2}T_{e3}$) is a grey powder that is a compound of two metallic elements (Bismuth and Telluride) and its alloys are widely used as materials for thermoelectric generator.

Table 5-2 Specification of TEG

Digi-Key Peltier TEG [CP85438-12708]	Value	Unit
Max. temperature difference ΔT_m (hot-to-cold side) at $T_h = 27\text{ }^\circ\text{C}$	68	K
Max. Current	8.4	A
Max. Voltage	15.4	V

Dimensions	40×40×3.8	Mm
Resistance R_{TEG}	1.5	Ω
Max. operating temperature	138	$^{\circ}\text{C}$
Ceramic (alumina)plate thickness h_a	2×0.8	mm
Thermocouple leg dimension(length x width x height)	1×0.7×2.2	mm
Number of Thermocouples	127	

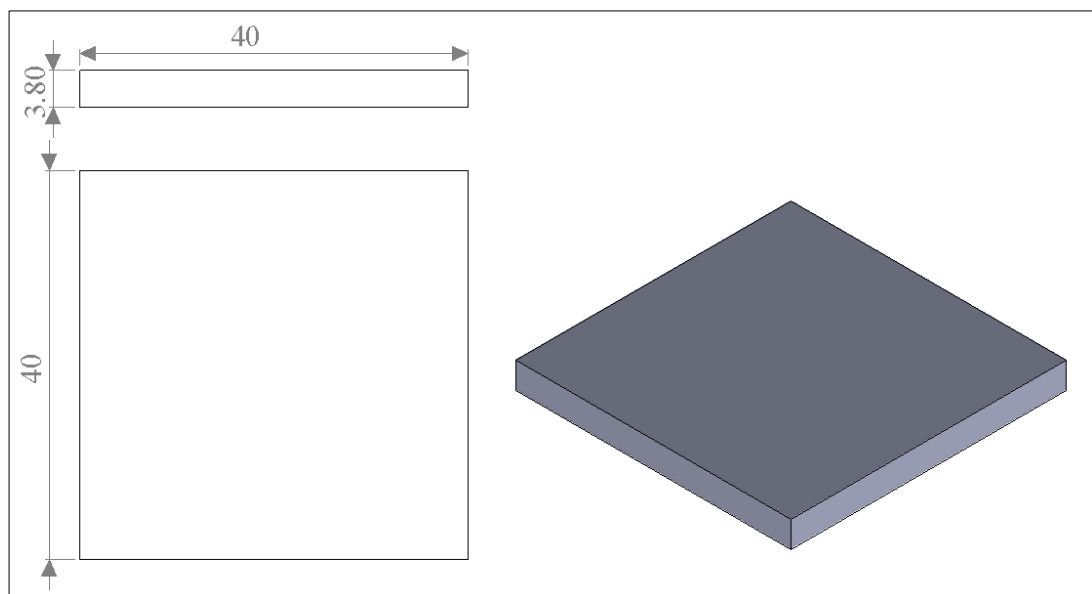


Figure 5-3 Peltier TEG

5.4.2 Heat Sink

The heat sink plays an important role in thermal EH, acting to maintain a temperature difference by efficiently transferring heat from the cold side of the thermoelectric generator module efficiently to the surrounding environment. Here, a medium size black aluminium heat sink which type (SK 100/100) of thermal resistance of $1.5\text{ }^{\circ}\text{C}/\text{W}$, was used, see Figure 5-4[151].

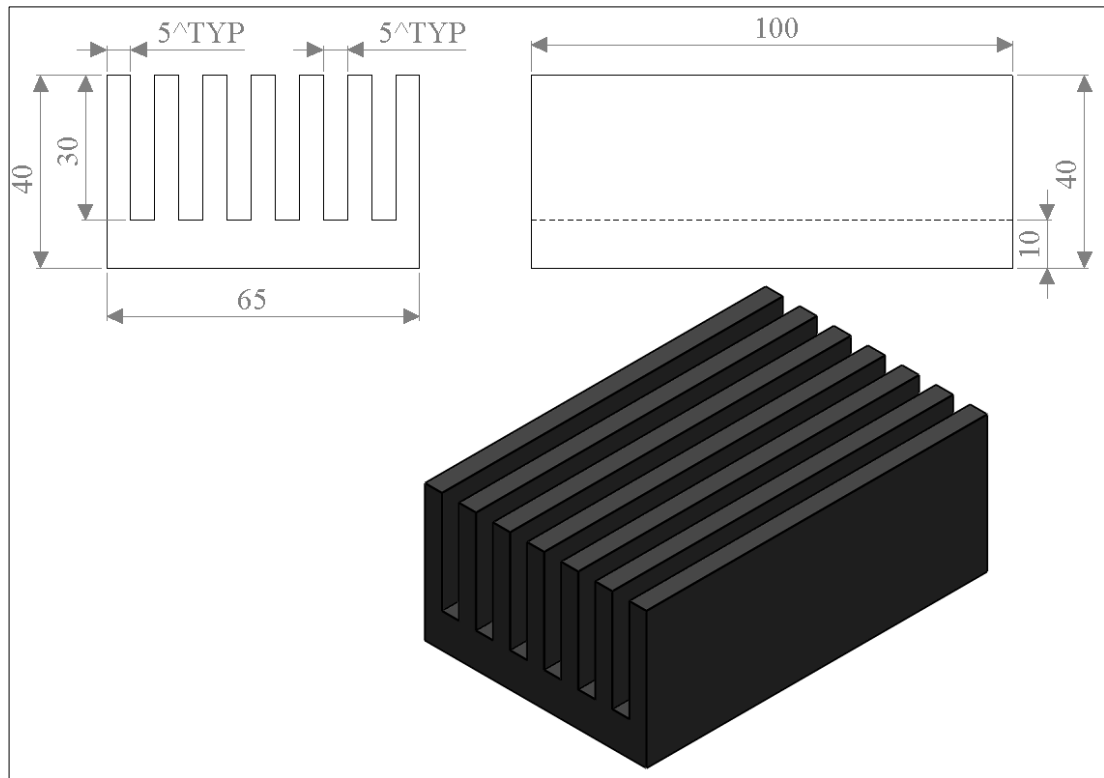


Figure 5-4 Aluminium Heat sink (SK 100/100)

5.4.3 Thermal Insulation and Conductance

A layer of thermal insulation is employed to maintain the temperature difference between the hot and cold sides, and the low thermal conductance of the material reduces unwanted heat loss and improves the heat transfer efficiency between the heat source and the heat sink. The thermal insulation had thickness of 6mm and thermal conductivity 0.22 W/m-K. The detailed shape of the insulation is shown in Figure 5-5.

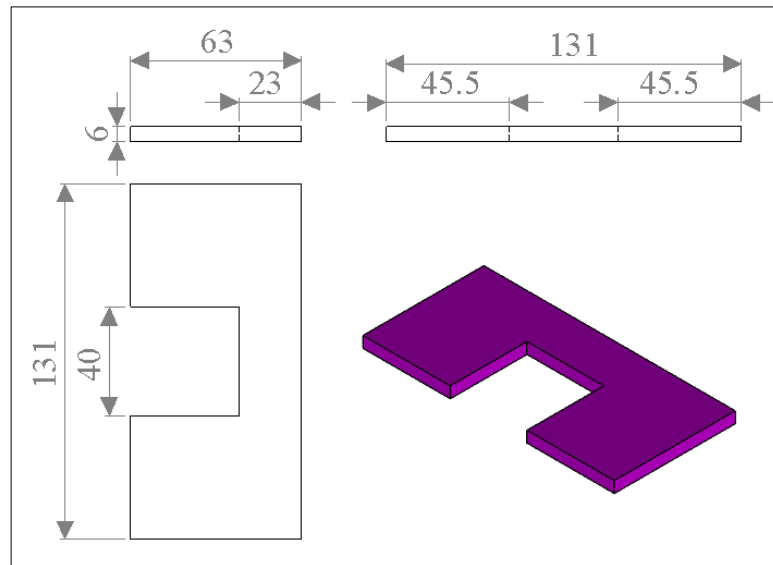


Figure 5-5 Thermal insulation material geometry

5.4.4 Insulation Material (Bond-Ply 100mm x100mm)

Two pieces of Insulation material have been chosen, which is called Bond-ply 100mm x100mm, made is fiberglass, and 1.0 mm thick as shown in Figure 5-6. The heat sink transfer pad was double sided adhesive with thermal conductivity (2.5 W/m-K) and used to maintain the temperature difference between hot and cold sides of TEG.

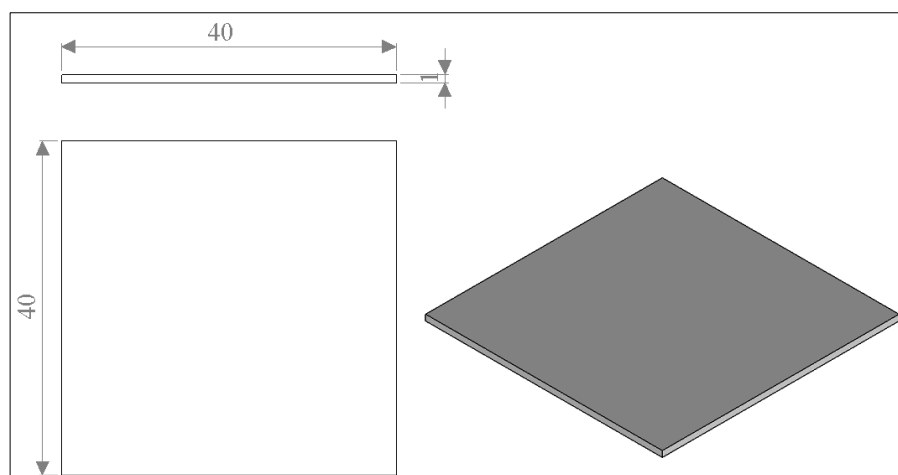


Figure 5-6 Insulation material (Bond-Ply)

5.4.5 Aluminium

Two small sheets of aluminium were used, one 1 mm thick as a heat dissipator on the cold side (Figure 5-7, and the other as a collector on the hot side (Figure 5-8). Aluminium is well suited for these tasks due to its large thermal conductivity, 120 W/mK.

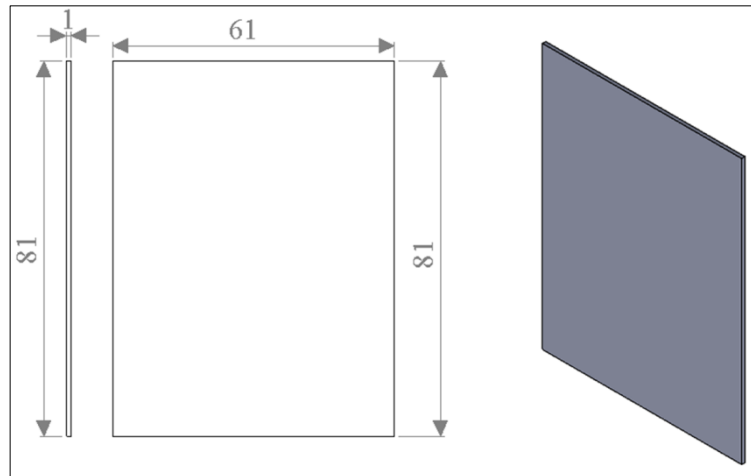


Figure 5-7 Aluminium for cold side

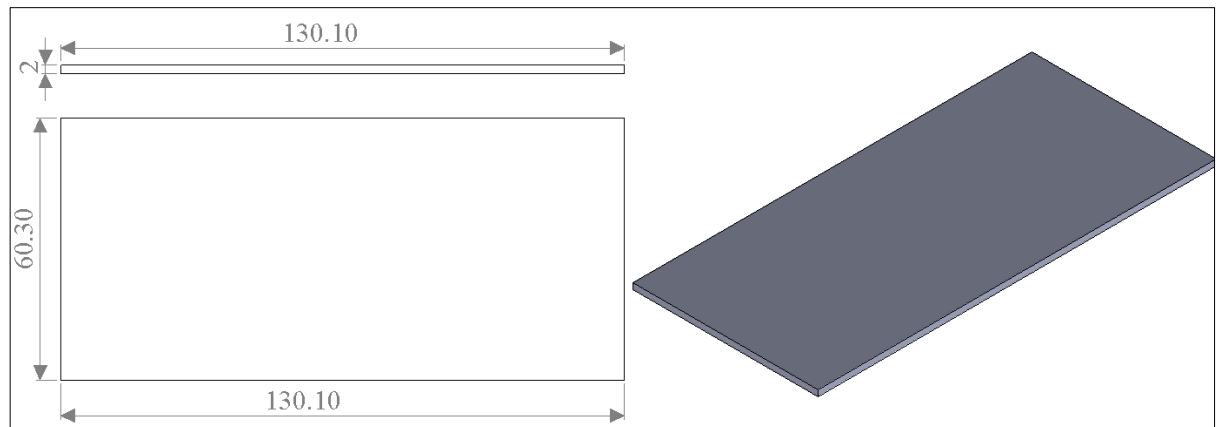


Figure 5-8 Aluminium for hot side

5.5 Model Boundary Conditions

The accuracy of the simulation depends on determining accurate, the initial and boundary conditions, the characteristics of the thermal design and the thermal

properties of the materials used. The initial condition analysis will include factors such as the ambient temperature, thermal parameters, heat source temperature and the initial temperature for the different materials.

5.5.1 Heat Source

The simulated thermal design used a heat source of 45°C, this is the temperature of the gearbox while ambient temperature is 24°C, based on the speed were set to 100% and 70% load, which was using this temperature as heat source that it will discuss about experimental works in Chapter 7.

5.5.2 Calculations of Convective Heat Transfer Coefficient.

The convective heat transfer coefficient (h W/m².°C) is very important in ensuring results of the software simulations are accurate. Convection method of heat transfer can be categorized into two types: The free convection type occurs when energy transfer from a hot surface to the surrounding fluid medium takes place when the movement of the fluid is due only to temperature/density differences within the fluid. An example of this is ambient air circulating around a stationary fluid pipe containing hot fluid in a closed room. The forced convection type occurs when flow is caused by external means such as fans. Convection energy loss is usually modelled using the cooling law by Newton [152].

$$Q = hA(T_{surf} - T_{air}) \quad (5-1)$$

Where Q signifies the heat power rate in Watts, h is the coefficient of convective heat transfer (W/(m².k)), T_{surf} is the surface temperature (°C), T_{air} is the ambient temperature (°C) as seen in equation (5-1) [146].

Touseconvection associated equations, some parameters such as temperatures and ambient, mess, specific heat and area of the TEG module should be obtained[145, 150, 151, 153-156].

On the other hand, since the other machine parts are stationary, $6 \text{ W/m}^2\cdot\text{C}$ for the natural convective coefficient have been applied based on experimental work that have carried out previous[157, 158].

5.6 The Mesh Structure of the Thermal Design Model

There are two meshing options embedded in this software package. They are thecurvature mesh and the standard mesh. Curvature mesh has been chosen for this research as they suit better for complex CAD module as it optimises automatically, the mesh density, within a specific limit based on the structure shape. The mesh sensitivity analysis was performed for the thermoelectric power generation system to check mesh independency.

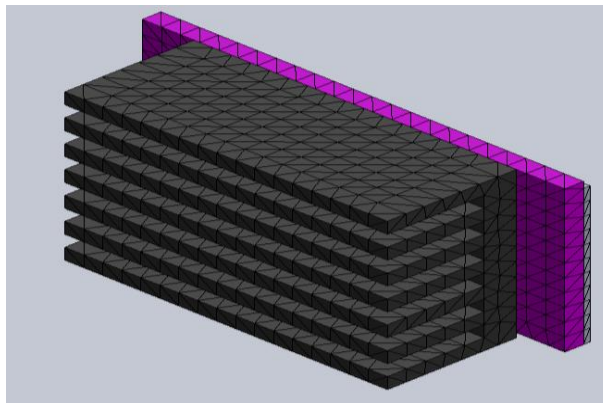


Figure 5-9Cross Section of thermal design Mesh Structure

5.7 Result and Discussion

Figure 5-10shows the simulated temperature distribution throughout the TEG with heat source temperature of $45 \text{ }^\circ\text{C}$ while ambient temperature is 24°C . The

predicted temperature difference, ΔT , was obtained from the simulated hot and cold sides temperatures of the TEG.

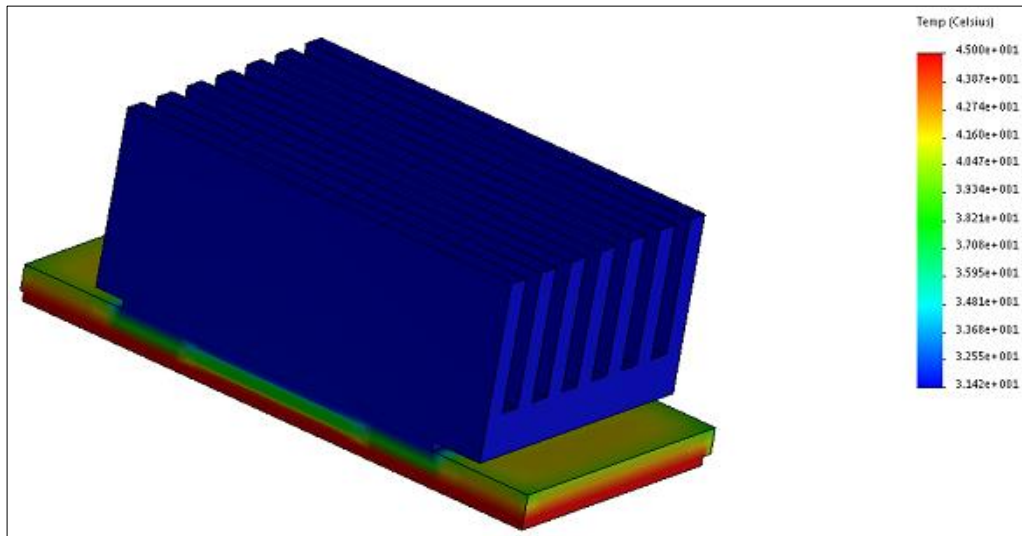


Figure 5-10 Thermal temperature distribution simulation for the thermal design with 45 °C heat source

Figure 5-11 shows result of simulated temperature difference ΔT between hot side and cold side of the TEG module was °C of 6.3°C after one hour, for the heat source 45 and ambient temperature is 24°C. This temperature difference of 6.3°C produced 160mV open circuit voltage as shown in Figure 5-12. From the figure, It can see that the temperature difference across the TEG after 1000 (sec) between the hot and cold sides was still increase slightly. Meantly, because the temperature difference produced when there is different of temperature between the cold and hot sides of the TEG which was started after 1000 (sec).

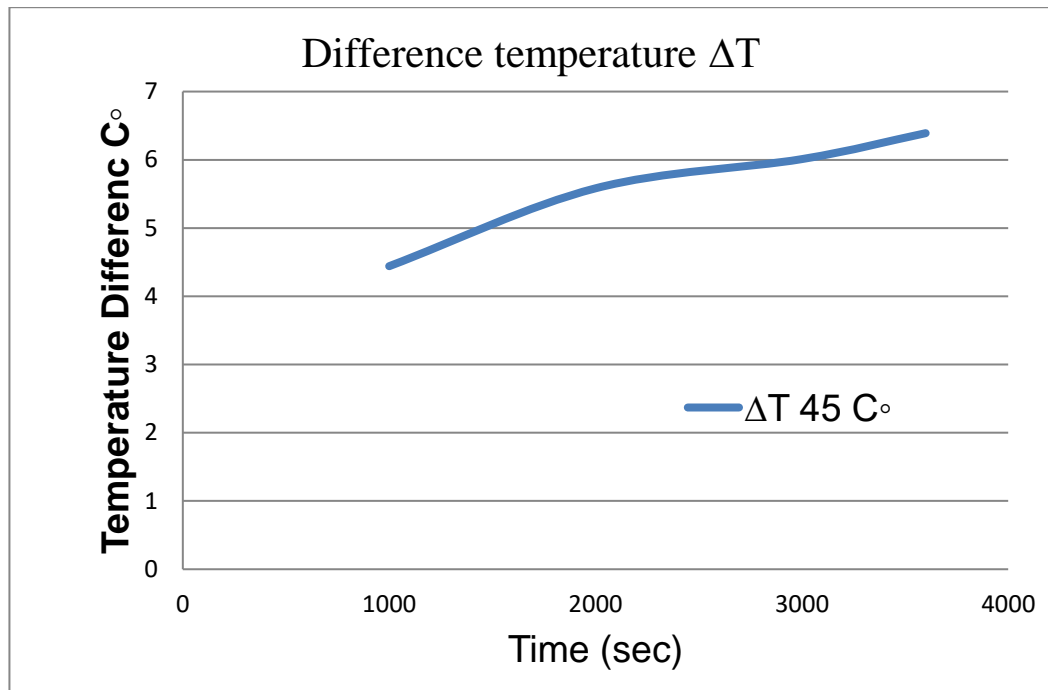


Figure 5-11 Simulated temperature difference between hot and cold sides for heat source of 45 °C and ambient temperature 24°C

After obtained the result of simulated temperature difference using the following equation to calculate the voltage generated by the TEG module, see figure (5-12)

$$V_G = N \beta \alpha_{ab} \Delta T \quad (5-2)$$

V_G Open circuit voltage

N Number of thermocouples

α_{ab} Seebeck coefficient

β Coefficient

ΔT Temperature difference between TEG's hot T_h and cold sides T_c

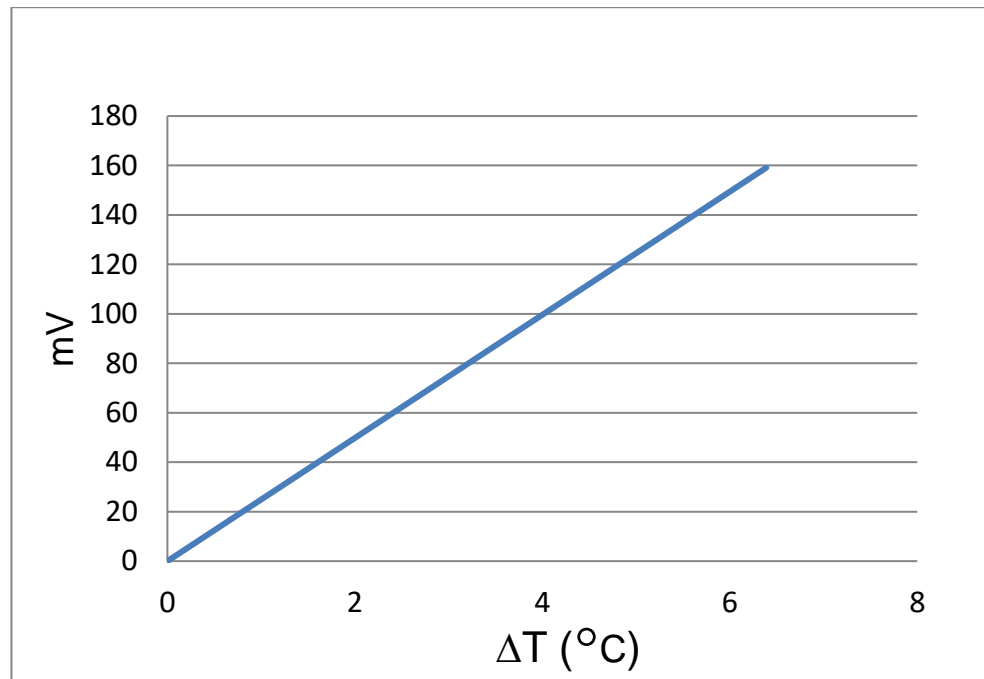


Figure 5-12 Simulation results of TEG open circuit voltage of temperature difference in the rang 0 to 6.3C

5.8 Summary

The purpose of this chapter was to develop a Finite Element Model to analyse and simulate the thermal behaviour of the TEG. This was done successfully using proprietary software after having determined such necessary parameters as: material properties, boundary conditions, mesh and loads. It will be shown in Chapter 7 that the results of simulated the temperature difference with the TEG are correlated closely with the theoretical calculations. A discussion will be presented at that point.

Chapter 6. Design and Implementation of Thermal Energy Harvesting System

In this chapter, a design for thermal energy harvesting system suitable for a WSN is proposed and built. To optimise the design for thermal energy harvesting, three different specifications of heat sinks were tested.

The proposed system is shown to be readily useable for thermal energy harvesting which is a simple and low cost design.

6.1 Introduction

Generally, EH systems have three parts: a load, a source of energy and an harvesting design. The source of energy, which is an ambient energy source to be harvested, will largely determine the design of the harvesting system and the technique used to harvest the input ambient energy and convert it to electrical power. The load is the WSN and this consumes the electrical power provided. Each part has its own characteristics, so only when these features to interact correctly with each other can the design of the energy harvesting system be optimised.

One of the most difficult aspects of designing an EH system is determining the structure of the system. As stated Chapter 2, many different EH systems have been designed, and it is difficult to say that any one system has the best performance. Hence, different EH designs exist for different systems intended for different purposes. In addition, the energy sources existing at the different places vary with time, and the sensor nodes on the same network may have different EH sources. Thus, stability and flexibility are considered as essential features of EH design that is successful. In designing an energy harvesting system this is highly efficient, many different design parameters and factors including the system size and cost, energy efficiency and the systems life span, must be considered.

6.2 Experimental Setup to Evaluate Heat Sinks

In evaluating the thermal EH system performance, a test platform was constructed. In this work, three different sizes of commercially available heat sinks with different specifications (Fischer Electronic SK 100/50 SA, SK 100/100

SA and SK 47/150 SA) were tested in the laboratory to characterize the performance of each, with the open circuit voltages recorded. In addition, their efficiency was evaluated over a range of temperature differences; 30 °C to 80 °C were used. More information about Heat sinks, see section 6.3.3.

6.3 System Design and Implementation

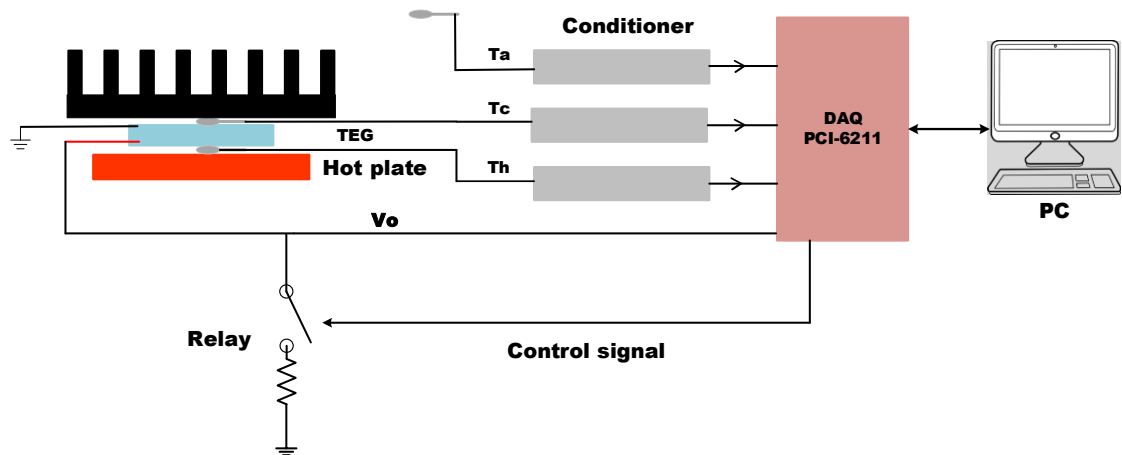


Figure 6-1 Schematic of experimental setup

Figure 6-1 shows the general thermal EH system architecture used to evaluate the different sizes of heat sinks. The experimental setup consists of four main parts: the thermal generator module, the heat source, the thermocouples (which use the Seebeck effect to generate an electrical voltage from a temperature difference) and the data acquisition (DAQ) system. The parameters measured, were the hot side temperature, cold side temperature, ambient temperature, open circuit voltage and current over a 1 Ω resistor of TEG. The maximum of output voltage of the conversion from the TEG system is maintained about 300mV.

6.3.1 Thermal Energy Harvesting Design

The thermal efficiency is an important factor for any thermal EH design; a high efficient TEG is the basic requirement for a successful EH system. However,

the high performance efficiency of the thermoelectric generator is dependent of the performance efficiency of the TE module and the thermal energy passing through the module.

The temperature difference across the module, and heat flow through it, are important factor in determining the efficiency of the full EH system. Hence, maintaining a large temperature difference across the TE module with efficient heat dissipation on the cold side are essential requirements. A good thermal conductor, such as a metal is considered as most suitable for the heat sink and good heat dissipation.

The thermal EH system was built, as illustrated in Figure 6-2, and consisted of: the TEG (Peltier TEG module from Digi-Key, code number CP85438) sandwiched between two pieces of thin aluminium with thickness 1.0 mm, one piece to work as a heat collector on the hot side and the other to act as a heat spreader on the cold side, see Figure 5-7 and Figure 5-8. A layer of thermal insulation material was double sided adhesive with thermal conductivity (0.22 W/m-K) and with thickness 1.0 mm, was shaped to fit around the TEG module and separate the aluminium plates, see Figure 5-6, to maintain the temperature difference between the hot and cold sides. Additional thermal insulation was placed around the TEG module see Figure 5-5, to better isolate the heat source from the heat sink because the heat source is physically close to the heat sink.

The heat sink plays an important role in the thermal energy harvester and is used to maintain a temperature difference between the hot and cold sides by dissipating heat from the cold side of the TEG efficiently to the surrounding air.

Figure 6-2 shows the set up with a medium size heat sink with thermal resistance of $1.5\text{ }^{\circ}\text{C}/\text{W}$.

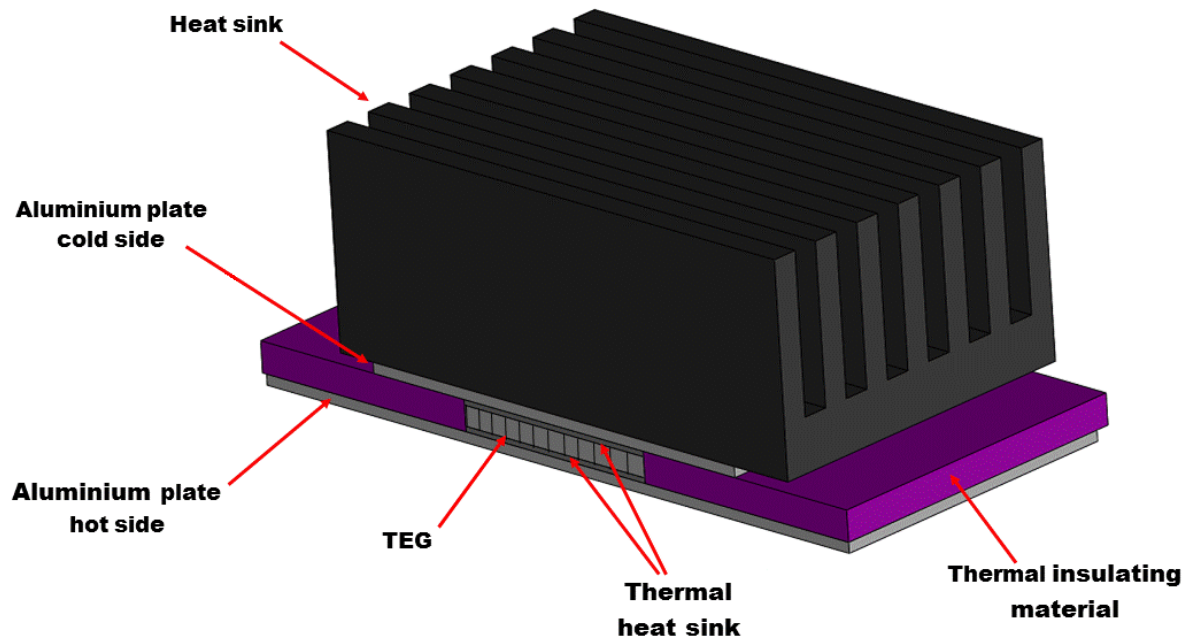


Figure 6-2 Structure of the Thermal EHsystem

Obviously, if the hot plate can be thermally isolated from the air surrounding the heat sink, more heat flow will pass through the module. The insulating material around the outside of the TEG is used to block this heat flow as shown in Figure 6-2.

6.3.2 Peltier

A commercially available Peltier TEG module Digi-Key, code number CP85438[159] was chosen as the TEG module, see Figure 6-3 and specifications are given in Table 5-2. This TEG has 127 thermocouples and a heat transfer area of 278 mm^2 . There are many materials which can produce a useable voltage from the temperature differences likely to be found with this particular usage, WSN attached to the surface of a gearbox, the important

differences are cost, availability and efficiency. CP85438-12708 was chosen as the TEG module [160], because of its low cost, small size and acceptable values of thermal conductance and power factor.

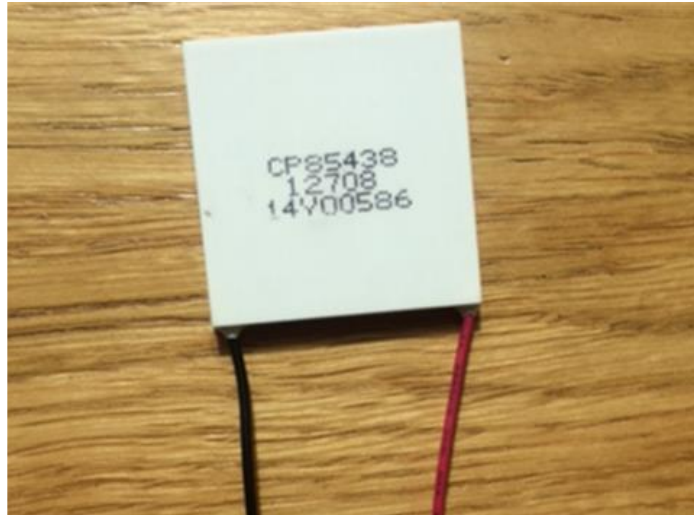


Figure 6-3 Peltier TEG module from Digi-Key, code number CP85438

6.3.3 Heat Sink

Three black anodised aluminium heat sinks of different sizes (Heat sink A, Heat sink B and Heat Sink C, see Table 6-1 and Figure 6-4) have been tested to assess which is the most effective heat sink for heat dissipation on the cold side. In testing the efficiency of heat transfer, same TE module was attached to each of the three different size heat sinks with testing done in the same environment, a room with steady temperature 21°C. A more efficient heat sink should dissipate a greater volume of heat from the TEG cold side.

It would be expected that the thermal resistance of the heat sink would be a key parameter in determining its performance, the lower the thermal resistance the lower the temperature on the cold side. These Heat sink were chosen as the EH

thermal module due to their low cost, acceptable value of thermal resistance and reliable company.

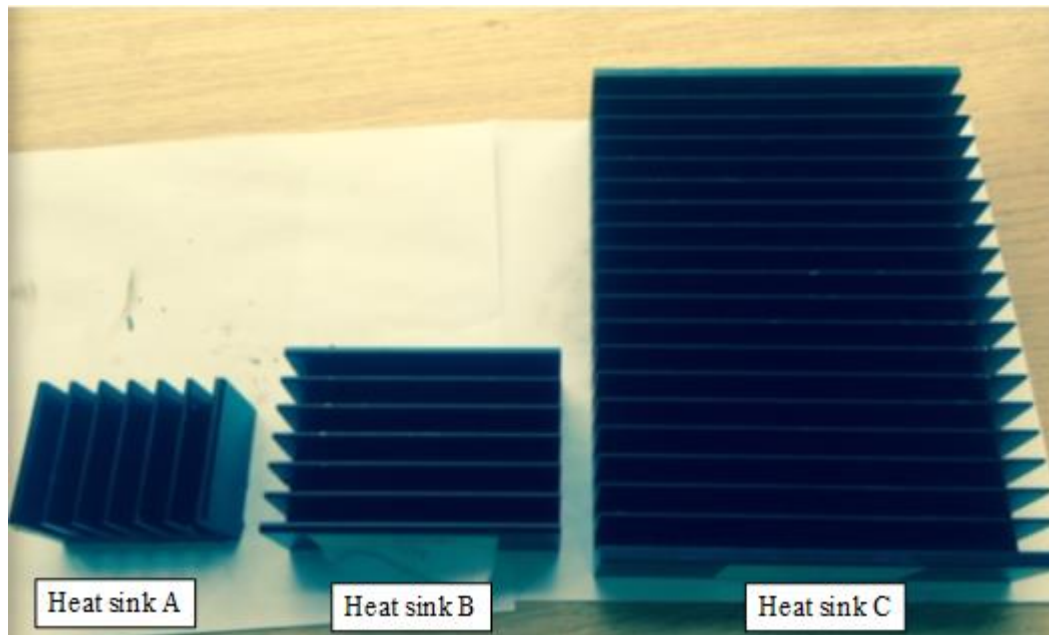


Figure 6-4 Picture of Heat sinks

Table 6-1 Heat sink specifications

Model	Height (mm)	Length (mm)	Width (mm)	Thermal resistance
Heat sink (A) SK 100/50	40	50	66	2.5 °C/W
Heat sink (B) SK 100/100	40	100	66	1.5 °C/W
Heat sink (C) SK 47/150	40	150	200	0.5 °C/W

6.3.4 Thermal Insulation Material

Thermal insulation is employed to maintain the temperature difference between the hot and cold sides, to reduce the unwanted heat loss and improve the heat transfer efficiency. Parameters to be considered when choosing thermal insulation include density ρ , thermal conductivity λ , thermal resistance R , thickness of thermal insulation layer and temperature limits[121].

Thermal resistance can be defined it is a heat property and a measurement of a temperature difference by which an object or material resists a heat flow. In addition, the thermal resistance of material is measure of its ability to resist the passage of heat. It is an effective way of comparing the performance of material of different types and thicknesses.

Two types of thermal insulation material have been used in this the thermal EH design. First, using suitable material the gearbox can be thermally insulated from the surrounding air and the heat it generates is channelled through the TEG, to generate an increased voltage, see Figure 6-5. The heat is then dissipated from the aluminium heat sink



Figure 6-5 Thermal insulation material

Second, the chosen insulation material is called Bond-Ply, made is fiberglass, see Figure 5-6. There are plenty of cheap and common insulation materials available commercially. Selection of insulation material for the gearbox should be based on effectiveness, durability and its capacity to adapt to the shape of the gearbox. The chosen insulation material is Bond-Ply. Table 6-2 shows Several material properties of insulation materials.

Table 6-2 Material properties of insulation materials

Insulating material	Thermal conductivity (W/m K)	Mass density (kg/m ³)	Thickness in mm
cork	0.045-0.055	80-500	3.3
wool	0.04	20-25	1.27
cotton	0.04	20	
air, motionless	0.0025	1.2	
Bond-Ply 100	0.22	15-25	1.00

6.4 Heat source

A commercially available hot plate (IKA, RCT basic, see Figure 6-6) has been used as the heat source for easily control of the hot side temperature. The key features of the hot plate are listed in Table 6-3. The claimed accuracy of the temperature was $\pm 1\text{K}$ [58]. (See section 6.7.2)



Figure 6-6 the Hot plate IKA, RCT basic

Table 6-3 the hot plate specification

Max temperature (° C)	360
Top plate material	Aluminium
Dimensions	6.5 in x 3.25 in x 10.75 in
Power	230 V
Weight [kg]	2.5
Heat control accuracy [$\pm\text{K}$]	1

6.5 Voltage Booster Design

The voltage output of the TEG module is usually very small, from several mW to a few hundreds of mW, depending on the temperature difference between hot side and cold side.

The output voltage of the TE generator due to both its absolute level and the variation in level due to changes ambient and working conditions is not appropriate to directly charge or power the sensor node. Thus, a DC-DC boost converter is added as a power conversion circuit at the TEG output to boost the low input voltage from the TEG to a higher, more useful, output voltage. Such a device is an essential part of the design of efficient EH systems.

Such a DC-DC converter should, of course, function over a wide input power and voltage range [161]. Because of its high system efficiency, low cost and suitable size an integrated DC-DC boost converter produced by Linear Technology LTC3108 (Ultra-low Voltage Step-Up Converter and Power Manager)[162][150, 159] was used as the circuit regulator for this research project. The schematic for boosting converter the DC-DC is shown in Figure 6-8. This DC-DC boost converter can boost an input voltage ranging from 20 mV to 500 mV to an adjustable one from 2.35 V to 5 V. Figure 6-7 shows a transformer with turn ratio of 1:100 is used for accepting the voltage at the input, which can go as low as 20 mV. The output voltage is fixed at 3.3 V for directly powering the sensor node.

In this project, a The backup capacitor with a capacity of 0.33 F was employed for storing extra energy harvested. It is used when there is no energy harvesting or if the output voltage of the TEG is insufficient enough for continuous operation

of the node. It accumulates energy for a relatively long time and then provide power to the sensor node for short periods, during which signal is collected and transmitted to a central device (DAQ system).

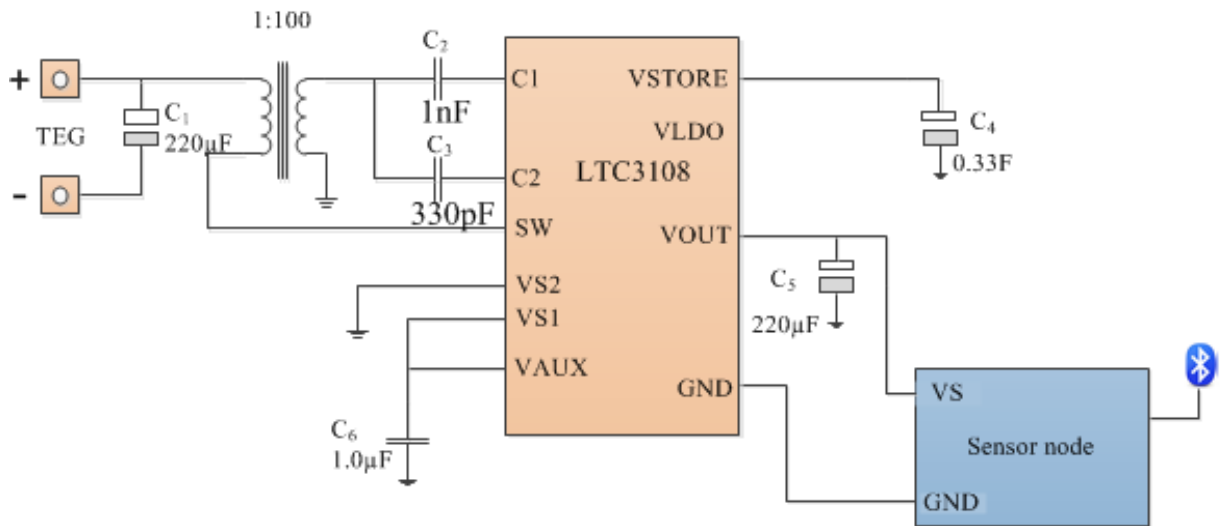


Figure 6-7The DC-DC boost converter Schematic diagram

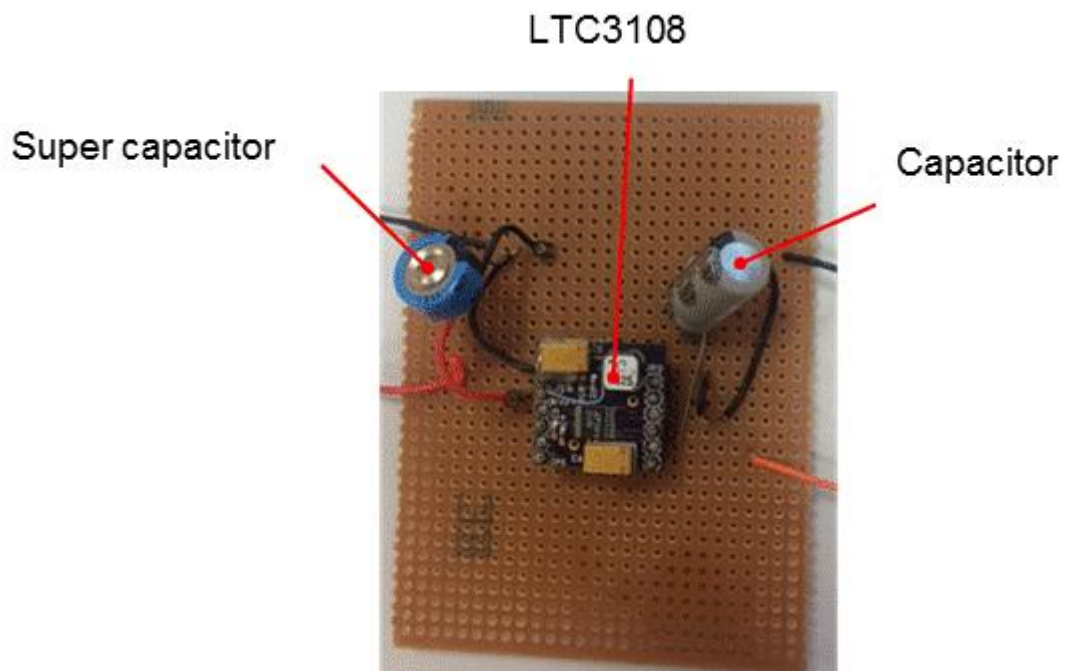


Figure 6-8Photo of DC-DC boost converter

6.6 The Buffering Effect of Capacitor

The importance of high performance is that buffering effect plays an important role in determining the working life of the EH system. To ensure continuous system operation even when the external energy source is weak or temporarily insufficient, the energy to be used to power the WSN should be stored in either a rechargeable battery or a super-capacitor, which is, thus a very important component for the design of a system with a long lifetime. Because of its high charging/discharging efficiency and unlimited charge/ discharge period, the super-capacitor is usually used as the primary buffer and is directly charged from the EH system.

6.7 Data Acquisition System and Experimental Procedure

Data acquisition have been taken is the process of measuring a physical phenomenon such as voltage, current, temperature and/or pressure. Here a DAQ (National Instruments, Multifunction I/O device, PCI-6211) system was used, this consisted of sensors, measurement hardware, and a computer with programmable software, including the capacity to provide screenshots of relevant parameters.

The monitored parameter include temperature on both cold and hot TEG module sides, The TEG module open circuit voltage and its current over a 1 Ω resistorwithaccuracy 1%. The open circuit voltage and current aremeasured alternatively, using a relay. The time interval for these measurements for collecting data is set as 6s for one hour experimental work.

6.7.1 Thermocouple Conditioner

The thermocouple is a temperature sensor, which consists of two wires of dissimilar metals joined together at one end called the measurement (hot) junction [163].

They convert a temperature difference into electricity via the Seebeck effect. Here, type K thermocouples were used. Type K has one wire composed Chromel and the other wire is Alumel (95% Nickel, 2% Magnesium, 2% Aluminium). These thermocouples are the most common type in use, and are inexpensive. The measurements made here are well within the acceptable range which extends to from 0 °C to over 1000 °C with an accuracy of about ± 1.5 K.

The thermocouple conditioner was made in our lab with operating temperature range of -55 to +125 and powered range between +5 to 15 V specifications. The input to the thermocouple conditioner is the signal from the thermocouple and the output is a linearized voltage of 20 mV/°C. The output provides a measure of the temperatures of hot and cold sides and surrounding air as shown in Figure 6-9.



Figure 6-9 Thermocouple conditioner

6.7.2 Experimental Procedure

For each test there were five channels to be viewed; hot side temperature, cold side temperature, ambient temperature and open circuit voltage and current.

The procedure for the experiment was:

- Place the TEG module on the hot plate, see Figure 6-11
- The test is to take six measurements for each Heat sink.
- Start the DAQ software and wait to the temperature to settle down and stabilise as shown in Figure 6-10.

When the temperatures of the hot side and cold side become stable, collect data every 6 seconds

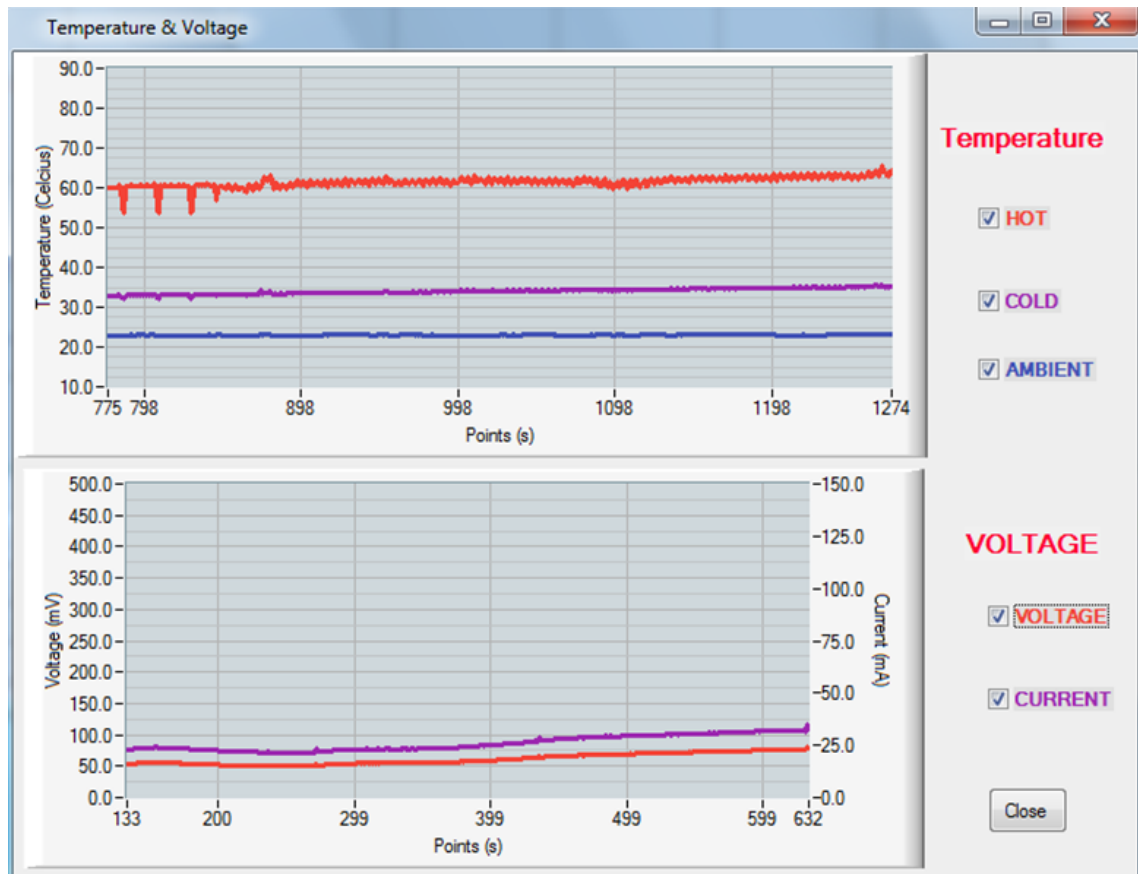


Figure 6-10 Screenshots measurements made by of DAQ software

The test consisted of, firstly, turned on the hot plate and setting the temperature required using the temperature regulator. Leaving the hot plate for about 25 minutes until the temperature became stable. The room temperature remained at about 21°C. The TEG was then placed on top of the hot plate, as shown in Figure 6-11, and data collection commenced. Unfortunately, the hot plate also heats the surrounding air and by so doing, reduces effectively the performance of the heat sink. For this research, thermally insulating material was used to shield the body of the heat sink from the heat source. The temperature of the hot plate was set, sequentially, to 30, 40, 50, 60, 70 and 80°C.

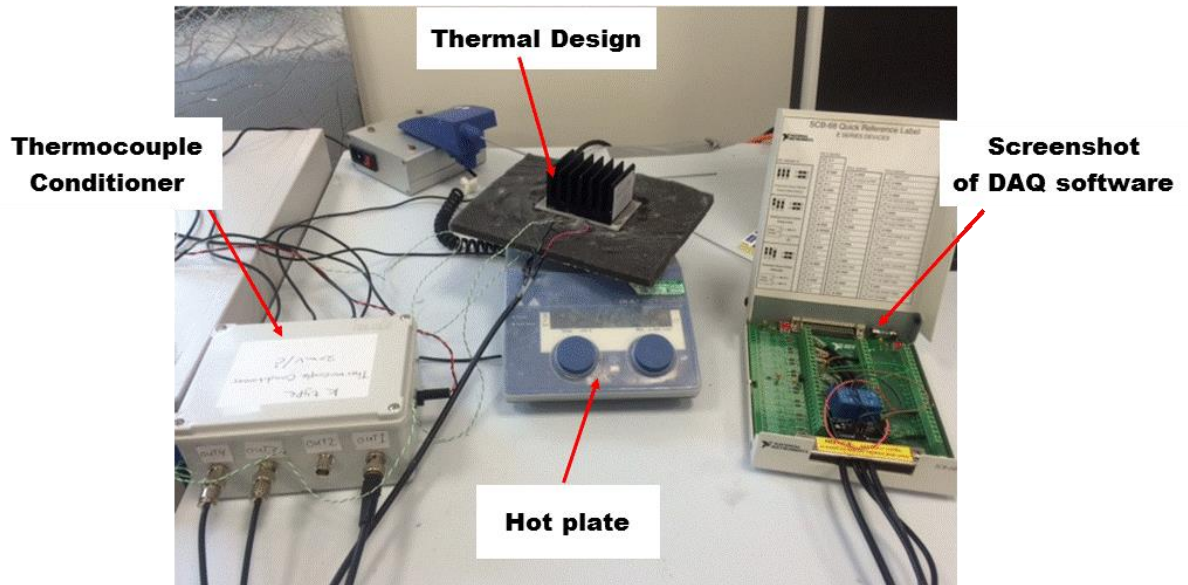


Figure 6-11 Experimental step

6.8 Results and Discussion

Figure 6-12 shows the measurements made for smallest of the heat sinks (A); hot side temperature (T_h), cold side temperature (T_c) and ambient temperature (T_a), it also shows difference temperature ($T_h - T_c$), open circuit voltage (V_G) and current through the 1 Ω resistor.

It can be observed that the values of T_h , T_c and T_a are nearly constant; that ambient temperature is in the range 19-20.5 $^{\circ}$ C, that the temperature difference ($T_h - T_c$) depended on the value of T_h . It can be seen that for the plate temperatures of 30, 40, 50, 60, 70 and 80 $^{\circ}$ C the corresponding values of V_G were 30, 65, 100, 150, 190 and 220 mV.

Figure 6-15 also shows that the current through a 1 Ω resistor for the plate temperature of 30, 40, 50, 60, 70, and 80 $^{\circ}$ C the corresponding values of 10, 25, 40, 50, 75, and 80 mA.

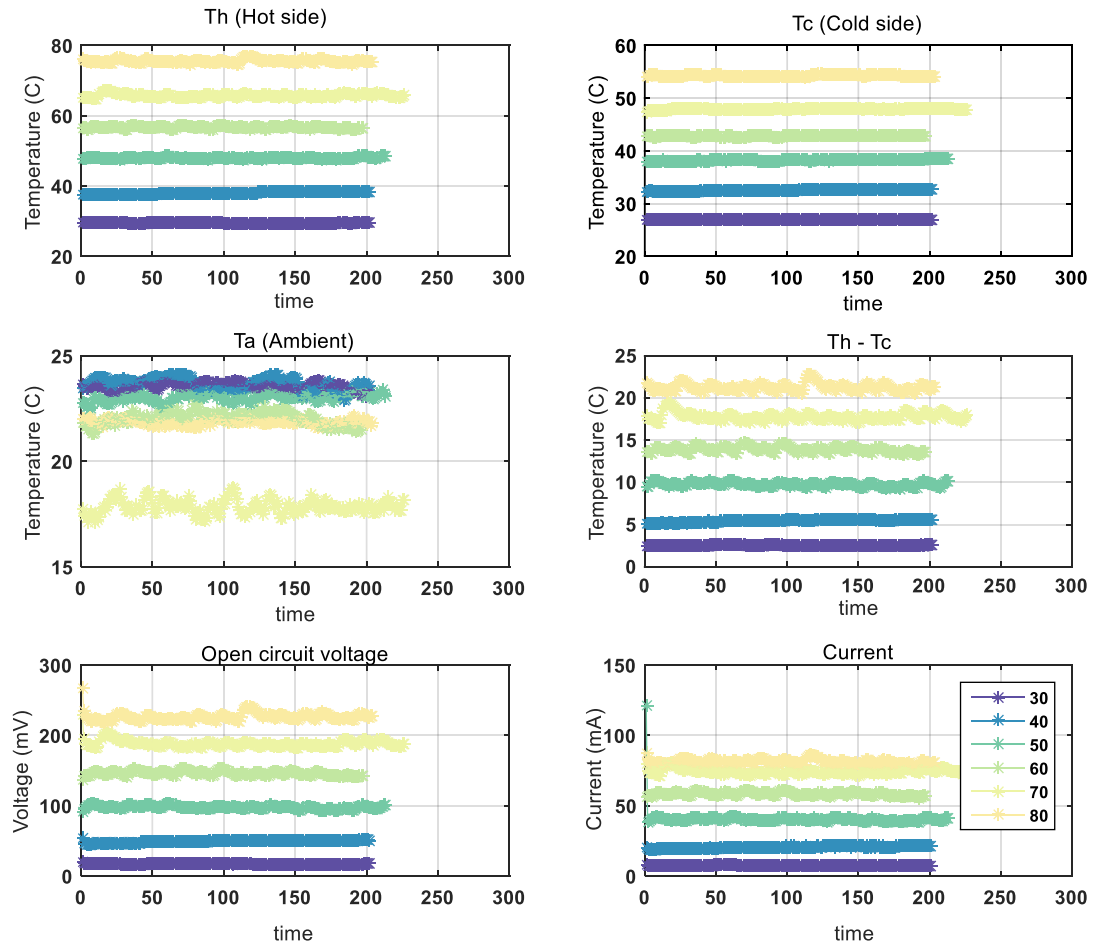


Figure 6-12 Heat sink (A)

Figure 6-13 shows the measurements made for intermediate heat sink (B). The ambient, room, temperature was in the range 20-25 °C. The temperature difference ($T_h - T_c$) is in the range 2-22 °C with ($T_h - T_c$) depending on the value of T_h .

It can be seen that for the plate temperatures of 30, 40, 50, 60, 70 and 80 °C the corresponding values of V_G were 30, 60, 100, 160, 200 and 250 mV. From the figure, it can also be seen that the current can reach about 100 mA for temperature 80 °C. However, for the plate temperature of 30 °C, it can produce 5 mA.

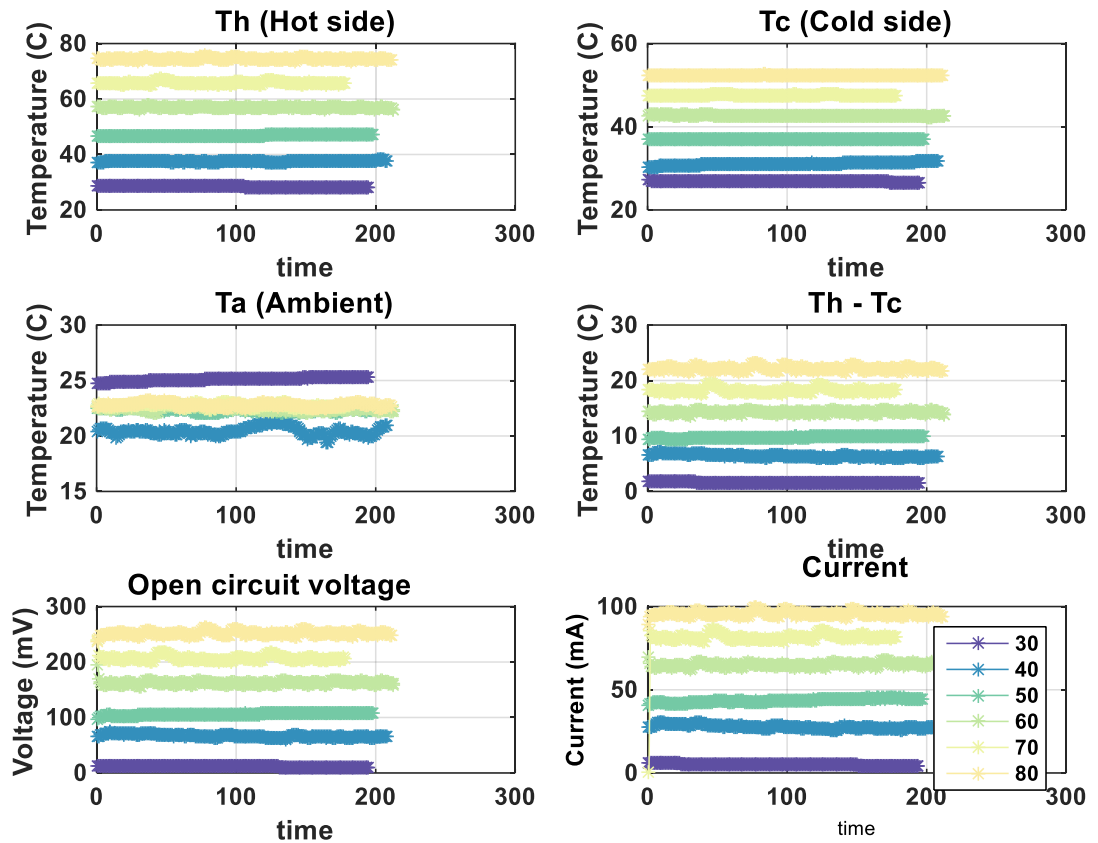


Figure 6-13 Heat sink (B)

Figure 6-14 shows the measurements made for the largest of the three heat sinks (C). It can be seen that for the plate temperatures of 30, 40, 50, 60, 70 and 80 °C the corresponding values of V_G were 30, 80, 140, 190, 250 and 300 mV. However, the temperature 30 °C produces voltage about 30mV.

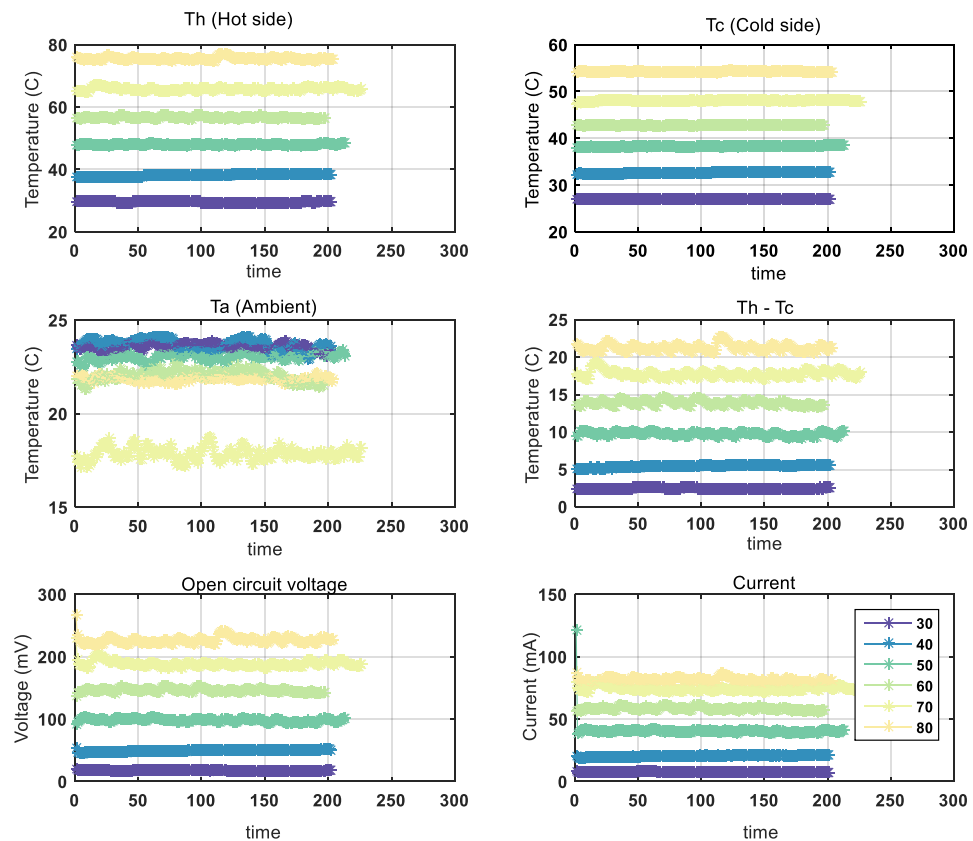


Figure 6-14 Heat sink (C)

Figure 6-15 shows plots of the measured open circuit voltage as a function of the measured temperature difference across the TEG module. It can be seen that the open circuit voltage increases linearly with temperature difference for all three all heat sinks. Clearly heat sink (C) produces the largest voltage for a given temperature difference.

Figure 6-15 also shows that the current through a 1Ω resistor also increases linearly with temperature difference for all three heat sinks. Given that it produces the largest voltage we see heat sink (C) also produced the largest current for a given temperature difference, i.e. a current of about 100 mA for a temperature difference of $40 \text{ }^{\circ}\text{C}$.

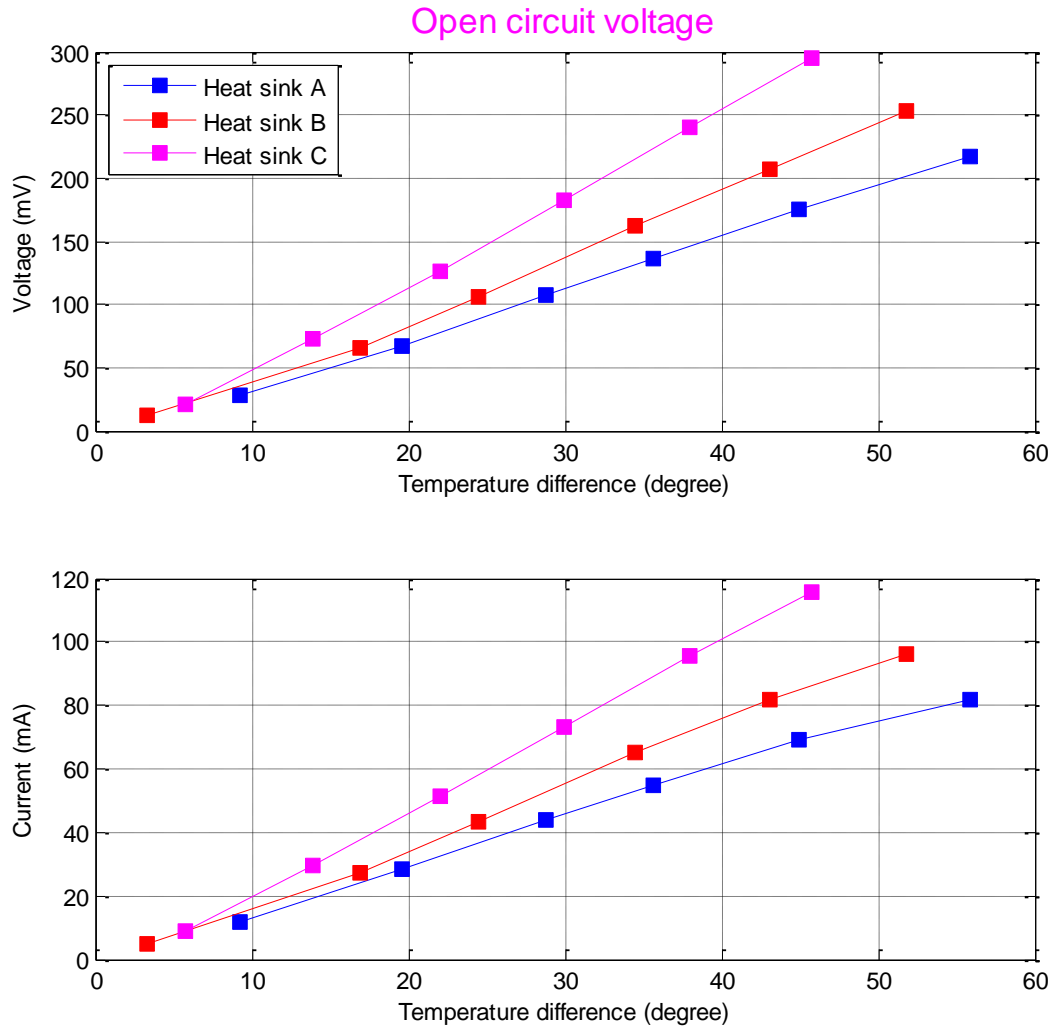


Figure 6-15 Measured open circuit voltage

Figure 6-16 shows the power output of the TEG for each of the three heat sinks. It can be observed that the power generated by the TEG module is greatest for the largest of the three sinks, because it is the most effective at dissipating heat and so produces a lower cold side temperature for a given heat side temperature. Heat sink C is the most effective.

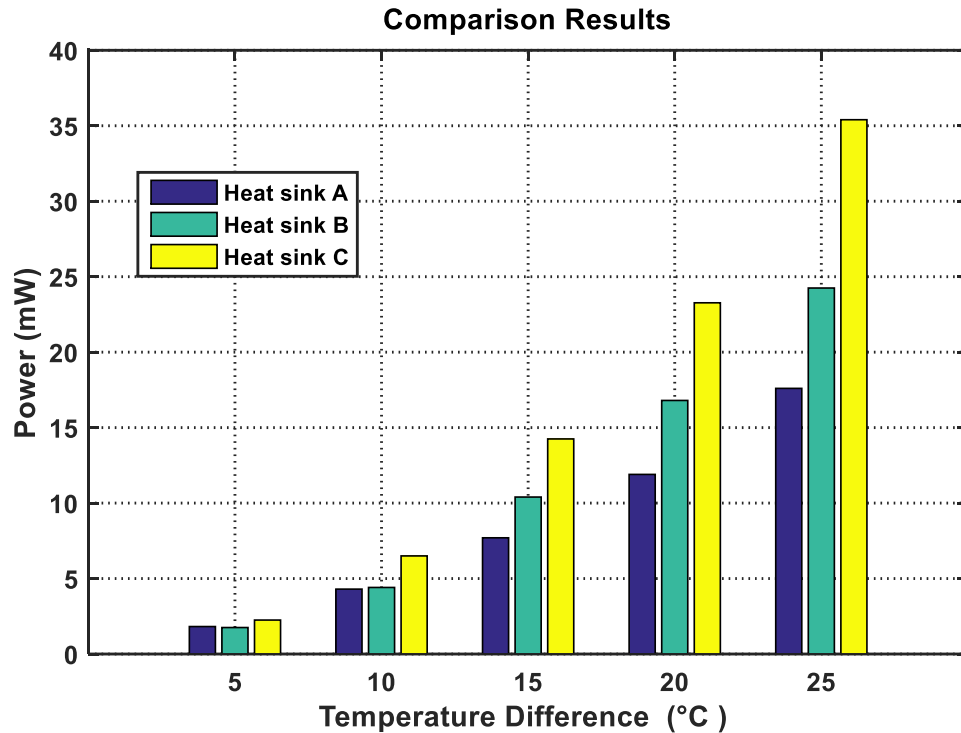


Figure 6-16 Result comparison for the three Heat sinks

6.9 Summary

The heat transfer performances for the three various heat sinks specifications were tested to determine which was the most effective at powering a Peltier TEG module. TEGs convert heat energy into electricity dependent on the temperature difference across them and it was found, as expected, that the heat sink which provided the greatest heat dissipation facilitated the greatest difference temperature across the TEG transfer and the largest open circuit voltage.

Chapter 7. The Optimisation of Thermal Energy System with Temperature Sensor for Monitoring a Gearbox

Efficiency is an important factor in the design of energy harvesting systems. Other factors which constrain the design of such systems are the cost and size (both volume and mass).

For this chapter, a thermal energy harvesting system has been designed in powering the wireless sensor node to monitor the temperature of a gearbox. The system design is based on the results presented in the previous chapter. This chapter describes improving the efficiency of the thermal energy harvesting system. The system being proposed enhances the efficiency of its energy as follow: Firstly, the designing of the Thermoelectric generator in order to increasing the efficiency of the energy conversion and secondly, developing an algorithm to effectively manage the power in order to improve the efficiency of the energy consumption.

Then, the chapter describes the experimental work of using the thermal energy harvesting design developed to power the WSN to monitor the temperature of the gearbox. The chapter concludes with a presentation of results obtained and a comparison of model predictions and experimental results.

7.1 Introduction

Thermal is another energy source which can be converted from our environment. Typically, sources of heat can be taken using many different forms, such as industrial machines, the human body, sunlight and exhaust gases. Recent improvements in materials that are thermoelectric have renewed the interest in TE generators.

The reason this thesis considers the development of a thermal EH system is to extend the work of those who have successfully applied thermal EH in other areas, to the condition monitoring of machines, in this case a Helical gearbox.

7.2 Experimental Setup

In order to evaluate its performance efficiency, the designed TEG system was tested in the laboratory on an industrial gearbox with a room temperature of 24 °C. The TEG was optimized to harvest the electrical power from the heat generated by the gearbox being monitored. The power generated was from the temperature gradient across the TEG obtained by sandwiching the TEG between two thin aluminium plates, placing one plate against the hot surface of the gearbox and attaching the second plate to a heat sink open to the surrounding air. The harvested power is then used to power a WSN to transmit the measured temperature to monitor the condition of the gearbox.

7.2.1 Gearbox Test Rig

The experimental test rig can be seen in Figure 7-1. The component parts consist of a 15 kW, prime driver (3 phase ACIM), 2 back-to-back two stage helical gearboxes in order to couple the AC motor together with a load generator by the use of spider rubber couplings that are flexible. The couplings

include a hard rubber with 150 mm diameter, three-jaw type with power transmission capabilities up to 100 kW at 1600 rpm. The transmission power is 3 kW for each gearbox. GB1, which is the first gearbox, operates in reducing the speed while GB2 increases the speed. In this way, the system maintains speed quite sufficient enough at the DC in producing an adequate load on the AC motor. The specifications for the gearboxes, AC motor, couplings and DC motor are given in, Table 7-1.

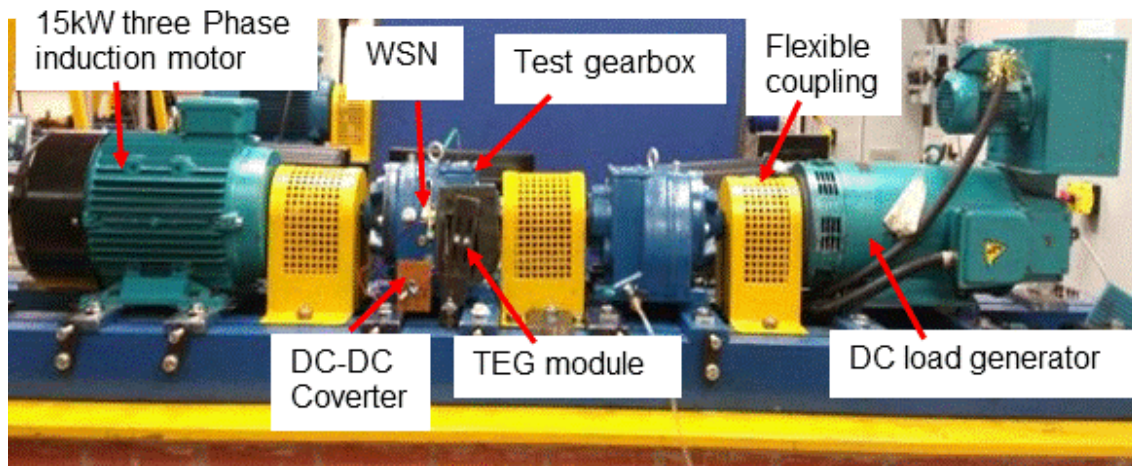


Figure 7-1 Test Rig

Table 7-1 Specifications for the AC motor as provided by manufacturer

Manufacturer	Invensys, Brook Crompton
Model of the Motor	T-DA160LA
Poles Number	4
Motor Frequency	50 Hertz
Motor Power	3 Phase 15 kW
Voltage at 50 Hz frequency	415 Volts
Rated Current	27.13 Amps
Connection	Delta Δ connection
Rated Speed	1460 rpm
Power factor (Cos Φ)	0.87
Full load torque	98.3 <u>N.m</u>
Stator resistance	0.8607 Ω
Stator Leakage Inductance	0.01678 H

7.2.2 Wireless Measurement System

When designing the EH system, the sensor node characteristics are vital as the power the system must provide is closely determined by the sensor node power consumption. Thus, an understanding of the behaviour and performance of the WSN is a necessary part of designing an efficient EH system. A Texas Instruments Sensor Tag CC2650K, sensor node was chosen as the target sensor node to be powered by thermal EH.

The WSN chosen should be small, inexpensive and energy efficient. The low cost and low power requirements requires that the sensor node must use a processor with low power consumption such as (BLE), a short transmission range and low power consumption sensor. Thus, the WSN is constrained in its computation and communication capabilities. Selecting an appropriate sensor meant balancing these requirements.

There are many other factors, each of which plays an important role in selecting a sensor such as environmental conditions, design parameters and sensor parameters.

7.2.2.1 Temperature Sensor

As stated above, the temperature sensor node was an integrated WSN, a Texas Instruments Sensor Tag CC2650STK, see Figure 7-2. The Sensor Tag was used due to its low power consumption, low cost, miniature design, low maintenance, and EH is included.

This compact sensor node integrates 10 low-power MEMS sensors and a two core BLE microcontroller CC2650 [164]. Two temperature sensors are available on the node, one for measuring object temperature and the other for ambient temperature. Another benefit of this module is that its programs are open source, which meant it could be customized for data acquisition as could the intelligent signal processing algorithms embedded on it.

The SensorTag is specially designed for low power consumption applications and it is claimed to offer years of battery life from a single lithium CR2302 coin battery currently costing about £1 [164]. Here, the coin battery was not used;

instead the SensorTag was powered by the energy harvested from waste heat from the gearbox.



Figure 7-2 Texas Instruments SensorTag CC2650K

The main features of the SensorTag are listed below:

- Power supply range: 1.8 V to 3.8 V,
- Operation temperature range: -40 to 125 °C,
- Accuracy ± 1 °C from 0 to 60 °C,
- Mass 30 g
- Ultra- low power
- Converts temperature to 12-Bit,
- BLE specification and IEEE802.15.4PHY
- Adds support for more low power sensors
- 10 sensors channels suitable for a wide range of sensors, including accelerometers and temperature measurement.

The SensorTag has a high performance ARM Cortex M3 (CC2650) with cloud connectivity which means the SensorTag can be accessed and controlled from

almost anywhere. Importantly the SensorTag offers seamless integration with mobile phone apps.

7.2.2.2 CC2540 USB Evaluation Module Kit

The CC2540 USB Evaluation Module Kit supplied with the SensorTag is shown in Figure 7-3. The kit contains one CC2540 BLE USB dongle which can be used to enable BLE on computer PC. It can also be used for analysing BLE protocol and for software and system level debugging (Texas Instruments provide a free internet tool SmartRF Packet Sniffer to assist with this). [127].

The CC2540 contains a number of features that make it suitable for systems that require very low power consumption. These include short transition times between operating modes and very low-power sleep modes [165]



Figure 7-3 Texas Instruments CC2540 USB Module

Relevant features of the CC2540 USB Module are listed below:

- Bluetooth V4.0 compliant protocol stack for Single-Mode BLE Solution
 - Complete Power-Optimized Stack, Including Controller and Host
 - Sample Application and Profiles
 - L2CAP

- Generic Application for GAP
- Development Tools
 - SmartRF Software
 - Supported by IAR Embedded Workbench
 - CC2540 Mini Development Kit

7.3 Thermal Image

An advanced thermal camera ThermoCAM S65 from FLIR systems was used to determine where on the gearbox it was best to place the TEG module to maximise electricity generation and to determine the temperature of the body of the gearbox. The thermal camera's sensitivity can reach $\pm 0.08^{\circ}\text{C}$ at 30°C and can be used to measure temperature in the range 0°C to 500°C . The thermal camera produces an image with 320×240 pixels, thus an acceptably accurate thermal distribution can be obtained. The camera is shown in Figure 7-4 and its specifications are shown in Table 7-5.

Table 7-2 Thermal CAM S65 technical Specification

Field of view/min focus distance	$24^{\circ} \times 18^{\circ} / 0.3 \text{ m}$
Spatial resolution (IFOV)	1.3 mrad
Electronic zoom function	2, 4, 8, interpolating
Focus	Automatic or manual
Digital image enhancement	Normal and enhanced
Detector type	Focal plane array (FPA) uncooled microbolometer; 320×240 pixels
Spectral range	7.5 to $13 \mu\text{m}$
Thermal sensitivity @ 50/60Hz	0.08°C at 30°C
Built-in digital video	Built-in digital video
Temperature ranges measurement	-40°C to $+120^{\circ} \text{C}$, Range 1



Figure 7-4 Thermal CAM S65

7.3.1 Thermal Camera Test Result

Figure 7-5 and Figure 7-6 show the temperature distribution of the surface of the gearbox at 10 min and 60 min after start-up. In the thermal image, the temperatures are represented by various kinds of colours whose corresponding temperature can be found in the colour bar shown at the right side. It can be seen that the best place to put the TEG module is vertical position of the gearbox surface.

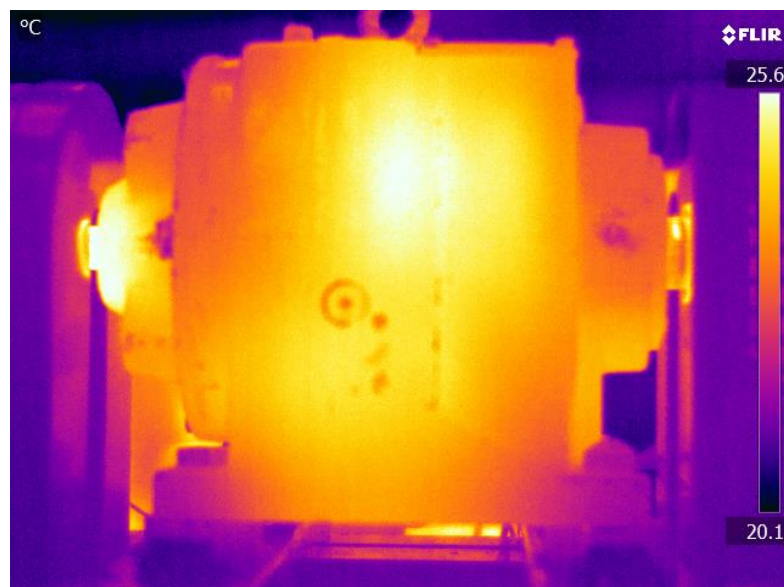


Figure 7-5 The thermal images of the gearbox after (10min)

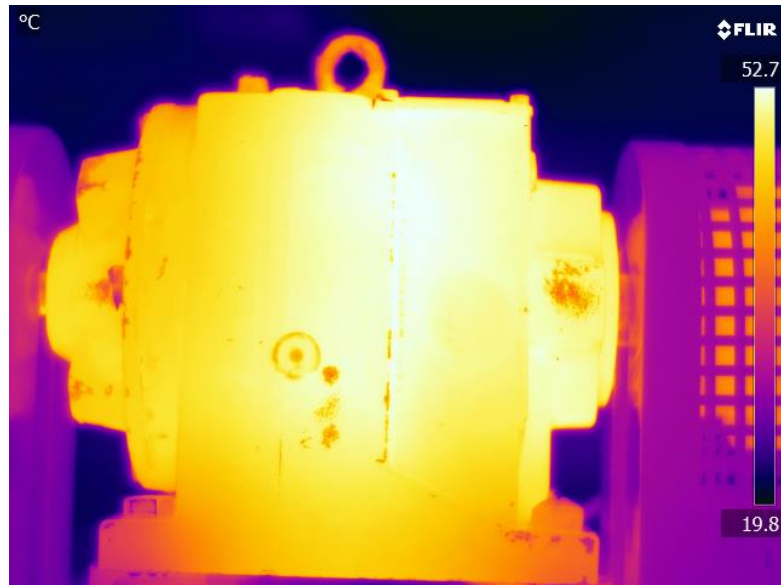


Figure 7-6 The thermal images of the gearbox after (60min)

7.4 The TEG System Evaluation

As mentioned in the preceding sections, the EH efficiency of the TEG is the most important factor in determining the efficiency of the entire system. Therefore, the procedure for the first evaluation is to confirm how much of the thermal energy might be harvested from an industrial machine such as a gearbox using the TEG module. Figure 7-7 shows the experimental setup used to evaluate the proposed TEG system.

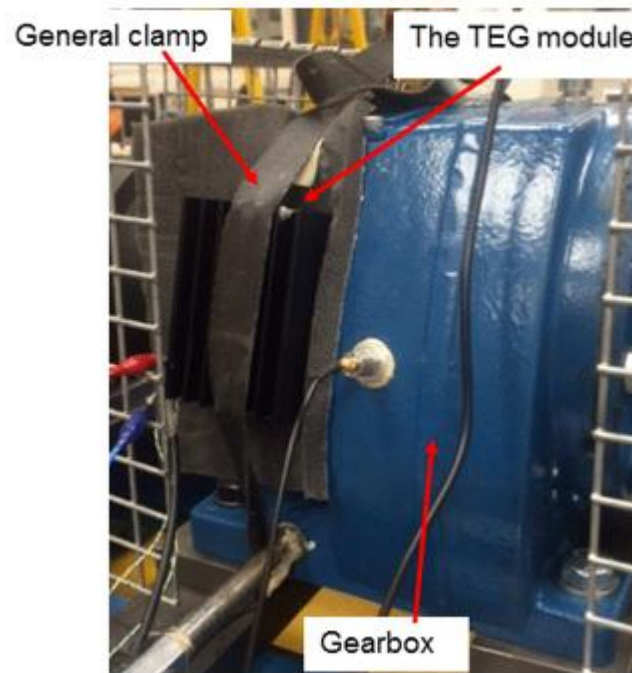


Figure 7-7 Experimental setup for thermal energy harvesting system

7.4.1 Test Procedure

To simulate a constant load and variable speed operating conditions common to industrial machines, the tests were carried out for different AC motor speeds for a fixed load applied (fixed load variable speed operation).

The test conditions were: the AC motor was run at the given operating speed (70% and 100% full speed) for one hour for test each cycle. The load was fixed during the cycle. Figure 7-8, is a photo of the tooth breakage fault seeded into the gearbox, 40% of one of the teeth was removed.



Figure 7-8 Tooth breakage fault

The data was collected for every run and each test was repeated at least six times, to ensure that repeatable results were being collected and random errors would be substantially reduced on averaging.

The TEG system was held close to the body of gearbox by holding it vertically with clamp which the best place as shown in the thermal images. The heat from the body of the gearbox is collected by the TEG module and converted to electricity to power the SensorTag. Meanwhile the working condition of the TEG module is monitored by an external data acquisition system to evaluate its performance.

7.4.2 Results and Discussion

The TEG module measured; hot side temperature, T_h , cold side temperature, T_c , temperature difference between hot and cold sides, $T_h - T_c$, open circuit voltage and current through a 1Ω resistor, and are presented in Figure 7-9. It is observed that both T_h and T_c have larger values for the higher speed case than for the lower. This was expected since more heat is generated when the gearbox is driven at a higher speed.

It is the temperature difference, ΔT ($T_h - T_c$), that generates the electrical power and it was noted that the difference in ΔT obtained with lower and higher speeds was negligible initially, but once the duration of the test exceeded about quarter of an hour, the difference in ΔT settled down to between 0.5 °C and 1 °C with the faster speed producing the greatest difference, which would be expected given the greater heat generated at the higher speed.

Somewhat surprisingly ΔT for both the high and low speed cases appeared to decrease for the first 15 minutes of operation, reaching minimum values around 1000 s. As expected T_h , T_c , and ΔT all reached their maximum values at the end of the test run.

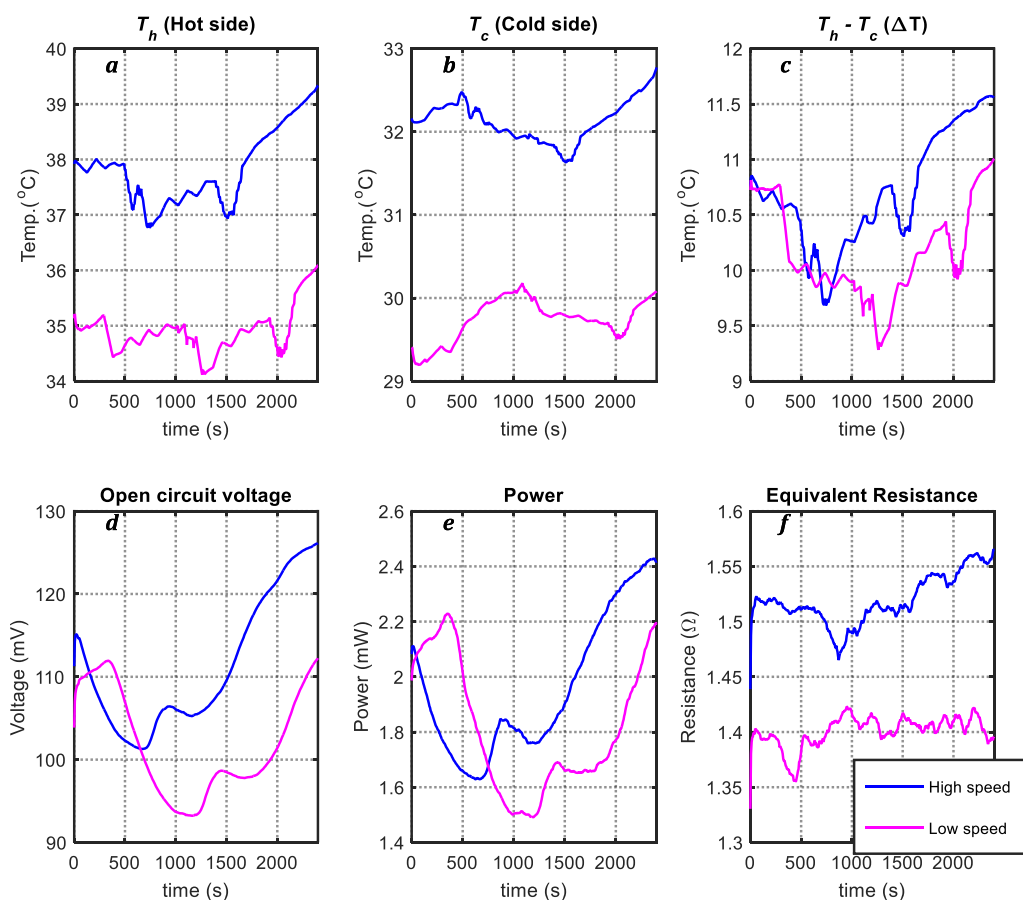


Figure 7-9 TEG module performance for high and low speed gearbox tests

The trace of the open circuit voltage followed the plots for ΔT closely (which is good). The measured values of the open circuit voltage generated by the TEG module ranged from 95 mV to 125 mV, which meets the input voltage requirement of the DC/DC booster circuit. By measuring the voltage across the 1 Ω resistor, the power consumption of the resistor was calculated as V^2/R (?) and is shown in Figure 7-9(e) which indicates the power output of the TEG module that can be harvested. Note that after about 1000 seconds, even at the lower speed the power available is about 1.5 mW, though at 2400 s and nearer to the steady state operating conditions the power output is 2.2 mW. Again there is a surprise, it appears that - at least initially - the lower speed produces more electrical power than the higher speed. However, after about 12 or so minutes it is observed that the power output for the higher speed is greater than that for the lower speed.

By using the open circuit voltage and current through the 1 Ω resistor, the equivalent resistance for the TEG module can be computed and is shown in Figure 7-10(f). It appears that the internal resistance of the TEG is significantly different from the 1 Ω resistor, 1.5 and 1.4 Ω respectively for the faster and slower speed. There is a difference of about 0.1 Ω observed between the internal resistances for two speed conditions.

Apart from temperature difference on its two sides, the power output capability of the TEG is also affected by the Seebeck coefficient, which is influenced by the temperature. Due to this phenomenon of the material, the internal resistance of the TEG module also changes with the temperature.

7.5 Development Features of the TEG Design Test Rig

7.5.1 The Initial Design Evaluation

Initially the clamp used to attach the TEG to the gearbox was a general laboratory clamp as shown in Figure 7-10, that was considered to be not very professional because the TEG module was not fitted properly into the gearbox and adversely effected to the output results and thus a new design of clamp was developed and used.

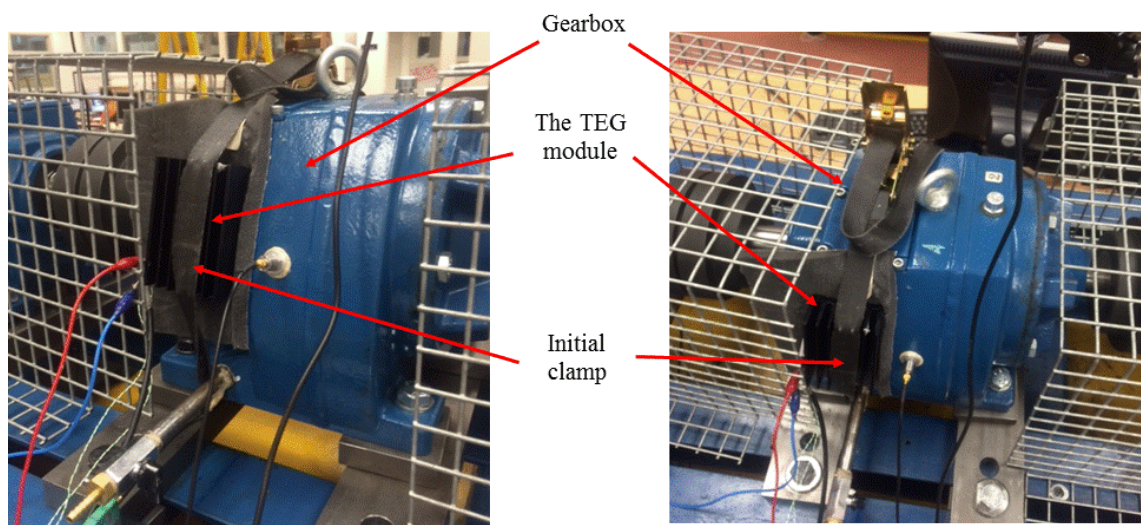


Figure 7-10 Picture of the TEG module held general laboratory clamp

7.5.1 The Developed Clamp

Figure 7-11 illustrates the clamp designed, developed and manufactured in the engineering workshops in the University of Huddersfield. The new clamp ensured a better fit of the TEG module into the gearbox than the general laboratory clamp. The 3D solid model is shown in Figure 7-11(b). Figure 7-12 is a second photo and schematic of the TEG attached to the gearbox. The TEG module was attached to the body of the gearbox by clamping it in a vertical position.

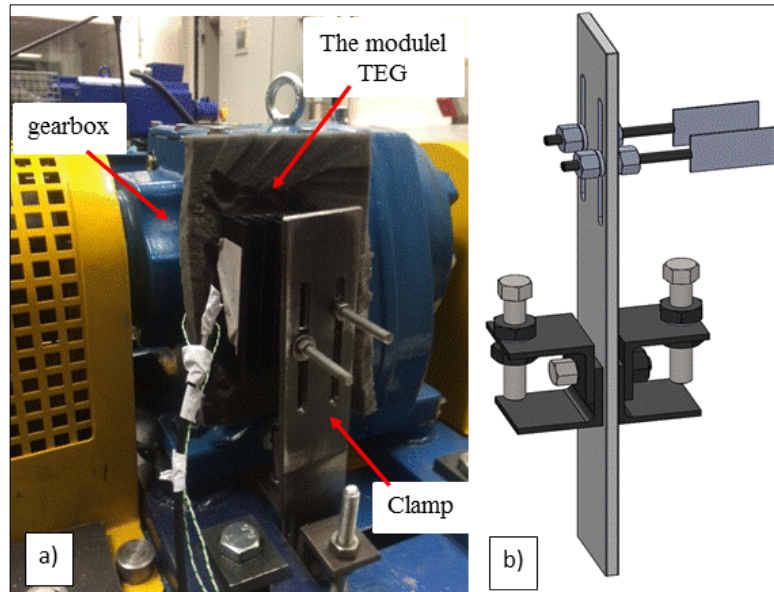


Figure 7-11 a) Module with developed clamp, b) illustrated of solid model of the developed clamp

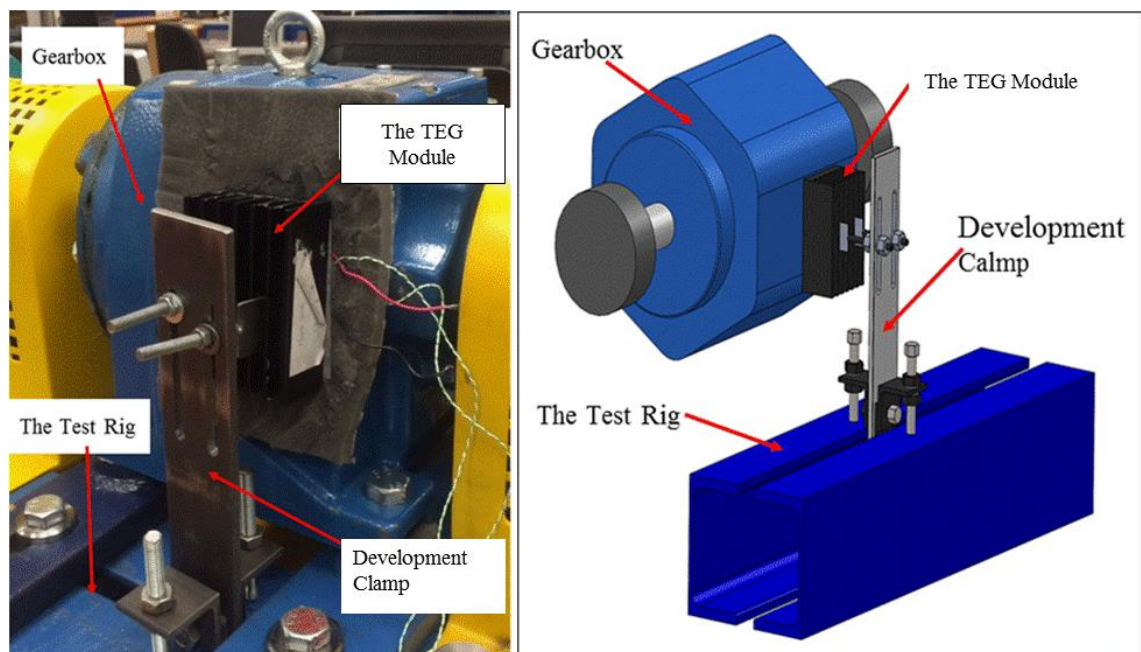


Figure 7-12 Photo of TEG module attached to gearbox using bespoke clamp and schematic of the clamp

Figure 7-13 shows results obtained with both clamps. It can be seen the developed clamp gave better results. Therefore, the developed clamp produces higher difference temperature hence produces high voltage.

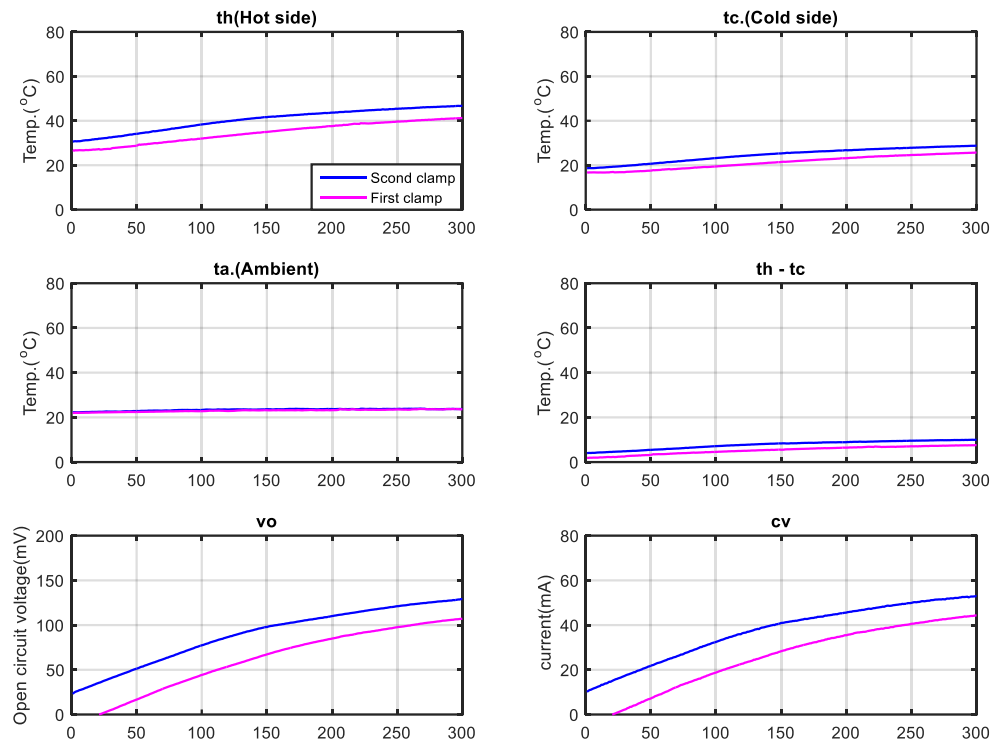


Figure 7-13 Results using different clamps

There were two ways to get the data from the SensorTag, first, by using an app on a smartphone, second using the CC2540 USB Evaluation Module Kit. By connecting the sensor tag from the application running on a smartphone, the sensor information on the sensor tag can be easily acquired via BLE, as shown in Figure 7-14.

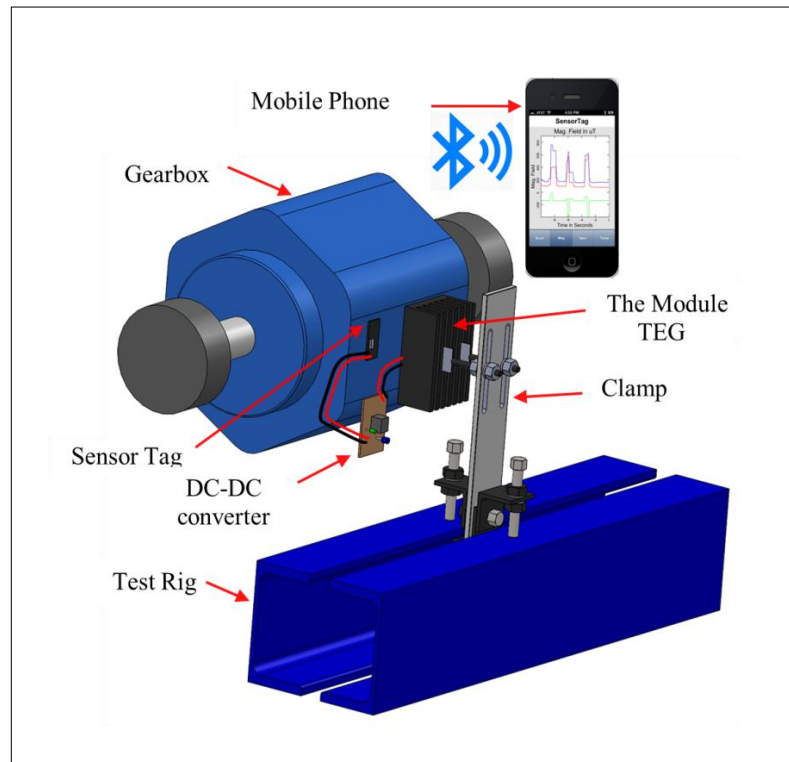


Figure 7-14 The TEG powered wireless temperature measurement

Figure 7-15 shows the experimental test system to which the TEG module was attached and USB module receiving the data. By connecting the sensor to the CC2540 USB Evaluation Module Kit via BLE data was transferred to a computer.

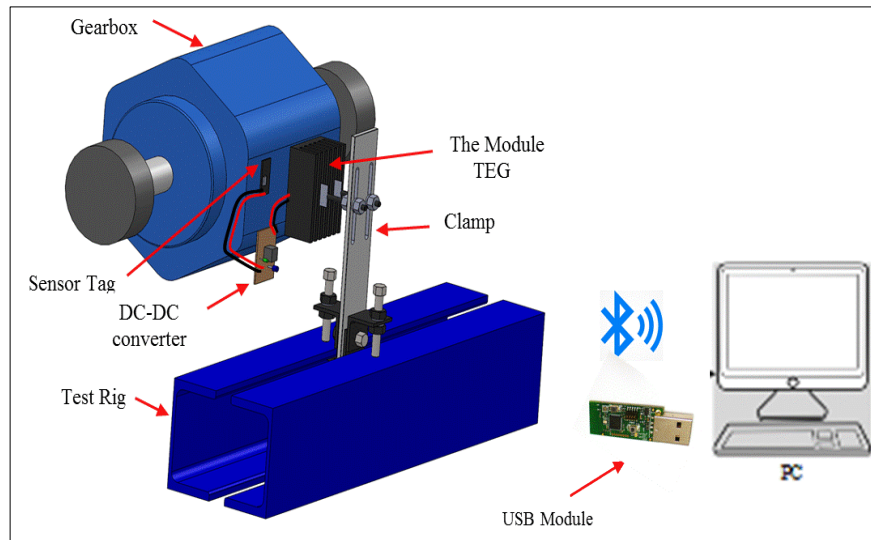


Figure 7-15 Test system

7.6 Results and Discussion

In the experiments the performance of the TE generator system was explored and evaluated based on comparing a healthy gearbox and gearbox under abnormal operation. In the first test, the AC motor was run at 80% load and full speed.

The experimental results are shown in Figure 7-16. It can be seen that the maximum harvested energy is as much as 10 mW when the temperature difference is around 17.5 which is maintained between the hot side and cold side with temperature difference of the gearbox under abnormal operation than healthy gearbox. Clearly the faulty condition generates more heat than the healthy condition, and this means more electrical power is generated and the power harvested by the TEG module for abnormal operation is higher than that for the healthy condition.

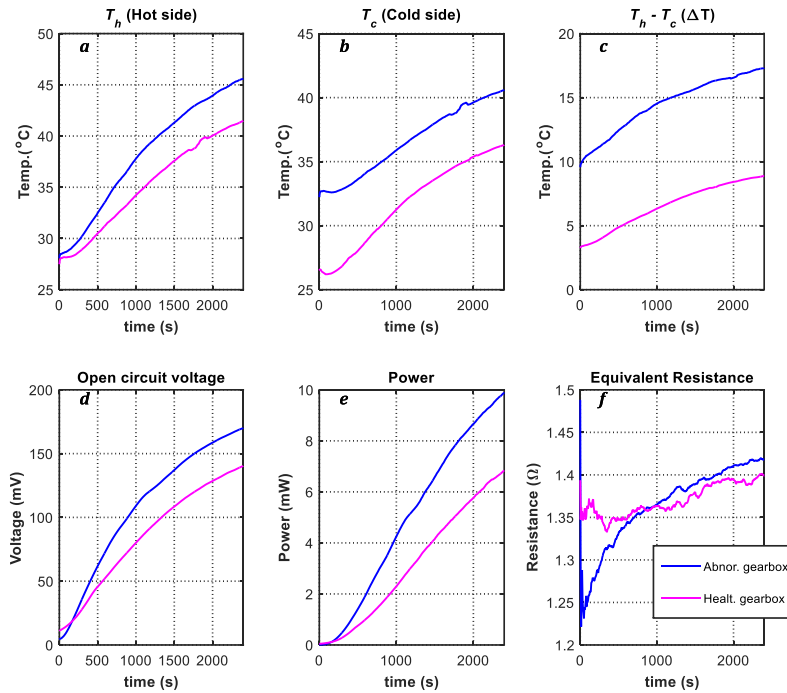


Figure 7-16 TEG module performance for high and low speed gearbox test

By running the gearbox at 70% speed for about one hour, the super capacitor can be fully charged to about 5.2V.

The integrated temperature sensor measures both the object and ambient temperature. As shown in Figure 7-17, the ambient temperature was about 30.9 °C while the object gearbox temperature is around 45.1°C. By programming the sensor node to operate periodically, it can achieve automated temperature monitoring without requiring an external power source such as a battery for the sensor node.

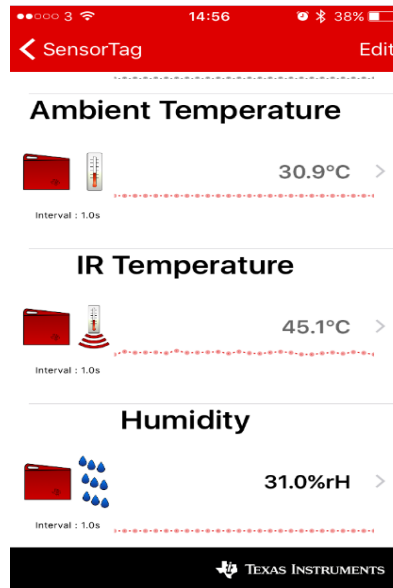


Figure 7-17 Screen shot of measurement on a mobile phone

Figure 7-18 shows the experimental test system to which the TEG module was attached the gearbox and by USB Module receiving the data.

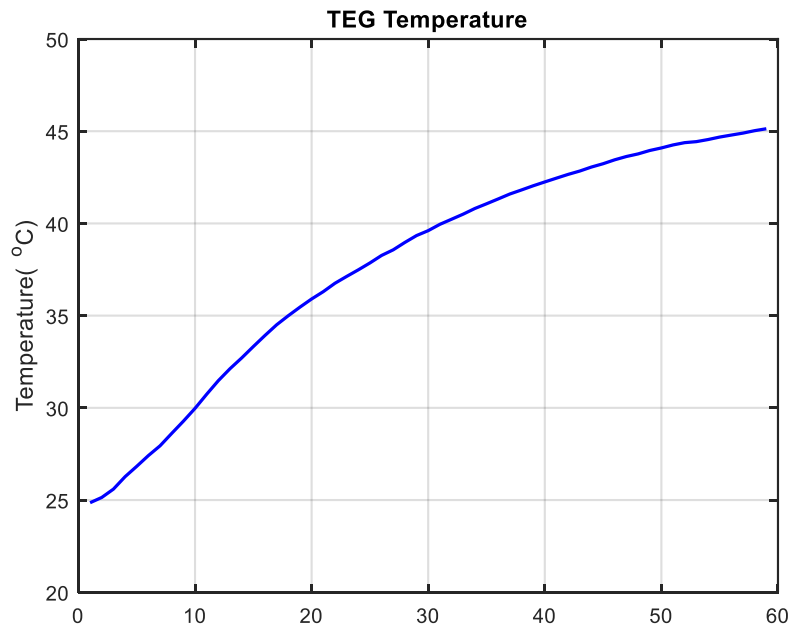


Figure 7-18 Temperature of gearbox by sensor tag

7.7 Comparison of the Results from Three Different Research Elements

This section presents a comparison of the results from the theory developed to underpin the Finite Element Analysis simulation and the experimental investigation.

Experimental data was compared with the simulation results for open circuit voltage, see Figure 5-19. The following equation for voltage generation in a TEG module, was used to predict the open circuit voltage:

$$V_G = N\alpha_{ab}\beta\Delta T \quad (7-1)$$

V_G Open circuit voltage,

N Number of thermocouples

α_{ab} Seebeck coefficient,

β Coefficient,

ΔT Temperature difference between TEG's hot T_h and cold sides T_c .

Regarding the Figure 7-20, the correlation between the two sets of results is good with an accuracy for the predicted results of about 85 %. Therefore, the results have shown a good agreement to that of the open circuit voltage value of 160 mV that have been calculated using the previous equation.

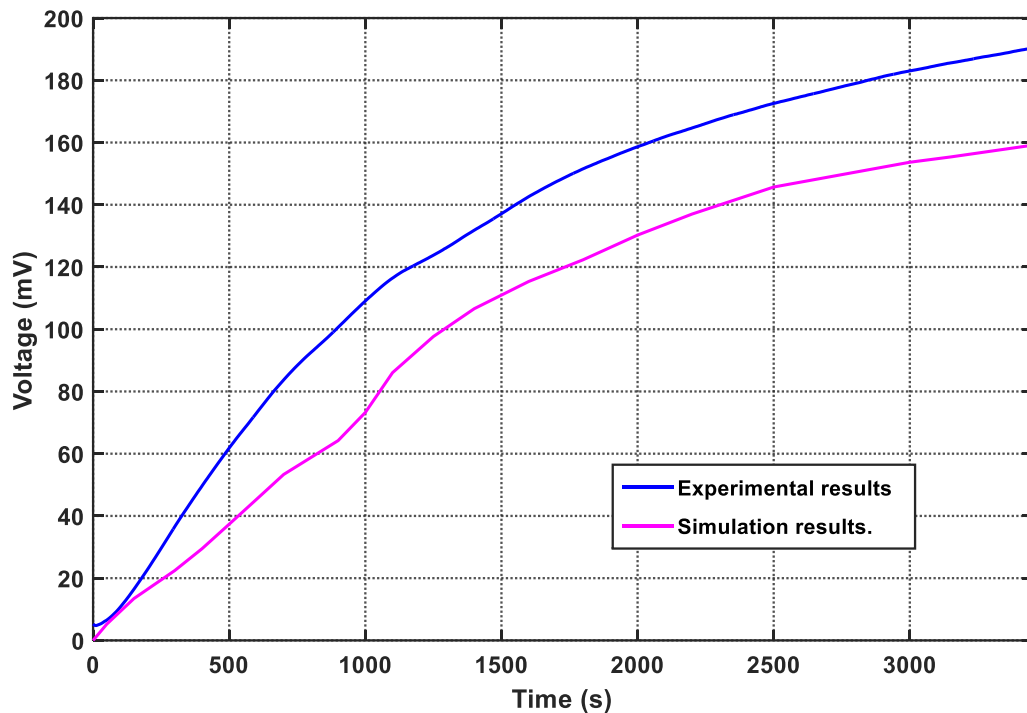


Figure 7-19 Comparison of open circuit voltage obtained by experiment and simulation

7.8 Summary

In this chapter, the author has successfully applied a highly efficiency thermal EH system to power a WSN using the design and structure developed in previous chapters. The TEG system has been sized optimally based on the theoretical model. The results show that the TEG system was able to harvest up to 10 mW of electrical energy from the industrial gearbox running under steady state conditions, and that the temperature of the gearbox was successfully measured by the sensor node and transmitted to a smart phone without needing the provision of external power to the sensor node. These results have shown a good agreement to that of the theoretical calculations. The simulation results are in good agreement the experimental results, the value of the model's predictions are consistently about 85% of the experimental values.

Chapter 8. Monitoring of Gearbox Using a Wireless Temperature Node Powered Thermal Energy Harvesting Module

Condition monitoring (CM) of gearbox is a crucial activity due to its importance in power transmission for many industrial applications. Monitoring temperature is an effective mean to collect useful information about the healthy conditions of the gearbox.

This chapter investigates the use of a wireless temperature node to detect the presence of a fault in a gearbox transmission system under different conditions. The wireless temperature node was integrated a novel feature, it is supplied with power by a thermoelectric generator module mounted on the gearbox house to be monitored so that the measurement system avoids the shortage of using a wired power sources or the requirement for recharging or changing batteries. The temperatures from lubricating oils and housing are modelled to implement model based detection.

8.1 Test Facility and Method

The gearbox test rig, shown in Figure 8-1, was used in this experimental study and has been described in Section 7.2.1. The construction allows the study of different faults seeded into the gearbox transmission system under different conditions. The TEG module was mounted directly into the surface of gearbox to power up the wireless temperature node, which it was mounted directly on the gearbox while another wireless temperature sensor measured oil of the gearbox as shown in Figure 8-1. The temperatures of the oil and surface of the gearbox were measured simultaneously.

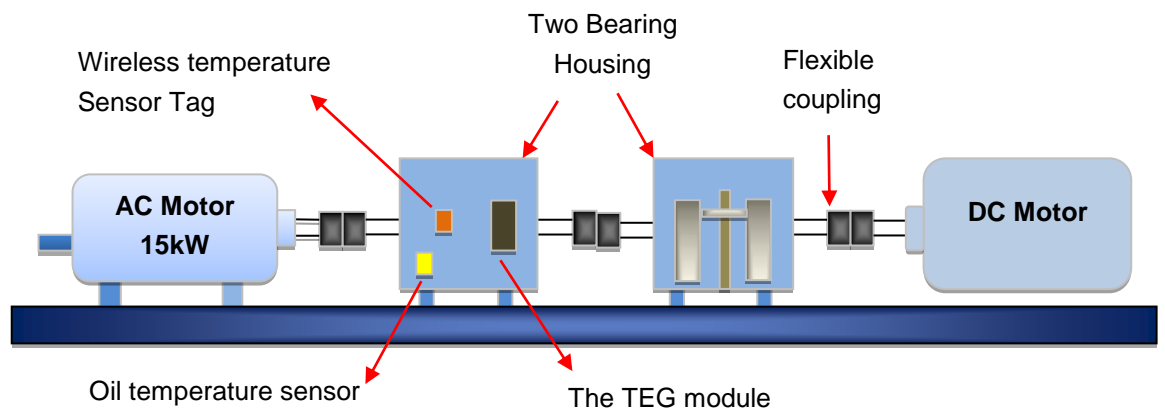


Figure 8-1 Test rig schematic showing sensor placements

8.2 Test Procedure

The test rig was operated at fixed speed with a 100% full AC speed of the motor, at four load settings increments: 100%, 70%, 30% and 0%. The aim is to investigate the detection process under variable load operation and constant speed, which are commonly used in real life applications.

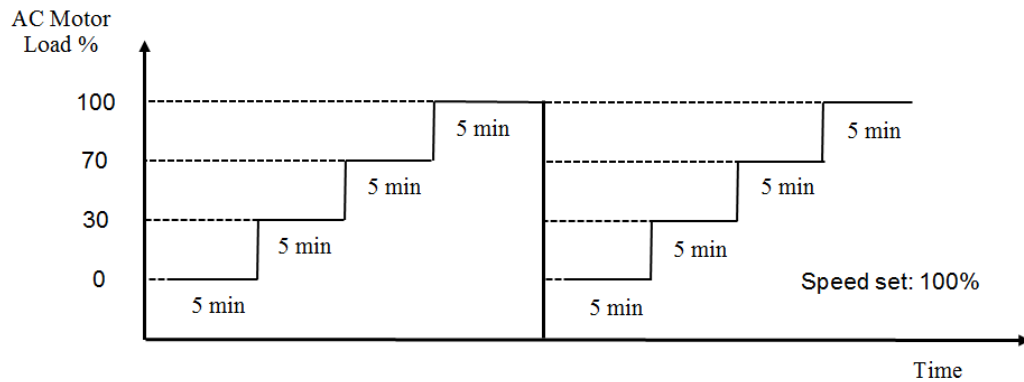


Figure 8-2 Test cycle

Each of the load setting have been operated on for five minutes period and was changed automatically by the PLC controller to the next step. Overall, for all four loads the cycle lasted 20 minute and was repeated once as shown in Figure 8-2. Three different faults have been studied, i.e. tooth breakage, oil level reduction (600ml less than the specification of 2600 ml) and 0.13 mm shaft misalignment between the gearbox and the driving motor. These represent some faults in mechanical transmission systems that commonly occur the most[166]. Tests that have been performed are to investigate the temperature based performance fault detection system and its capabilities to diagnose temperature analysis.

8.3 Wireless Measurement

An integrated WSN, Texas Instruments Sensor Tag CC2650STK, shown in Figure 7.2 and described in Section 7.2.2.1, has been used to measure the temperature of the surface of the gearbox, the measured temperature data is send to the USB module (see Figure7-3, and Section 7.2.2.2).

8.4 Result and Discussion

The experimental works have been performed to detect different gearbox faults, tooth breakage, oil level and shaft misalignment. The gearbox was tested under

three different defective conditions, in which the temperatures of the oil and surface of gearbox have been measured simultaneously.

8.5 Baseline

Figure 8-3 shows the oil temperatures of the gearbox measured by thermocouple and the housing temperature of the gearbox measured using the sensor tag, the surface temperature called housing temperature. From this Figure, it can be seen that the oil temperatures of the three cases under abnormal working conditions vary from about 41 °C to 46 °C. However, the housing temperature of the gearbox fluctuates between about 33 °C and 36 °C.

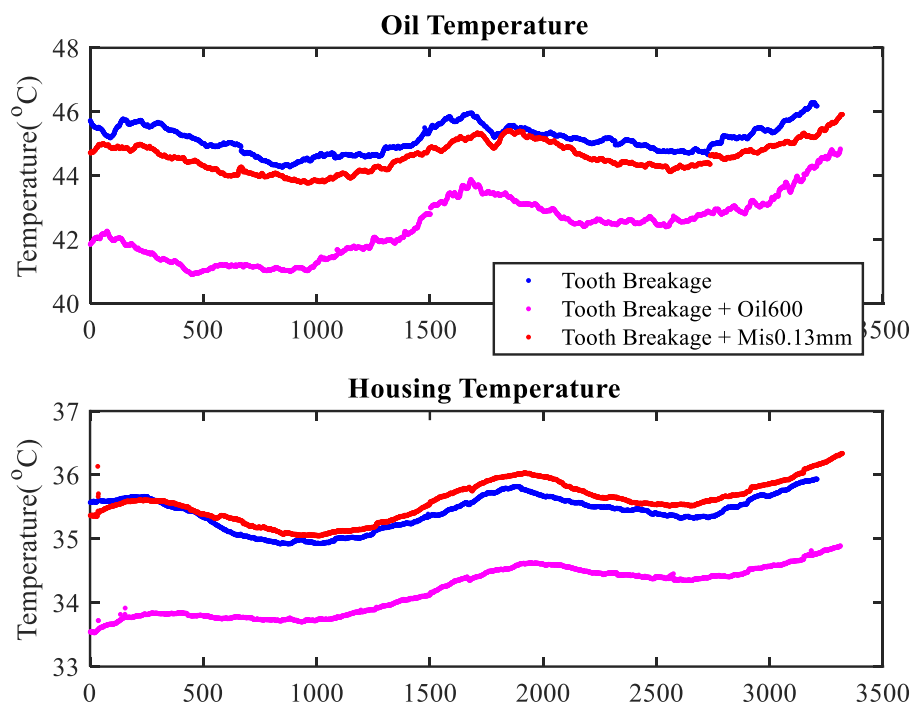


Figure 8-3 Surface temperature and oil temperature of the gearbox with different conditions measured by WSN

The temperature difference between oil and surface is largely due to the fan cooler of the AC-motor. Tooth breakage generates the highest lubricating oil temperature. However, the condition of tooth breakage and shaft misalignment (0.13) generates the highest housing temperature. Tooth breakage and

reduction of oil level (600 ml) gives the lowest temperature of both oil and housing.

Figure 8-4 shows the relationship of the housing temperature and oil temperature of gearbox for all four loads. It can be observed that the temperatures of the gearbox with tooth breakage and tooth breakage and shaft misalignment at different loads are higher than for tooth breakage and reduction in oil level. However, the oil and housing temperatures are lowest for tooth breakage and reduced oil level.

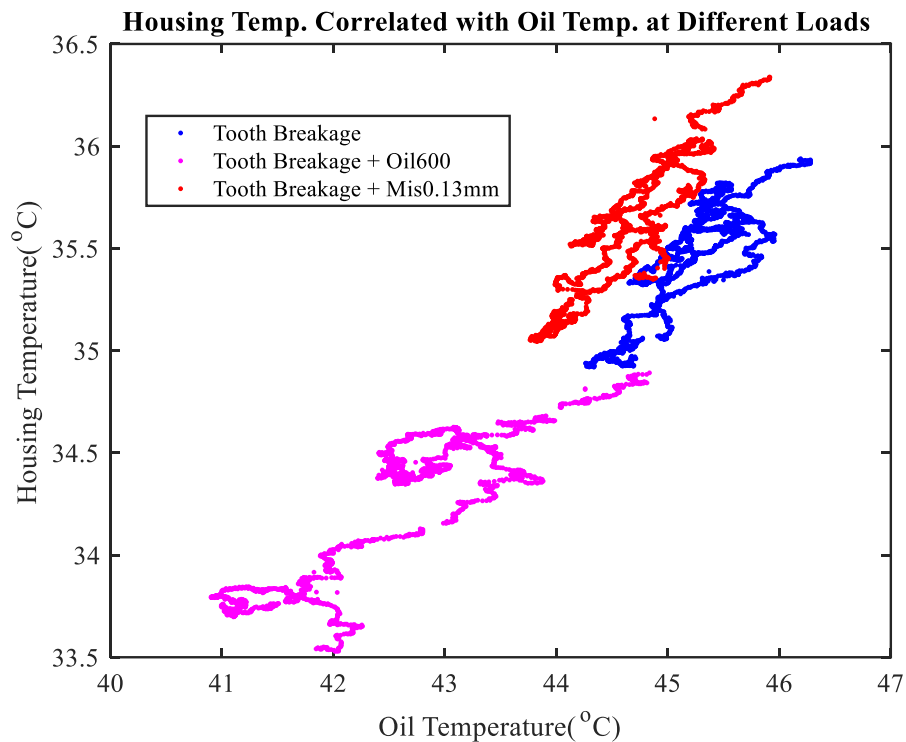


Figure 8-4 Results of surface temperature and oil temperature for all four loads

In this study, a model has been developed based on polynomial fitting of training and predicting temperatures. In which, baseline condition with tooth breakage fault was developed to define the limitation of acceptable gearbox working

condition. The developed model is based mainly on data-driven modelling, which has been used to build models for complementing the interaction dynamics of gearbox transmission temperature. A model algorithm is used to determine the relationship between the gearbox oil and housing temperatures based on a training data set that represents the gear system thermal behaviour. The model would be useful in solving a practical problem with complex periodic signals such as the gearbox faults.

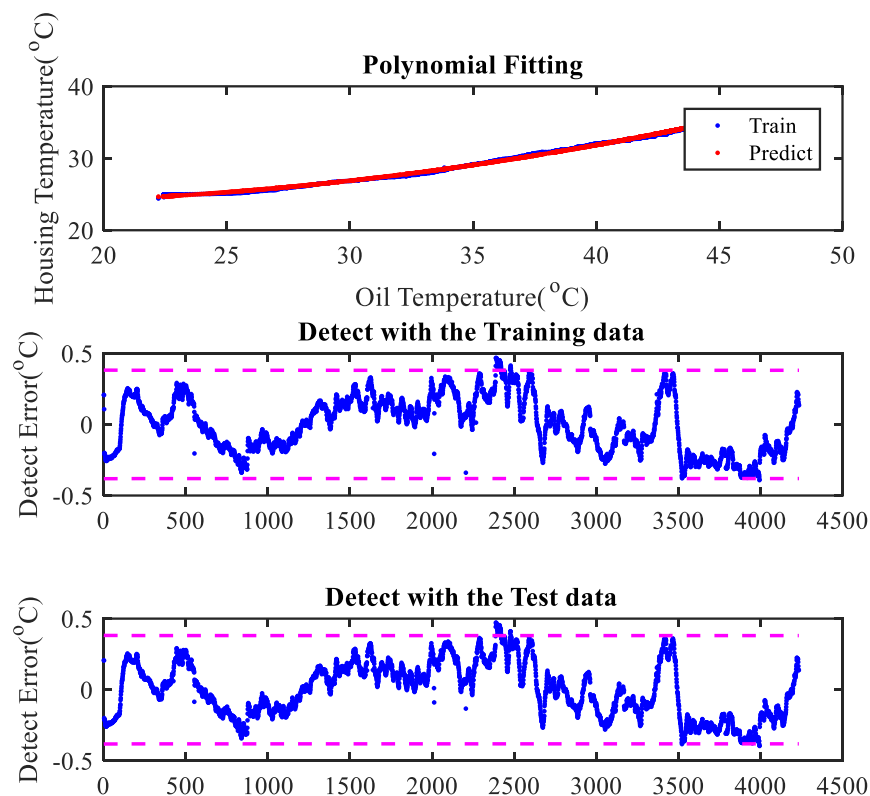


Figure 8-5 Data drive model based on gearbox temperature

This model can be used to monitor the occurrence of an abnormality condition of the gearbox. Figure 8-6 illustrates the transmission paths of the generated heat to the gearbox housing during the gear meshing process, the oil and bearing are the main transmission paths of the generated heat to the gearbox housing. The main sources of heat generation are the friction induced between the teeth

contact surfaces during the gear meshing and the friction due to oil viscosity. Greater transmission load increases the contact friction between the meshing gears, hence the oil temperature increased based on the applied load conditions. Thereby, three different conditions have been simulated under different operating conditions, to confirm the developed model. These faults are mainly related to the transmission paths of heat mesh generation.

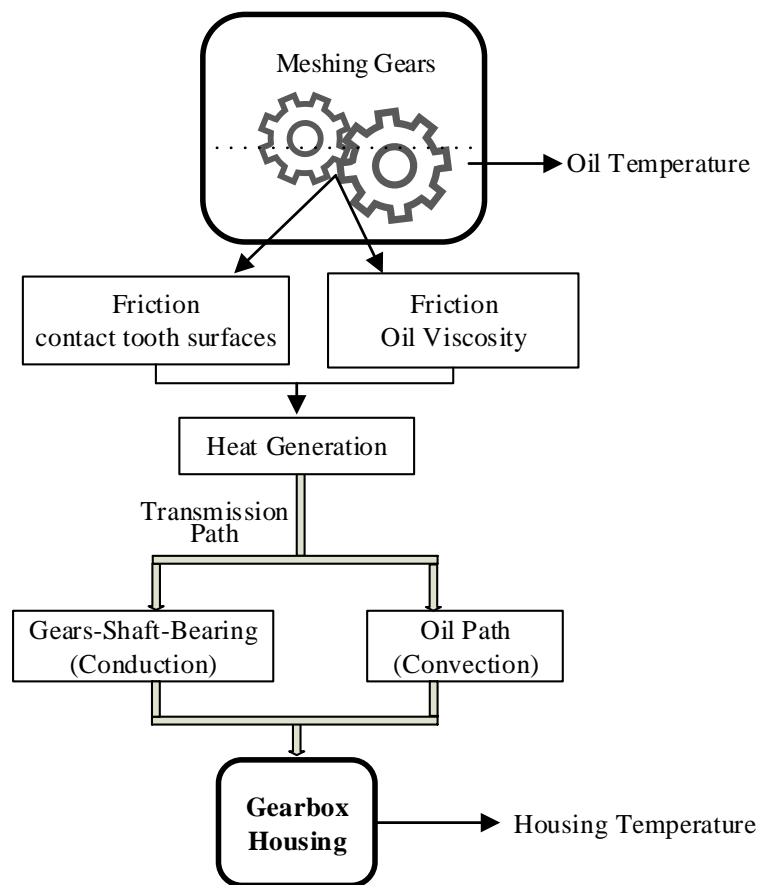


Figure 8-6 Transmission path of gear mesh temperature

8.5.1 Oil Level Reduction

Figure 8-8 depicts the relationships between the oil temperature and the housing temperature of the gearbox when the oil level was decreased by 600ml. The oil temperature and gearbox housing temperature are generally increased with increasing load.

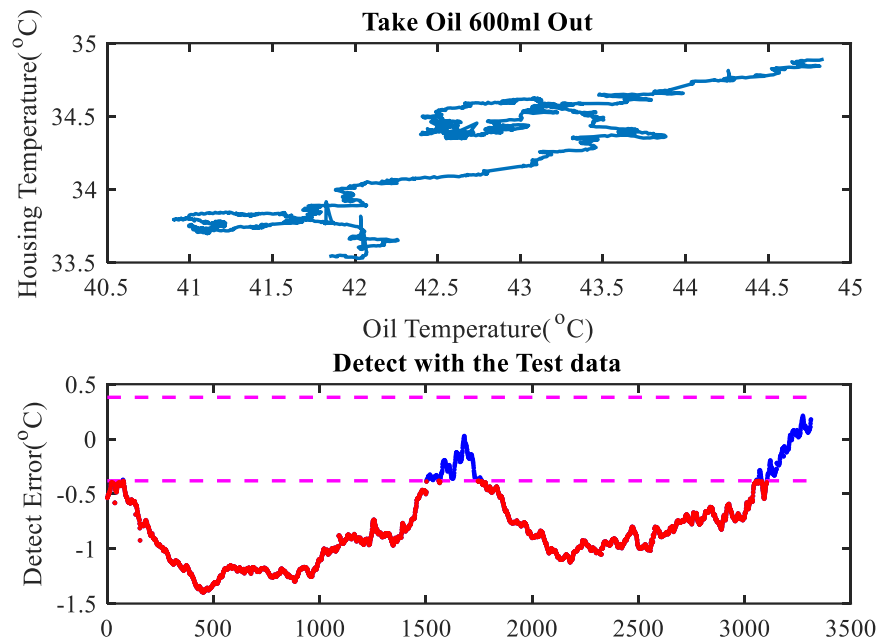


Figure 8-7 Results of surface temperature at reduced oil level

The lower plot in Figure 8-8, the detection model signal, is changed significantly with reduction in oil level condition. This confirms that a change has occurred in the transmission paths of gear mesh temperature which, in this case, can be mainly related to the oil transmission path. The detection signal is changed based on the lower oil level and the detect error model is outside of baseline range.

8.5.2 Shaft Misalignment

Figure 8-9 illustrates the same relation of the gearbox temperatures under the effect of shaft misalignment at all four loads. In which, the conduction path of the gear temperature via the bearing is influenced and more heat is generated that increases the oil and the housing temperatures. The detection model signal is changed due to the shaft misalignment condition and most of the detect signal is out of the acceptable limited region.

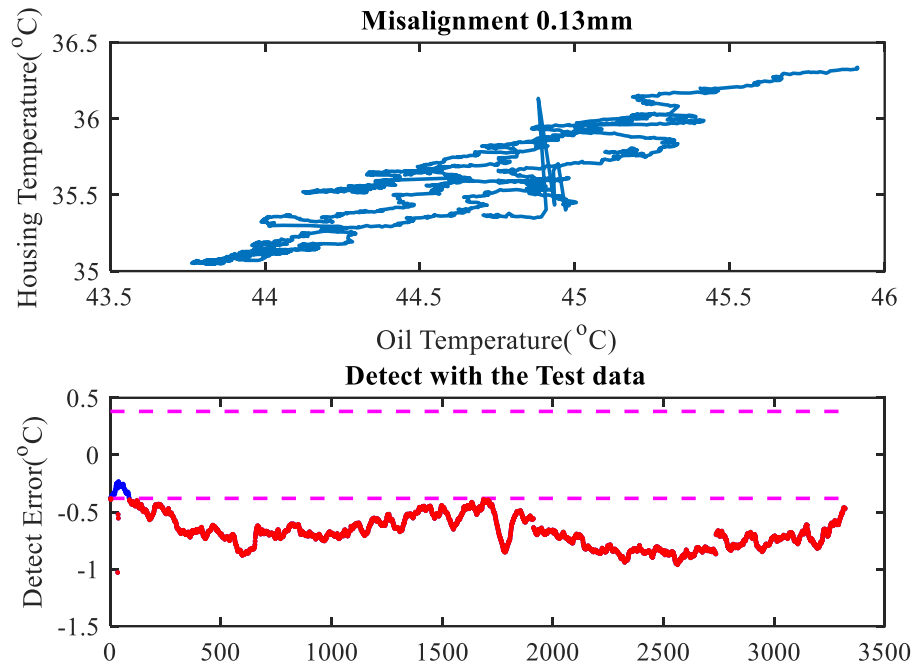


Figure 8-8 Results of surface temperature at shaft misalignment

8.6 Conclusion

Modelling the temperatures measured internally (oil) and externally (surface) is effective for the detection of abnormal gearbox operations. The model allows an accurate description between the internal heat generation due to gear friction and oil viscous drag, the heat convection through the oil and the conduction by the shaft-bearing. Therefore, any changes occurring in these aspects can be detected by a model-based approach. Especially, common deteriorations in gear meshing conditions such as tooth breakage, lubricating problems, and installation complications of the gearbox, which alter either the friction losses or heat conduction paths, have been demonstrated to be detectable using the approach proposed. Moreover, the fabricated wireless temperature node is reliable, and accurate to obtain the temperatures without using any cables or external power supply. These unique features together with the outstanding performance of fault detection make it particularly suitable for online and

automated condition monitoring without any maintenances to the monitoring system.

.

Chapter 9. Conclusions and Future Work suggestions

This chapter gives a summary on the achievements of the research work that have been described in this thesis relating to the aim and objectives defined in Chapter 1, Section 1.5. It also contains conclusions based on the results obtained from the research undertaken. A summary of the author's contributions to knowledge are included. Finally, recommendations for future work are given that could advance the explorations presented in this thesis.

9.1 Introduction

This research project investigated thermal energy harvesting in order to power a WSN for measuring and transmitting measured temperatures for the condition monitoring of a gearbox with and without seeded faults. As a result of this research it is expected to reduce the cost of maintenance for industrial machinery. The research project has involved the successful development, construction and implementation of a new test rig. This was designed, developed and built in the engineering laboratories at the University of Huddersfield.

Temperature was selected as the measurement parameter because it has long been confirmed to be highly sensitive and effective for detection of several kinds of industrial machinery faults. Temperature is an important indicator of the health of many machine components such as the gearbox. The gearbox is an significant element in rotating machines, and has been generally used in industry. It also accounts for a high percentage of machines faults. Hence, a gearbox was used in this research.

9.2 Conclusions

The research has demonstrated that it is viable to harvest the thermal energy of a machine to power a wireless temperature sensor node used to monitor the health and performance of the machine. The research addressed key issues to achieve high power regeneration by the harvesting system to power the nodes, and leads to the following conclusions:

- 1- A TEG has been successfully employed to harvest energy to power the WSN for condition monitoring of a gearbox. The TEG can convert widely available waste heat from machines to usable electrical energy but its conversion efficiency is not high.
- 2- The temperature difference between the hot and cold sides of the Peltier module affects the power output of the TEG. In maintaining a high difference in temperature, a good heat sink is used to increase the heat dissipation from the cold side to the ambient air, and thermal insulation material is added around the Peltier module to maintain maximum difference between the hot and cold sides of the module.
- 3- Bluetooth Low Energy is employed as the wireless transmission protocol due to its low power consumption and its wide availability on current portable smart phones and tablets.
- 4- A new generation low power consumption Texas Instruments SensorTag CC2650STK, was selected as the sensor node because it integrates one processor for data acquisition and signal processing, and another processor specifically for BLE communication.
- 5- The backup capacitor was added for storing the energy harvested from the TEG. It accumulates energy for a relative long time and then provides power to the sensor node for short periods, during which the signal is collected and transmitted to a central device.
- 6- By using the designed TEG module together with the highly integrated sensor tag, the temperature of the gearbox was successfully measured by the sensor tag and received on a smart phone without the need to

provide external power to the sensor tag. This proves the feasibility of this kind of battery-less condition monitoring scheme.

- 7- The model provides an accurate description between the internal heat generations: gear friction and oil viscous drags, and heat transmission through the oil and the convection and by conduction along the shaft bearing. The results show that this monitoring approach allows comment fault cases: tooth breakage, oil shortage, and shaft misalignment to be separated under different loads, which demonstrates the outstanding performance of the system for online and automated condition monitoring.

9.3 Review of Research Objective and Achievements

The key achievements of this work are summarised alongside the specified objectives below:

Objective one: Investigate common condition monitoring strategies and techniques, and select one to use to monitor the health of a gearbox. To obtain a detailed understanding of energy harvesting and thermoelectricity generator design and function.

Achievement one: A number of the popular techniques for machinery condition monitoring were reviewed and it was found that temperature monitoring has been widely employed in the industry because of its high sensitivity to the occurrence of machines faults at an early stage and cheap measurement instrumentation. In Chapter 2, energy harvesting and thermoelectric generation are reviewed. It has been found that the TEG has the unique advantage of

harvesting thermal energy to produce electrical power from CM applications. Especially, heat losses which produce temperature differences happen all rotation machines. The electrical power produced is related to the temperature difference across the TEG, and hence TEGs have been widely used in different industrial applications and continuously improved by many researchers.

Objective two: To investigation the WSN network applications to the condition monitoring fields, including various protocols and challenges. Develop a detailed understanding of the Bluetooth Low Energy which will act as the wireless transmission protocol.

Achievement two: Chapter Three introduces the WSN as applied to condition monitoring. Different wireless communication protocols have been developed according to the application requirements. In addition, the motivation for using BLE are presented, and application described. For condition monitoring, the BLE was found to be more suitable for essential merits such as low power consumption and low cost.

Objective three: Provide background information regarding the development of the TEG model. A fundamental theoretical understanding of the generated voltage of the TEG model will be developed. Build and run 3D Finite Element computer model of the thermal design, and validate the model against experimental data.

Achievement three: The development of a mathematical model for the electric, voltage and power generated by the TEG has been completed. In Chapter 5, the SolidWorks Finite Element Analysis software package was used to create

the FE model and then simulation studies provide more accurate specification for designing a TEG system based on different heat source i.e. machines to be monitored.

Objective four: Develop and design a rig suitable to test the TEG and, WSN developed. Evaluate the performance of the TEG for TEH for three different specifications of heat sinks, in which, an industrial gearbox will be used as both a heat source for the TEG system and the monitored machines for WSN.

Achievement four: A TEG module was designed and fabricated with three heat sinks. In Chapter 6, the heat transfer performances of three different specifications of heat sinks were tested on the TEG. The largest heat sink was found to provide the greatest heat dissipation from the cold side to the ambient air. Tests were conducted by running the driving the AC motor of gearbox rig at full load for one hour at both a lower speed (70% maximum speed) and at a higher speed (100% maximum speed).

Objective five: Evaluate the performance of the TEG for energy harvesting to power the WSN for different test conditions. In addition, Investigate the use of a wireless temperature node to monitor and diagnose different faults on a gearbox transmission system under different conditions.

Achievement five: A comparison test has been completed to verify the performance of the TEG and the temperature WSN node on the gearbox operating at two speeds and with seeded faults. In Chapter 8, two temperature outputs from lubricating oils and housing were modelled to implement a model based detection. The model based detection scheme allows two common

gearbox faults, misalignments and oil shortages to be identified online under different operating conditions.

9.4 Contributions to Knowledge

The research work presented in this study is the development of a new energy harvester of waste heat for electrical energy generation and thereby to power a WSN based CM system. The novel parts of the research can be summarised as following:

First contribution: Design and optimise the THE system to power up wireless temperature sensor node for monitoring the status of gearboxes. The improvement actions for the TEG system are designing and the power consumption efficiency. Furthermore, it was found that the Bluetooth low energy based wireless measurement system can be employed as the wireless transmission protocol to transfer temperature signals for gearbox condition monitoring. Especially, the evaluation results show that the TEG systems can efficiently harvest thermal energy from industrial machines such as a gearbox

Second contribution: By using the thermal harvester TEG module to power the highly integrated sensor tag, the temperature of the gearbox was successfully monitoring and shown on a smart phone without providing external power or battery to the sensor tag.

Third contribution: The theoretical model of the energy harvesting system, based on a general systematic architecture, has been proposed in this thesis to predict the performances of the TEH system. Such a theoretical analysis is very

important for the design and implementation of an energy harvesting system in the real world. The theory model developed has shown to have predictive value with regard to the experimental results. The temperature difference between the hot and cold sides of thermoelectric device, has a substantial impact on generating the energy of the Thermal harvesting design. In addition, the parameters obtained were applied to the FE module of the system and validated against experimental results.

Fourth contribution: The wireless temperature node has been applied to monitor and diagnose different faults on a gearbox transmission system under different conditions. The temperature model based approach is novel which,

Uses the dependence of external temperature on the internal one and the heat transfer paths allows any changes relating to gear operations to be identified over wide operating conditions. This outstanding performance of fault detection together with the novel self-power temperature sensor nodes makes make it particularly suitable for online cost-effective and automated condition monitoring.

9.5 Recommendation for Future Work

Future work for the enhancement of the working life of a WSN based on energy harvesting systems should focus on the following:

Recommendation 1: In this thesis, with regards to the proposed energy harvesting model and the procedure of the design, only thermal energy harvesting has been considered. In future work, other environmental energy

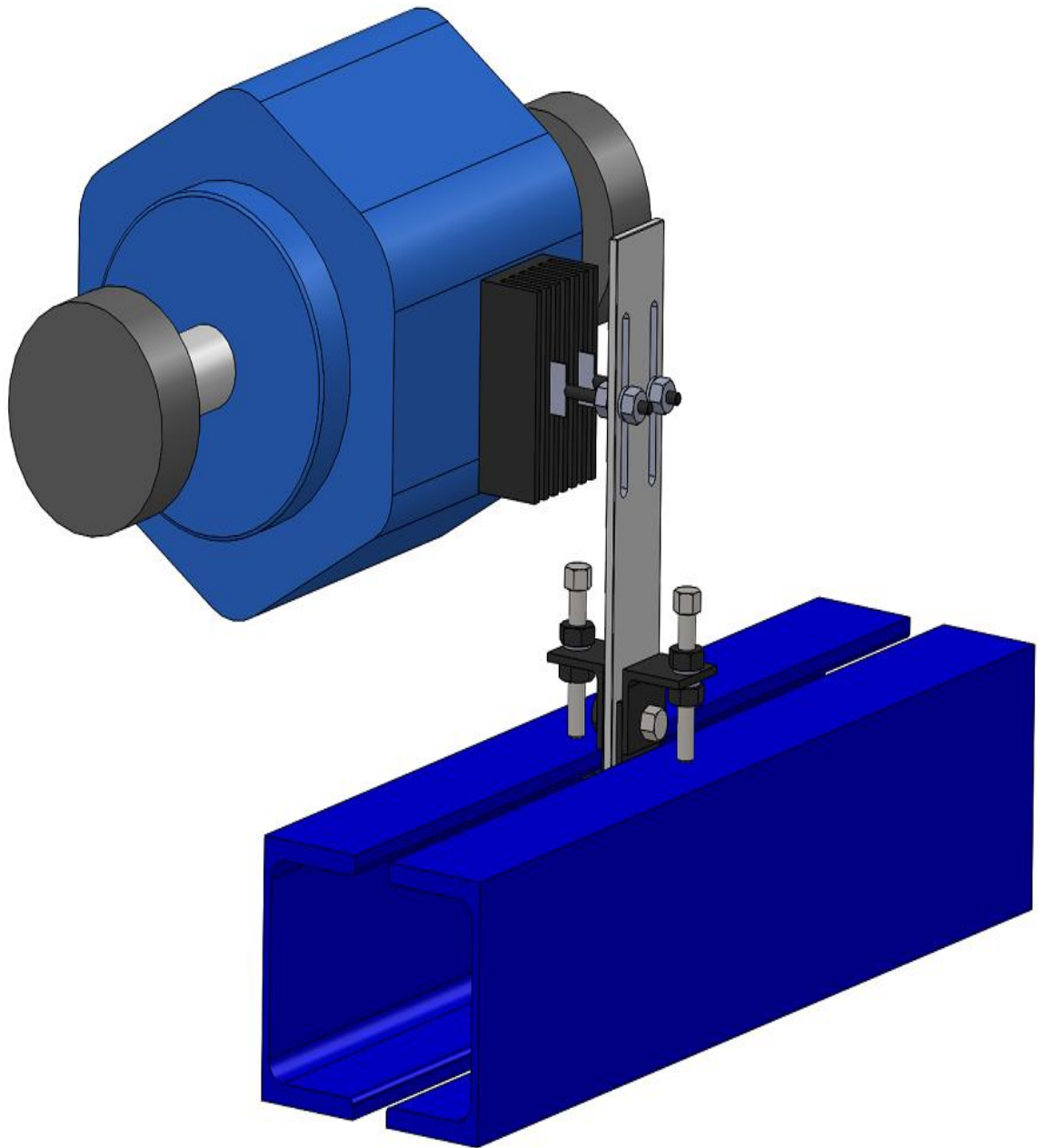
sources that are quite common including energy from vibration and solar needs to be considered.

Recommendation 2: The designed energy harvesting system design only predicts the system performance of thermal sources. Therefore, the model needs to be extended in accepting other forms of energy harvesting technologies, including EF energy harvesting, vibration energy harvesting, and so on.

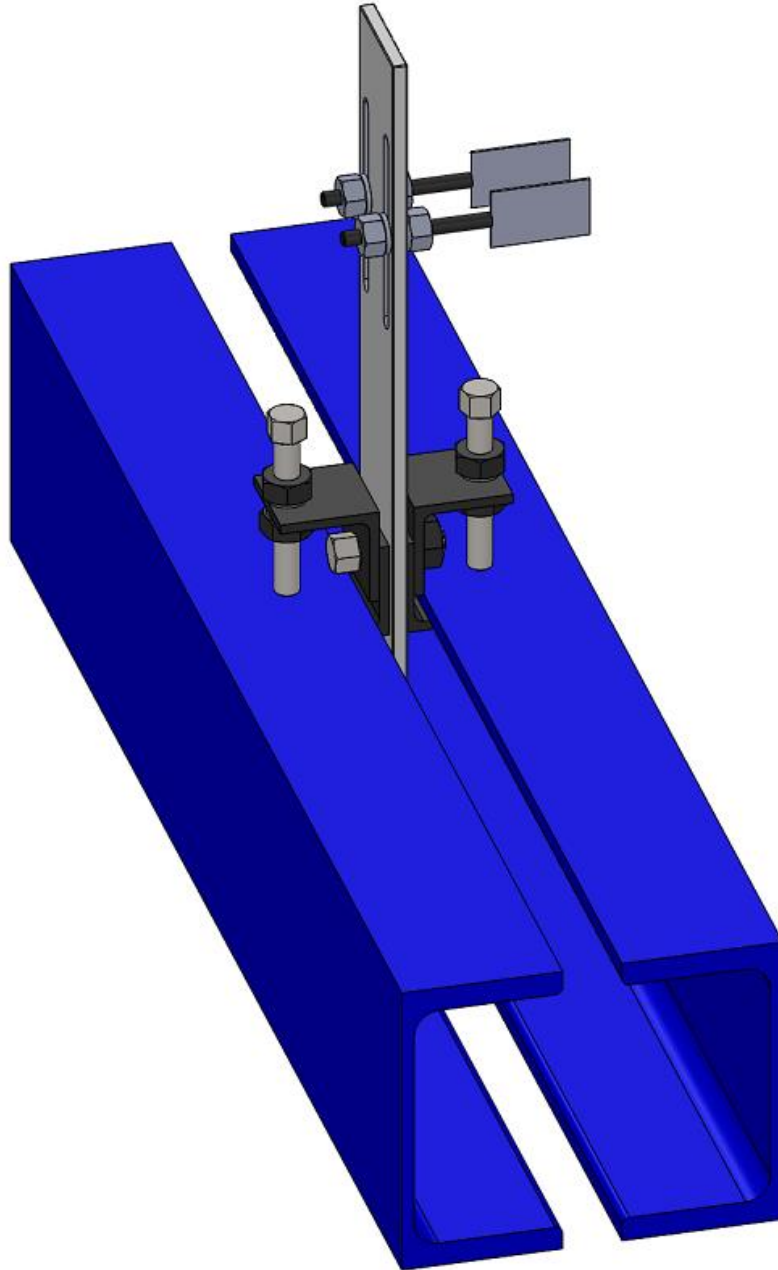
Recommendation 3: Fabricate the wireless sensor node into compact design, and construct suitable package in order to apply them to an industrial environment that is less conducive.

Recommendation 4: Different rotating machine such as bearings should be tested to evaluate and optimise the power that can be generated.

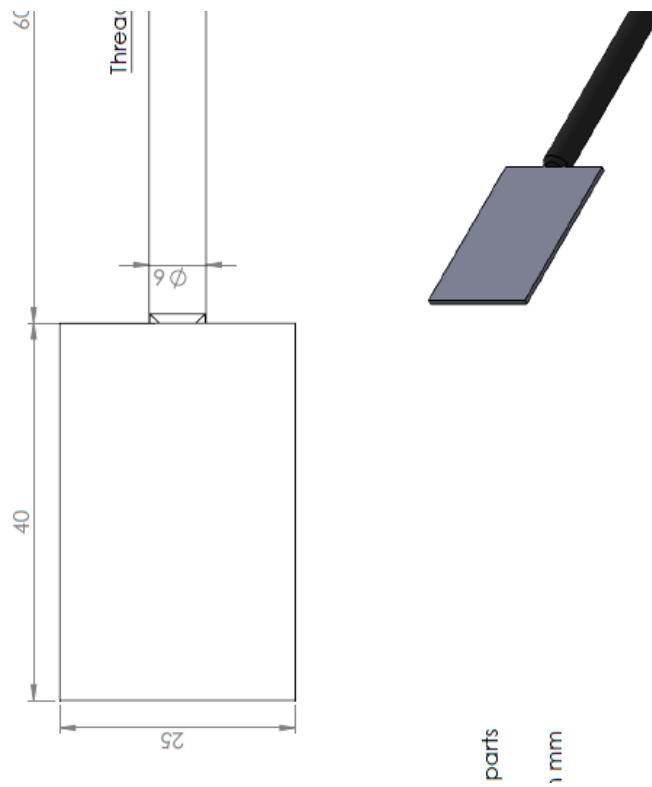
APPENDIX – A.1: Sold model



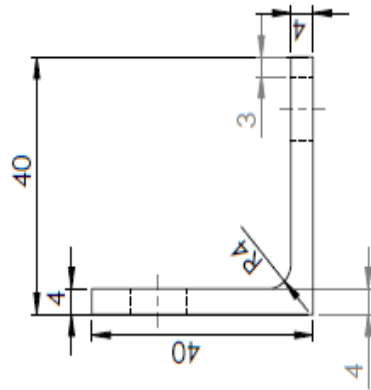
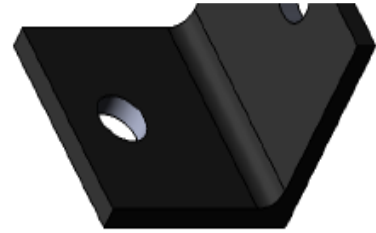
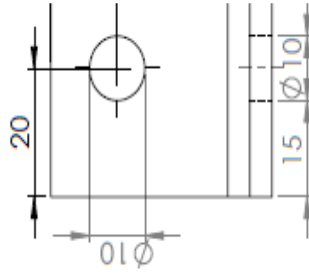
APPENDIX – A.2: Clamp



APPENDIX – B.1: Clamp support part design - 1

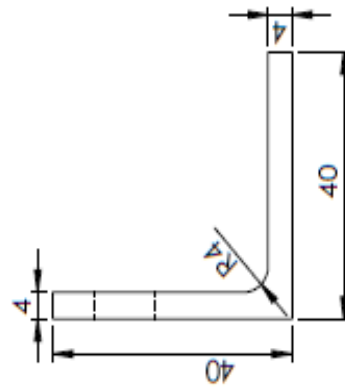
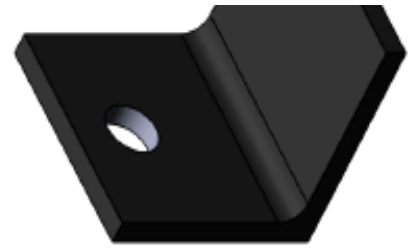
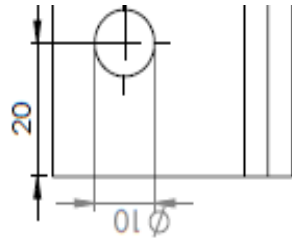


APPENDIX – B.2: Clamp support part design - 2



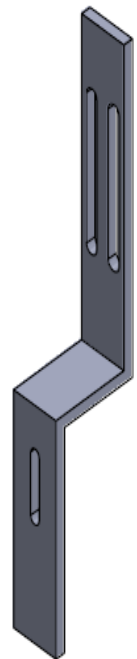
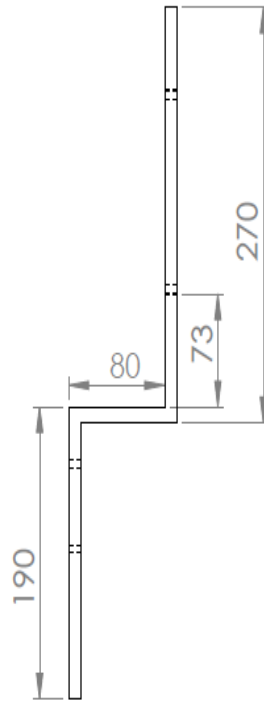
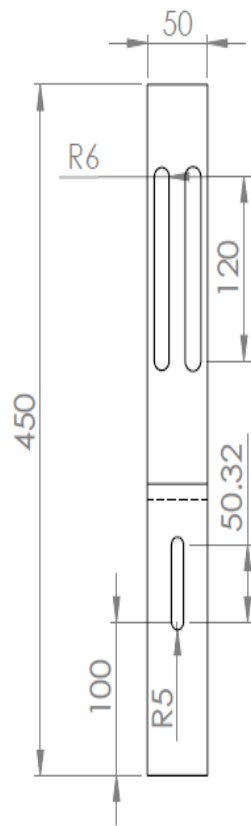
Manufacturing two parts
from N8 Steel
Standard M10+0.010 Tolerances
Dimensions are in mm

APPENDIX – B.3: Clamp support part design - 3

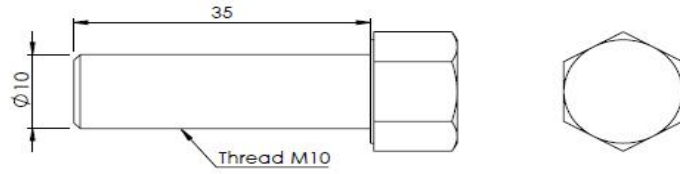


Manufacturing two parts
Material N8 Steel
Thread M10+0.010 Tolerances
Dimensions are in mm

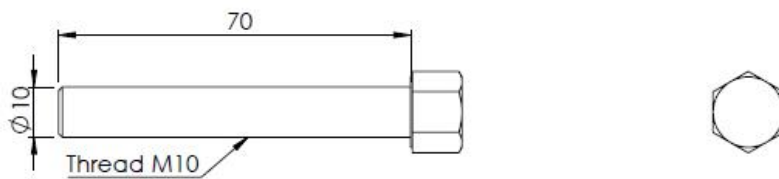
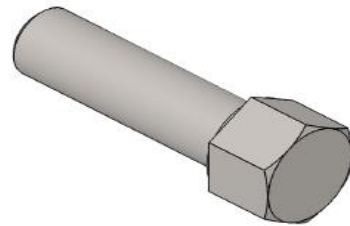
APPENDIX – C.1: Clamp support part design - 4



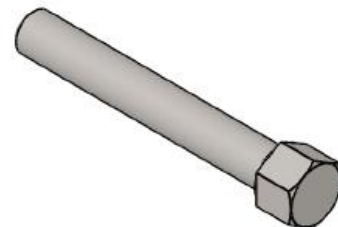
APPENDIX – D: Clamp support part design - 6



- One part
- All dimensions are in mm



- Two parts
- All dimensions are in mm



APPENDIX – E: Risk Assessment – University of Huddersfield

Brief description of activity: Investigation the Torsional Load Capacity of a V-Band Clamp		Assessment by: ALL Users	Assessment
ion: T4/03			
SPECIFIC TASK/ASPECT OF ACTIVITY: Test Rig			
Risks to health and safety	People at risk	Measures to manage the risks effectively	Wh
Lifting risk, heavy components and/or components falling risk	Users	Lift with knees Wear appropriate footwear Ensure components are 0.5 meters from the edge of the work space	Use
Back/arm strain	Users	Ensure correct stance is taken and pressure is gradually with no 'jarring' actions	Use
SPECIFIC TASK/ASPECT OF ACTIVITY: Test Rig			
Risks to health and safety	People at risk	Measures to manage the risks effectively	Wh
Lifting risk, heavy components and/or components falling risk	Users	Lift with knees Wear appropriate footwear Ensure components are 0.5 meters from the edge of the work space	Use
Back/arm strain	Users	Ensure correct stance is taken and pressure is gradually with no 'jarring' actions	Use

Risk assessment (DATA HS \ Forms \ H&S \ New risk assessment 190906) - University of Huddersfield

REFERENCE

- [1. Fakhfakh, T., et al. *Condition Monitoring of Machinery in Non-Stationary Operations*. in *Proceedings of the Second International Conference Condition Monitoring of Machinery in Non-Stationary Operations CMMNO'2012*. 2012. Springer.
2. Telford, S., M.I. Mazhar, and I. Howard. *Condition based maintenance (CBM) in the oil and gas industry: an overview of methods and techniques*. in *Proceedings of the 2011 International Conference on Industrial Engineering and Operations Management, Kuala Lumpur, Malaysia*. 2011.
3. Kelly, A., *Maintenance strategy*. 1997: Elsevier.
4. Higgs, P.A., et al. *A survey on condition monitoring systems in industry*. in *ASME 7th Biennial Conference on Engineering Systems Design and Analysis*. 2004. American Society of Mechanical Engineers.
5. Tavner, P., *Review of condition monitoring of rotating electrical machines*. IET Electric Power Applications, 2008. **2**(4): p. 215-247.
6. Lu, B., et al. *A review of recent advances in wind turbine condition monitoring and fault diagnosis*. in *Power Electronics and Machines in Wind Applications, 2009. PEMWA 2009. IEEE*. 2009. IEEE.
7. Aliwan, M., F. Gu, and A. Ball, *A Study of Wireless Vibration Sensors for Monitoring Bearing Faults*. eMaintenance, 2012: p. 95.
8. Hou, L. and N.W. Bergmann, *Novel industrial wireless sensor networks for machine condition monitoring and fault diagnosis*. IEEE Transactions on Instrumentation and Measurement, 2012. **61**(10): p. 2787-2798.
9. Eti, M.C., S. Ogaji, and S. Probert, *Reducing the cost of preventive maintenance (PM) through adopting a proactive reliability-focused culture*. Applied energy, 2006. **83**(11): p. 1235-1248.

10. Rybak, J.M., *Remote condition monitoring using open-system wireless technologies*. Sound and Vibration, 2006. **40**(2): p. 16.
11. Irfan, M., et al., *An on-line condition monitoring system for induction motors via instantaneous power analysis*. Journal of Mechanical Science and Technology, 2015. **29**(4): p. 1483-1492.
12. Heng, A., et al., *Intelligent condition-based prediction of machinery reliability*. Mechanical Systems and Signal Processing, 2009. **23**(5): p. 1600-1614.
13. Beebe, R.S., *Predictive maintenance of pumps using condition monitoring*. 2004: Elsevier.
14. Schwarzer, R., *Modeling health behavior change: How to predict and modify the adoption and maintenance of health behaviors*. Applied Psychology, 2008. **57**(1): p. 1-29.
15. Benbouzid, M.E.H., *A review of induction motors signature analysis as a medium for faults detection*. IEEE transactions on industrial electronics, 2000. **47**(5): p. 984-993.
16. Witten, I.H. and E. Frank, *Data Mining: Practical machine learning tools and techniques*. 2005: Morgan Kaufmann.
17. Wang, L. and R.X. Gao, *Condition monitoring and control for intelligent manufacturing*. 2006: Springer Science & Business Media.
18. Jardine, A.K., D. Lin, and D. Banjevic, *A review on machinery diagnostics and prognostics implementing condition-based maintenance*. Mechanical systems and signal processing, 2006. **20**(7): p. 1483-1510.
19. Kelly, A., *maintenance Strategy*. Elsevier. 1997: p. 79-124.
20. Elhaj, M., et al., *Numerical simulation and experimental study of a two-stage reciprocating compressor for condition monitoring*. Mechanical Systems and Signal Processing, 2008. **22**(2): p. 374-389.

21. Gungor, V.C. and G.P. Hancke, *Industrial wireless sensor networks: Challenges, design principles, and technical approaches*. IEEE Transactions on Industrial Electronics, 2009. **56**(10): p. 4258-4265.
22. Hu, F. and X. Cao, *Wireless sensor networks: principles and practice*. 2010: CRC Press.
23. Akyildiz, I.F., et al., *Wireless sensor networks: a survey*. Computer networks, 2002. **38**(4): p. 393-422.
24. Arampatzis, T., J. Lygeros, and S. Manesis. *A survey of applications of wireless sensors and wireless sensor networks*. in *Proceedings of the 2005 IEEE International Symposium on, Mediterrean Conference on Control and Automation Intelligent Control, 2005*. 2005. IEEE.
25. Cao, Q. and J.A. Stankovic. *An in-field-maintenance framework for wireless sensor networks*. in *International Conference on Distributed Computing in Sensor Systems*. 2008. Springer.
26. Pathan, A.-S.K., H.-W. Lee, and C.S. Hong. *Security in wireless sensor networks: issues and challenges*. in *2006 8th International Conference Advanced Communication Technology*. 2006. IEEE.
27. Sen, J., *A survey on wireless sensor network security*. arXiv preprint arXiv:1011.1529, 2010.
28. Ali, M., T. Voigt, and Z.A. Uzmi. *Mobility management in sensor networks*. in *Workshop proceedings of 2nd IEEE DCOSS*. 2006.
29. Dâmaso, A., et al., *Evaluating the power consumption of wireless sensor network applications using models*. Sensors, 2013. **13**(3): p. 3473-3500.
30. Rice, A. and S. Hay, *Measuring mobile phone energy consumption for 802.11 wireless networking*. Pervasive and Mobile Computing, 2010. **6**(6): p. 593-606.

31. Moschitta, A. and I. Neri, *Power consumption assessment in wireless sensor networks*. ICT-Energy-Concepts Towards Zero-Power Information and Communication Technology, 2014: p. 203-224.
32. Dietrich, I. and F. Dressler, *On the lifetime of wireless sensor networks*. ACM Transactions on Sensor Networks (TOSN), 2009. **5**(1): p. 5.
33. Raghunathan, V., S. Ganeriwal, and M. Srivastava, *Emerging techniques for long lived wireless sensor networks*. IEEE Communications Magazine, 2006. **44**(4): p. 108-114.
34. Niyato, D., et al., *Wireless sensor networks with energy harvesting technologies: A game-theoretic approach to optimal energy management*. IEEE Wireless Communications, 2007. **14**(4).
35. Yu, D., J. Cheng, and Y. Yang, *Application of EMD method and Hilbert spectrum to the fault diagnosis of roller bearings*. Mechanical systems and signal processing, 2005. **19**(2): p. 259-270.
36. Li, H., X. Zhang, and F. Xu, *Experimental investigation on centrifugal compressor blade crack classification using the squared envelope spectrum*. Sensors, 2013. **13**(9): p. 12548-12563.
37. Ho, D. and R. Randall, *Optimisation of bearing diagnostic techniques using simulated and actual bearing fault signals*. Mechanical systems and signal processing, 2000. **14**(5): p. 763-788.
38. Lee, V.C., *Energy harvesting for wireless sensor networks*. 2012, University of California, Berkeley.
39. Gilbert, J.M. and F. Balouchi, *Comparison of energy harvesting systems for wireless sensor networks*. international journal of automation and computing, 2008. **5**(4): p. 334-347.

40. Yeatman, E.M. *Energy harvesting: small scale energy production from ambient sources*. in *SPIE Smart Structures and Materials+ Nondestructive Evaluation and Health Monitoring*. 2009. International Society for Optics and Photonics.
41. Chalasani, S. and J.M. Conrad. *A survey of energy harvesting sources for embedded systems*. in *Southeastcon, 2008. IEEE*. 2008. IEEE.
42. Paradiso, J.A. and T. Starner, *Energy scavenging for mobile and wireless electronics*. *IEEE Pervasive computing*, 2005. **4**(1): p. 18-27.
43. Tan, Y.K. and S.K. Panda, *Review of energy harvesting technologies for sustainable WSN*, in *Sustainable wireless sensor networks*. 2010, InTech.
44. KHENG, T.Y., *Analysis, Design and implementation of Energy Harvesting Systems for Wireless Sensor Nodes*. 2010.
45. Baydar, N. and A. Ball, *A comparative study of acoustic and vibration signals in detection of gear failures using Wigner–Ville distribution*. *Mechanical systems and signal processing*, 2001. **15**(6): p. 1091-1107.
46. Márquez, F.P.G., et al., *Condition monitoring of wind turbines: Techniques and methods*. *Renewable Energy*, 2012. **46**: p. 169-178.
47. Li, W., et al., *A study of the noise from diesel engines using the independent component analysis*. *Mechanical Systems and Signal Processing*, 2001. **15**(6): p. 1165-1184.
48. Davies, A., *Handbook of condition monitoring: techniques and methodology*. 2012: Springer Science & Business Media.
49. Douglas, R., J. Steel, and R. Reuben, *A study of the tribological behaviour of piston ring/cylinder liner interaction in diesel engines using acoustic emission*. *Tribology International*, 2006. **39**(12): p. 1634-1642.

50. Elmaleeh, M.A., N. Saad, and M. Awan. *Condition monitoring of industrial process plant using acoustic emission techniques*. in *Intelligent and Advanced Systems (ICIAS), 2010 International Conference on*. 2010. IEEE.
51. Tavner, P., *Condition monitoring of rotating electrical machines*. Vol. 56. 2008: IET.
52. Harris, T., C. Seppala, and L. Desborough, *A review of performance monitoring and assessment techniques for univariate and multivariate control systems*. *Journal of Process Control*, 1999. **9**(1): p. 1-17.
53. De Silva, C.W., *Vibration and shock handbook*. 2005: CRC Press.
54. Gibson, R. and R. Plunkett, *A forced-vibration technique for measurement of material damping*. *Experimental Mechanics*, 1977. **17**(8): p. 297-302.
55. Mathew, S., et al., *Dye-sensitized solar cells with 13% efficiency achieved through the molecular engineering of porphyrin sensitizers*. *Nature chemistry*, 2014. **6**(3): p. 242-247.
56. Green, M.A., et al., *Solar cell efficiency tables (version 35)*. *Progress in photovoltaics: Research and applications*, 2010. **18**(2): p. 144-150.
57. Jeong, J. and D. Culler, *A practical theory of micro-solar power sensor networks*. *ACM Transactions on Sensor Networks (TOSN)*, 2012. **9**(1): p. 9.
58. Randall, J. and J. Jacot, *Is AM1.5 applicable in practice? Modelling eight photovoltaic materials with respect to light intensity and two spectra*. *Renewable Energy*, 2003. **28**(12): p. 1851-1864.
59. Jiang, X., J. Polastre, and D. Culler. *Perpetual environmentally powered sensor networks*. in *Proceedings of the 4th international symposium on Information processing in sensor networks*. 2005. IEEE Press.
60. Simjee, F. and P.H. Chou. *Everlast: long-life, supercapacitor-operated wireless sensor node*. in *Low Power Electronics and Design*, 2006.

- ISLPED'06. Proceedings of the 2006 International Symposium on.* 2006. IEEE.
61. Park, C. and P.H. Chou. *Ambimax: Autonomous energy harvesting platform for multi-supply wireless sensor nodes.* in *Sensor and Ad Hoc Communications and Networks, 2006. SECON'06. 2006 3rd Annual IEEE Communications Society on.* 2006. IEEE.
 62. Sodano, H.A., D.J. Inman, and G. Park, *A review of power harvesting from vibration using piezoelectric materials.* Shock and Vibration Digest, 2004. **36**(3): p. 197-206.
 63. Stanton, S.C., C.C. McGehee, and B.P. Mann, *Nonlinear dynamics for broadband energy harvesting: Investigation of a bistable piezoelectric inertial generator.* Physica D: Nonlinear Phenomena, 2010. **239**(10): p. 640-653.
 64. Moser, C., *Power management in energy harvesting embedded systems.* 2009, TU Munich.
 65. Roundy, S., P.K. Wright, and J.M. Rabaey, *Energy scavenging for wireless sensor networks.* 2003: Springer.
 66. Shenck, N.S. and J.A. Paradiso, *Energy scavenging with shoe-mounted piezoelectrics.* IEEE micro, 2001. **21**(3): p. 30-42.
 67. Wang, L. and F.G. Yuan. *Energy harvesting by magnetostrictive material (MsM) for powering wireless sensors in SHM.* in *The 14th International Symposium on: Smart Structures and Materials & Nondestructive Evaluation and Health Monitoring.* 2007. International Society for Optics and Photonics.
 68. Roundy, S.J., *Energy scavenging for wireless sensor nodes with a focus on vibration to electricity conversion.* 2003, University of California, Berkeley.

69. Edmison, J., et al. *Using piezoelectric materials for wearable electronic textiles*. in *Wearable Computers, 2002.(ISWC 2002). Proceedings. Sixth International Symposium on*. 2002. IEEE.
70. Glynne-Jones, P., et al., *An electromagnetic, vibration-powered generator for intelligent sensor systems*. *Sensors and Actuators A: Physical*, 2004. **110**(1): p. 344-349.
71. Meninger, S., et al., *Vibration-to-electric energy conversion*. *IEEE Transactions on Very Large Scale Integration (VLSI) Systems*, 2001. **9**(1): p. 64-76.
72. Mitcheson, P.D., et al., *Architectures for vibration-driven micropower generators*. *Journal of microelectromechanical systems*, 2004. **13**(3): p. 429-440.
73. Yuan., L.W.a.F.G., *Structural vibration energy harvesting by magnetostrictive materials (MsM)*. *The 4th China-Japan-US Symposium on Structural Control and Monitoring,, 2006*(147-152).
74. Hudak, N.S. and G.G. Amatucci, *Small-scale energy harvesting through thermoelectric, vibration, and radiofrequency power conversion*. *Journal of Applied Physics*, 2008. **103**(10): p. 5.
75. Rowe, D.M., *Thermoelectrics handbook: macro to nano*. 2005: CRC press.
76. Fahrenbruch, A. and R. Bube, *Fundamentals of solar cells: photovoltaic solar energy conversion*. 2012: Elsevier.
77. Stordeur, M. and I. Stark. *Low power thermoelectric generator-self-sufficient energy supply for micro systems*. in *Thermoelectrics, 1997. Proceedings ICT'97. XVI International Conference on*. 1997. IEEE.

78. Bitschi, A., *Modelling of thermoelectric devices for electric power generation*. 2009, Diss., Eidgenössische Technische Hochschule ETH Zürich, Nr. 18441, 2009.
79. Watkins, C., B. Shen, and R. Venkatasubramanian. *Low-grade-heat energy harvesting using superlattice thermoelectrics for applications in implantable medical devices and sensors*. in *Thermoelectrics, 2005. ICT 2005. 24th International Conference on*. 2005. IEEE.
80. Stark, I. *Invited talk: Thermal energy harvesting with Thermo Life*. in *International Workshop on Wearable and Implantable Body Sensor Networks (BSN'06)*. 2006. IEEE.
81. Simons, R. and R. Chu. *Application of thermoelectric cooling to electronic equipment: a review and analysis*. in *Semiconductor Thermal Measurement and Management Symposium, 2000. Sixteenth Annual IEEE*. 2000. IEEE.
82. Luo, Q., et al., *A novel water heater integrating thermoelectric heat pump with separating thermosiphon*. *Applied Thermal Engineering*, 2005. **25**(14): p. 2193-2203.
83. Knox, A., et al., *Megawatt-scale application of thermoelectric devices in thermal power plants*. *Journal of electronic materials*, 2013. **42**(7): p. 1807-1813.
84. Rowe, D.M., *Thermoelectrics, an environmentally-friendly source of electrical power*. *Renewable energy*, 1999. **16**(1): p. 1251-1256.
85. Zhang, X. and L.-D. Zhao, *Thermoelectric materials: Energy conversion between heat and electricity*. *Journal of Materiomics*, 2015. **1**(2): p. 92-105.
86. Snyder, G.J. and E.S. Toberer, *Complex thermoelectric materials*. *Nature materials*, 2008. **7**(2): p. 105-114.

87. Faleev, S.V. and F. Léonard, *Theory of enhancement of thermoelectric properties of materials with nanoinclusions*. Physical Review B, 2008. **77**(21): p. 214304.
88. Ma, Y., R. Heijl, and A.E. Palmqvist, *Composite thermoelectric materials with embedded nanoparticles*. Journal of Materials Science, 2013. **48**(7): p. 2767-2778.
89. Kazeoka, M., et al., *Improvement in thermoelectric properties of (ZnO) 5 In 2 O 3 through partial substitution of yttrium for indium*. Journal of materials research, 1998. **13**(03): p. 523-526.
90. Goldsmid, H. and R. Douglas, *The use of semiconductors in thermoelectric refrigeration*. British Journal of Applied Physics, 1954. **5**(11): p. 386.
91. Zhang, X., et al., *Alpha Stable Distribution Based Morphological Filter for Bearing and Gear Fault Diagnosis in Nuclear Power Plant*. Science and Technology of Nuclear Installations, 2015. **2015**.
92. Leonov, V., et al., *Thermoelectric converters of human warmth for self-powered wireless sensor nodes*. IEEE Sensors Journal, 2007. **7**(5): p. 650-657.
93. Prijić, A., et al., *Thermal energy harvesting wireless sensor node in aluminum core PCB technology*. IEEE Sensors Journal, 2015. **15**(1): p. 337-345.
94. Xin, L. and Y. Shuang-Hua. *Thermal energy harvesting for WSNs*. in *Systems Man and Cybernetics (SMC), 2010 IEEE International Conference on*. 2010.
95. Ihn, J.-B. and F.-K. Chang, *Detection and monitoring of hidden fatigue crack growth using a built-in piezoelectric sensor/actuator network: II. Validation using riveted joints and repair patches*. Smart materials and structures, 2004. **13**(3): p. 621.

96. Lynch, J.P. and K.J. Loh, *A summary review of wireless sensors and sensor networks for structural health monitoring*. Shock and Vibration Digest, 2006. **38**(2): p. 91-130.
97. Lynch, J.P., et al. *Design of a wireless active sensing unit for structural health monitoring*. in *NDE for Health Monitoring and Diagnostics*. 2004. International Society for Optics and Photonics.
98. Matthews, R., et al. *A wearable physiological sensor suite for unobtrusive monitoring of physiological and cognitive state*. in *Engineering in Medicine and Biology Society, 2007. EMBS 2007. 29th Annual International Conference of the IEEE*. 2007. IEEE.
99. Singh, K.J. and D.S. Kapoor, *Create Your Own Internet of Things: A survey of IoT platforms*. IEEE Consumer Electronics Magazine, 2017. **6**(2): p. 57-68.
100. Cañedo, J. and A. Skjellum. *Adding scalability to Internet of Things gateways using parallel computation of edge device data*. in *High Performance Extreme Computing Conference (HPEC), 2016 IEEE*. 2016. IEEE.
101. VINEELA, A. and S. MEZEER, *EVOLUTION OF WIRELESS SENSOR NETWORKS TOWARDS THE INTERNET OF THINGS*.
102. Akyildiz, I.F., et al., *A survey on sensor networks*. IEEE Communications magazine, 2002. **40**(8): p. 102-114.
103. Yap, F.G. and H.-H. Yen, *A survey on sensor coverage and visual data capturing/processing/transmission in wireless visual sensor networks*. Sensors, 2014. **14**(2): p. 3506-3527.
104. Lu, W.W., *Compact multidimensional broadband wireless: the convergence of wireless mobile and access*. IEEE Communications Magazine, 2000. **38**(11): p. 119-123.

105. Pei, Z., et al. *Application-oriented wireless sensor network communication protocols and hardware platforms: A survey*. in *Industrial Technology, 2008. ICIT 2008. IEEE International Conference on*. 2008. IEEE.
106. Bogias, A.C., *A wireless 802.11 condition monitoring sensor for electrical substation environments*. 2012, Cardiff University.
107. Ab-Rahman, M.S., A.H. Asmir, and K. Jumari, *Development of camera and GSM interfacing system for home security surveillance*. *Scientific Research and Essays*, 2013. **8**(38): p. 1858-1871.
108. Palacios, R., et al., *Analytical procedure to obtain internal parameters from performance curves of commercial thermoelectric modules*. *Applied Thermal Engineering*, 2009. **29**(17): p. 3501-3505.
109. Rappaport, T.S., *Wireless communications: principles and practice*. Vol. 2. 1996: Prentice Hall PTR New Jersey.
110. Alliance, W.-F., *Securing Wi-Fi wireless networks with today's technologies*. White paper, February, 2003.
111. Wright, P., D. Dornfeld, and N. Ota, *Condition monitoring in end-milling using wireless sensor networks (WSNs)*. *Transactions of NAMRI/SME*, 2008. **36**.
112. Hodge, V.J., et al., *Wireless sensor networks for condition monitoring in the railway industry: A survey*. *IEEE Transactions on Intelligent Transportation Systems*, 2015. **16**(3): p. 1088-1106.
113. Guo, P. and N. Bai, *Wind turbine gearbox condition monitoring with AAKR and moving window statistic methods*. *Energies*, 2011. **4**(11): p. 2077-2093.
114. Xue, X., V. Sundararajan, and W.P. Brithinee. *The application of wireless sensor networks for condition monitoring in three-phase induction motors*. in *Electrical Insulation Conference and Electrical Manufacturing Expo, 2007*. 2007. IEEE.

115. Shahidi, A., et al. *Wireless temperature and vibration sensor for real-time bearing condition monitoring*. in *Microwave Symposium Digest (IMS), 2013 IEEE MTT-S International*. 2013. IEEE.
116. Gupta, L.A. and D. Peroulis. *Wireless temperature sensor for condition monitoring of mechanical seals*. in *Microwave Conference (EuMC), 2012 42nd European*. 2012. IEEE.
117. Feng, G., et al., *Investigation of wireless protocols for remote condition monitoring*. 2013, University of Huddersfield.
118. Bayón, R.M., et al., *A Wireless Portable High Temperature Data Monitor for Tunnel Ovens*. *Sensors*, 2014. **14**(8): p. 14712-14731.
119. Peng, D. and S. Wan, *Industrial Temperature Monitoring system design based on zigbee and infrared temperature Sensing*. *Optics and Photonics Journal*, 2013. **3**(02): p. 277.
120. Lee, D., *Wireless and powerless sensing node system developed for monitoring motors*. *Sensors*, 2008. **8**(8): p. 5005-5022.
121. Luo, Z., *A simple method to estimate the physical characteristics of a thermoelectric cooler from vendor datasheets*. *Electronics cooling*, 2008. **14**(3): p. 22-27.
122. Raza, S., et al., *Building the Internet of Things with Bluetooth smart*. *Ad Hoc Networks*, 2017. **57**: p. 19-31.
123. Bluetooth, S., *Bluetooth core specification version 4.0*. Specification of the Bluetooth System, 2010.
124. Chang, K.-H., *Bluetooth: a viable solution for IoT?[Industry Perspectives]*. *IEEE Wireless Communications*, 2014. **21**(6): p. 6-7.
125. Padgett, J., *Guide to bluetooth security*. NIST Special Publication, 2017. **800**: p. 121.

126. Abbas, Z. and W. Yoon, *A survey on energy conserving mechanisms for the internet of things: Wireless networking aspects*. *Sensors*, 2015. **15**(10): p. 24818-24847.
127. Gomez, C., J. Oller, and J. Paradells, *Overview and evaluation of bluetooth low energy: An emerging low-power wireless technology*. *Sensors*, 2012. **12**(9): p. 11734-11753.
128. Fakhri, F. and D. Darjat, *IMPLEMENTATION BLUETOOTH LOW ENERGY ON THE MEDICAL SUPPORTING DEVICE*. 2011, Diponegoro University.
129. Gomez, C. and J. Paradells, *Wireless home automation networks: A survey of architectures and technologies*. *IEEE Communications Magazine*, 2010. **48**(6).
130. Ludovici, A., A. Calveras, and J. Casademont, *Forwarding techniques for IP fragmented packets in a real 6LoWPAN network*. *Sensors*, 2011. **11**(1): p. 992-1008.
131. Sirur, S., et al. *A mesh network for mobile devices using Bluetooth low energy*. in *SENSORS, 2015 IEEE*. 2015. IEEE.
132. Aakvaag, N., M. Mathiesen, and G. Thonet. *Timing and power issues in wireless sensor networks-an industrial test case*. in *Parallel Processing, 2005. ICPP 2005 Workshops. International Conference Workshops on*. 2005. IEEE.
133. Dzung, D., et al. *Design and implementation of a real-time wireless sensor/actuator communication system*. in *Emerging Technologies and Factory Automation, 2005. ETFA 2005. 10th IEEE Conference on*. 2005. IEEE.
134. Kushalnagar, N., G. Montenegro, and C. Schumacher, *IPv6 over low-power wireless personal area networks (6LoWPANs): overview, assumptions, problem statement, and goals*. 2007.

135. Montenegro, G., et al., *Transmission of IPv6 packets over IEEE 802.15. 4 networks*. 2007.
136. Doe, U., *Industrial wireless technology for the 21st century*. Report, Technology Foresight, 2004.
137. Mainwaring, A., et al. *Wireless sensor networks for habitat monitoring*. in *Proceedings of the 1st ACM international workshop on Wireless sensor networks and applications*. 2002. Acm.
138. Srinivasan, K.K., P.J. Mago, and S.R. Krishnan, *Analysis of exhaust waste heat recovery from a dual fuel low temperature combustion engine using an Organic Rankine Cycle*. *Energy*, 2010. **35**(6): p. 2387-2399.
139. Kumar, S., et al., *Thermoelectric generators for automotive waste heat recovery systems part I: numerical modeling and baseline model analysis*. *Journal of electronic materials*, 2013. **42**(4): p. 665.
140. Cheng, F., *Calculation Methods for Thermoelectric Generator Performance*, in *Thermoelectrics for Power Generation-A Look at Trends in the Technology*. 2016, InTech.
141. Chen, J., *Design and analysis of a thermoelectric energy harvesting system for powering sensing nodes in nuclear power plant*. 2016, Virginia Tech.
142. Zhang, H., Y. Mui, and M. Tarin, *Analysis of thermoelectric cooler performance for high power electronic packages*. *Applied thermal engineering*, 2010. **30**(6): p. 561-568.
143. Bottner, H. *Thermoelectric micro devices: current state, recent developments and future aspects for technological progress and applications*. in *Thermoelectrics, 2002. Proceedings ICT '02. Twenty-First International Conference on*. 2002.

144. Carmo, J.P., L.M. Gonçalves, and J.H. Correia, *Thermoelectric microconverter for energy harvesting systems*. IEEE Transactions on Industrial Electronics, 2010. **57**(3): p. 861-867.
145. Nesarajah, M., F. Felgner, and G. Frey. *Modeling and simulation of a thermoelectric Energy Harvesting System for control design purposes*. in *Mechatronics-Mechatronika (ME), 2014 16th International Conference on*. 2014. IEEE.
146. Bergman, T.L., et al., *Fundamentals of heat and mass transfer*. 2011: John Wiley & Sons.
147. Lineykin, S. and S. Ben-Yaakov, *Analysis of thermoelectric coolers by a spice-compatible equivalent-circuit model*. IEEE Power Electronics Letters, 2005. **3**(2): p. 63-66.
148. Prijic, A., et al., *Thermal Energy Harvesting Wireless Sensor Node in Aluminum Core PCB Technology*. Sensors Journal, IEEE, 2015. **15**(1): p. 337-345.
149. Dalola, S., et al., *Characterization of thermoelectric modules for powering autonomous sensors*. IEEE Transactions on Instrumentation and Measurement, 2009. **58**(1): p. 99-107.
150. Lienhard, J.H., *A heat transfer textbook*. 2013: Courier Corporation.
151. Hamil, A., et al., *Validation, Optimization and Simulation of Solar Thermoelectric Generator Model*. 2015.
152. Bergman, T.L. and F.P. Incropera, *Introduction to heat transfer*. 2011: John Wiley & Sons.
153. Virjoghe, E., et al., *Numerical Simulation of Thermoelectric System*. Latest trends on systems, 2002. **2**: p. 630-635.

154. Allouhi, A., et al. *Simulation of a thermoelectric heating system for small-size office buildings in cold climates*. in *2015 3rd International Renewable and Sustainable Energy Conference (IRSEC)*. 2015. IEEE.
155. Felgner, F. and G. Frey. *Object-oriented simulation model of thermoelectric devices for energy system design*. in *Electrotechnical Conference (MELECON), 2012 16th IEEE Mediterranean*. 2012. IEEE.
156. Varadrajana, E. and M. Bhanusri. *Design and simulation of unimorph piezoelectric energy harvesting system*. in *COMSOL conference, Bangalore*. 2013.
157. Li, Y., et al., *A review on spindle thermal error compensation in machine tools*. *International Journal of Machine Tools and Manufacture*, 2015. **95**: p. 20-38.
158. Haitao, Z., Y. Jianguo, and S. Jinhua, *Simulation of thermal behavior of a CNC machine tool spindle*. *International Journal of Machine Tools and Manufacture*, 2007. **47**(6): p. 1003-1010.
159. Nicholas s, H., Glenn G, Amatuucci, *Energy harvesting and Storage with lithium-Ion Thermogalvanic Cells*. *15th international Symposium on Solid Oxide Fuel Cell*, 2008.
160. Xiao, H., X. Gou, and C. Yang. *Simulation analysis on thermoelectric generator system performance*. in *System Simulation and Scientific Computing, 2008. ICSC 2008. Asia Simulation Conference-7th International Conference on*. 2008. IEEE.
161. Pathirana, W. and A. Muhtaroglu. *Low voltage DC-DC conversion without magnetic components for energy harvesting*. in *Energy Aware Computing, 2012 International Conference on*. 2012. IEEE.
162. LTC3108. *Instruments*, *T. Sensor*.
<http://cds.linear.com/docs/en/datasheet/3108fc.pdf> 2012.

163. Kumar Rai, V., *Temperature sensors and optical sensors*. Applied Physics B: Lasers & Optics, 2007. **88**(2).
164. Instruments, T. *Sensor Tag CC2650STK*.
http://processors.wiki.ti.com/index.php/CC2650_SensorTag_User's_Guide
http://processors.wiki.ti.com/index.php/CC2650_SensorTag_User's_Guide.
165. Lindh, J. and C. Lee, *Measuring Bluetooth Smart Power Consumption*. 2015.
166. V Spyropoulos, D. and E. D Mitronikas, *A review on the faults of electric machines used in electric ships*. Advances in Power Electronics, 2013. **2013**.